Title
Steady-state Visually Evoked Potentials: Improving Experimental Design and Identifying Sources of Variability

Author
Head, Austin Louis

Publication Date
2016

Peer reviewed|Thesis/dissertation

UNIVERSITY OF CALIFORNIA

Los Angeles

Steady-state Visually Evoked Potentials: Improving Experimental Design and Identifying Sources of Variability

A dissertation submitted in partial satisfaction of the requirements for the degree Doctor of Philosophy in Biomedical Engineering

by

Austin Louis Head

2016

ABSTRACT OF THE DISSERTATION

Steady-state Visually Evoked Potentials: Improving Experimental Design and Identifying Sources of Variability

by

Austin Louis Head

Doctor of Philosophy in Biomedical Engineering

University of California, Los Angeles, 2016

Professor Mark S. Cohen, Chair

The original experiments presented in this manuscript began with the objective of utilizing steady-state visually evoked potentials (SSVEPs) as a tool for the study of visual attention and of attention disorders. The early outcomes of these experiments were not successful in reproducing effects that were reported to be quite robust by the relevant literature. This failure to replicate prior results precluded further interpretation of the data and launched a reexamination of the experimental design. Efforts to improve the application of SSVEPs specifically to the study of attention also led to a questioning of the assumptions about the properties of SSVEPs and to a thorough exploration into their sources of variability. This manuscript describes the development of precise methods for generating SSVEPs, presents the results of experiments investigating poorly understood SSVEP characteristics, and reveals sources of variability that can hinder SSVEP research. The outcomes of this project demonstrate

that subtle stimulus parameters such as contrast and duty cycle can considerably impact SSVEP data. The culmination of this endeavor is a multimodal imaging study illustrating the relationship between evoked potentials across a range of frequencies as well as the distinctions between responses to periodic and aperiodic stimuli.

The dissertation of Austin Louis Head is approved.

James Warwick Bisley

Martin M. Monti

Dan Ruan

Mark S. Cohen, Committee Chair

University of California, Los Angeles

2016

DEDICATION

For Amanda, my family, and my childhood dreams of becoming a scientist.

TABLE OF CONTENTS

LIST OF TABLES AND FIGURES

ACKNOWLEDGEMENTS

The attention studies presented in Chapter 2 and the exploratory research presented in Chapter 3 were supported by NIMH grant R43MH099709 to Gregory V. Simpson, who also contributed significantly as P.I.

The experiments in Chapter 4, particularly the simultaneous EEG/fMRI study, were supported by NIH grant 5R21MH096239-02 to Mark S. Cohen, who also contributed significantly as P.I.

The experimental design, data collection, and analyses described in this manuscript also were aided by Agatha Lenartowicz, Samantha O'Connell, Samantha Betts, Sean Noah, Catherine Haber, Danni Ji, Sarah Heath, Edward Lau, Andrew Cho, Steven Lu, Cameron Rodriguez, Pamela Douglas, Xia Hongjing, Wei Li, Ariana Anderson, Wesley Kerr, Don Vaughn, Malina Beatrice, Shruthi Chakrapani, Ally Karacozoff, Mitch Yin, Jen Bramen, and Dianna Han.

VITA

Education:

2015 M.S. University of California, Los Angeles, Biomedical Engineering
2009 B.S. University of Houston, Biomedical Engineering

Research Training:

2009-2016: Graduate Student Researcher
Staglin Center for Cognitive Neuroscience, *University of California, Los Angeles* (Los Angeles, CA)
Doctoral Advisor: Mark S. Cohen, PhD

- Designed experiment paradigms to study visual evoked responses and visual attention in adults using EEG, fMRI, and concurrent EEG/fMRI
- Developed high-precision hardware and software to provide stimuli and to record responses for noise-sensitive EEG and MRI experiments
- Collected neuroimaging and physiological data on adult subjects using EEG, fMRI, ECG, and BCG, separately and concurrently
- Analyzed EEG and fMRI data using techniques including temporal averaging, wavelet transforms, Fourier analysis, convolution, etc.
- Created additional hardware and software solutions for various lab projects, including documentation and support
- Trained research assistants and undergraduate students on EEG and fMRI data collection, signal processing, and experimental design

2009: Software Programmer
University of Houston Cognitive Development Lab, *University of Houston* (Houston, TX)

- Updated legacy code in Matlab and Psychtoolbox to work with newer software versions and different operating systems
- Collaborated on experiment design related to language development
- Modified stimulus presentation scripts for alternative experimental setups

2008: Research Intern
The Methodist Hospital Research Institute, *Houston Methodist* (Houston, TX)

- Studied the Alzheimer's Disease Neuroimaging Initiative database, which includes clinical, imaging, and genetics data from 800 subjects
- Analyzed database using SQL and statistical methods including LDA

2007: Research Assistant
NSF-Funded Summer Nanotechnology Study Program, *Tohoku University* (Sendai, Japan)

- Traveled to Japan to study nanotechnology, culture, and language

- Designed and constructed microwave resonance cavities using CAD software and machine tools
- Assessed permittivity of carbon nanotube samples using resonance cavities, network analyzers, and a superconducting magnet

Teaching:

2011-2012: Graduate Teaching Assistant, Principles of Neuroimaging B, *UCLA*
2010-2011: Graduate Teaching Assistant, Principles of Neuroimaging A, *UCLA*

Honors:

2004-2009: National Merit Scholar, *University of Houston*
2007-2008: Dean's List, *University of Houston*

Publications:

Douglas, P., Pisani, M., Reid, R., **Head, A**., . . . Cohen, M. (2014). Method for Simultaneous fMRI/EEG Data Collection during a Focused Attention Suggestion for Differential Thermal Sensation. *Journal of Visualized Experiments JoVE,* (83). doi: 10.3791/3298

Douglas, P., Lau, E., Anderson, A., **Head, A**., . . . Cohen, M. (2013). Single trial decoding of belief decision making from EEG and fMRI data using independent components features. *Frontiers in Human Neuroscience Front. Hum. Neurosci., 7*(392). doi:10.3389/fnhum.2013.00392

Presentations:

2012: Increase in intra-individual variability of ultra-slow cortical EEG activity during sustained attention in adults with ADHD: Society for Neuroscience, (New Orleans, LA)

2007: Identifying Nanotube Permittivity through Microwave Cavity Techniques: Rice University Research Colloquium, (Houston, TX)

Organizations:

Society for Neuroscience
Engineering World Health (undergraduate board member)
University of Houston Honors College
University of Houston Biomedical Curriculum Board

CHAPTER 1: INTRODUCTION AND OVERVIEW OF METHODS

Background

A transient evoked potential is an electrophysiological recording of the nervous system's response to an external stimulus. An ideal transient evoked potential should capture a single deviation from the resting state of the nervous system, and the system should return to its resting state prior to subsequent stimuli. In contrast, a steady-state evoked potential represents the stable periodic response of the nervous system to repeating stimuli, consisting of spectral components at the stimulus frequency and its harmonics (Regan, 1989). The frequency specificity of steady-state evoked potentials contributes to the ease of identifying these signals and to their resilience against certain types of artifacts. The characteristic stability and noise resistance of steady-state visually evoked potentials (SSVEPs) has led to their inclusion in many cognitive and clinical neuroscience paradigms as well as in brain-computer interface (BCI) and other engineering applications (Vialatte et al, 2010).

SSVEPs have been shown to be less susceptible to certain artifacts common in electroencephalography (EEG), such as eye blinks and DC drift (Perlstein et al, 2003) as well as contamination from muscular activity (Gray et al, 2003), in large part due to the precise concentration of the SSVEP frequency components. In addition to aiding the detection and study of SSVEPs themselves, this frequency specificity can distinguish between responses to multiple simultaneous stimuli so long as the stimuli occur at unique frequencies. Known as frequency tagging, this method demonstrated the enhancement of SSVEPs as a result of spatial attention (Morgan et al, 1996). Frequency tagging has also been used to study binocular rivalry (Brown and Norcia, 1997) as well as to investigate and to localize mechanisms of attention control (Müller et al, 1998).

In recent decades, literature related to SSVEPs has focused primarily on their applications to cognitive neuroscience and particularly to BCI. Fewer experiments have investigated the mechanisms and phenomena solely of SSVEPs since the early fundamental work. Methods and implementations of SSVEP paradigms can differ substantially with little discussion of the effects of certain design choices on the SSVEP signal itself (Zhu et al, 2010). The characteristics of the driving stimuli and the techniques for their generation are inconsistent throughout the field. Strobe lamps, oscilloscopes, light-emitting diodes (LEDs), and computer monitors have all been used in SSVEP paradigms, and the variety of stimuli include full-field illumination, circular spots, concentric rings, checkerboards, and other patterns (Vialatte et al, 2010). The driving stimuli can be sinusoidal, rectangular, or triangular waveforms (Teng et al, 2011) at a range of frequencies, with stimulus durations ranging from under one second (Pastor et al, 2003) to several minutes (O'Connell et al, 2009). The degree to which different implementations may alter SSVEP outcomes remains largely unaddressed, as many questions about the underlying principles of SSVEPs have not yet been answered (Vialatte et al, 2010).

The diversity of stimulus methods alone is not necessarily problematic, but reported results also exhibit appreciable variability. One study found a rectangular wave with a 50% duty cycle as the optimum driving stimulus (Teng et al, 2011), but another study reported stronger SSVEPs using longer duty cycles as high as 89.5% (Lee et al, 2011). A third experiment found that a 50% duty cycle maximized BCI accuracy, but reported that lower duty cycles improved user comfort and resulted in less signal-to-noise ratio (SNR) variability (Cecotti, 2010). The choice of stimulus frequency also varies throughout the literature, and driving stimuli at differing frequencies have been shown to activate distinct cortical networks with effects on SSVEP attentional modulation (Ding et al, 2006). Unsurprisingly, various SSVEP paradigms have

produced differing results of SSVEP source localization (Vialatte et al, 2010). Publication bias in favor of positive outcomes and statistical significance has been widely discussed and empirically supported (Dwan et al, 2013), and this bias has been shown to impact the peer review process itself (Emerson et al, 2010). As such, the collective literature likely overstates the beneficial characteristics of SSVEPs while underestimating their limitations.

The remainder of this chapter discusses the advantages and disadvantages of two techniques often seen in this field. The details of a stimulus device built specifically for this project are included there as well. Chapter 2 of this manuscript presents initial attempts to reproduce and to expand upon reported effects of SSVEP attentional modulation. A lack of success in these early experiments inspired an iterative redesign process that developed an improved set of stimulus methods for studying attention using SSVEPs, as told throughout Chapter 3. The explorations into subtle aspects of SSVEP implementations brought awareness of inconsistencies in the literature regarding stability and variance in these effects. Chapter 4 describes a series of experiments investigating further sources of variability in SSVEPs and provides clarity regarding the fundamental principles governing the generation of SSVEPs as well as evoked responses to similar arrhythmic stimuli. Chapter 5 concludes the manuscript and reflects on the lessons learned throughout the process.

SSVEP Presentation Using Commercial Display Devices

Computer display devices such as LCD monitors are a popular choice for evoking SSVEPs, as they facilitate implementation and modification of designs, particularly with multiple stimuli or complex stimulus patterns. However, the refresh rate of each display sets substantial restrictions on the frequency and the waveform of the driving stimulus. CRT monitors have the capability to switch between a range of possible refresh rates, but these have been made

largely obsolete by LCD devices. Commercial LCD products commonly operate with a nominal frame rate of 60 Hz, in which case changes to the stimulus can occur only in increments of approximately 16.7 milliseconds. Some LCD monitors offer frame rates of 120 Hz or higher, widening the range of possible stimuli, but discretization always imposes some limits. These constraints affect rectangular wave stimuli less than other waveforms, and many SSVEP studies have successfully used computer displays through careful experimental design.

The frequency of a rectangular wave on a computer monitor should be chosen with attention to the frame rate. By definition, SSVEPs result from periodic stimulation (Regan, 1989). Accurate and consistent periodic stimuli can only be produced on a monitor when the period of the waveform is an integer multiple of the duration of a single frame. The number of frames in each stimulus period also restricts the duty cycle of the waveform to a small number of possible values (Volosyak et al, 2009). A 50% duty cycle is only possible with an even number of frames. The generation of stimuli with a particular duty cycle and the generation of multiple stimuli with the same duty cycle at different frequencies can be particularly difficult because of frame rate limitations. If two stimuli have different duty cycles, the stimulus with the longer duty cycle will appear brighter because of the increased fraction of time when the stimulus is on. Where differences of duty cycle are simply a consequence of design constraints, the luminance of stimuli with unequal duty cycles should be balanced such that all stimuli share the same average luminance.

Driving frequencies that do not conform to the frame rate of a monitor can be approximated using a variable stimulus period. A response resembling an SSVEP to an intended frequency can be elicited by alternating between two stimulus periods, one faster and one slower than the intended stimulus, to achieve the correct average frequency over the entire duration of

stimulation. Varying the amount of cycles at each of the two alternating periods allows a wide range of approximated stimulus frequencies. A publication demonstrating this method suggests that approximated SSVEPs are "mostly comparable" with SSVEPs evoked by a stimulus with a constant period, in terms of amplitude, SNR, and BCI accuracy (Nakanishi et al, 2013). However, approximated stimuli should be avoided whenever possible, as further investigation has confirmed that this method does result in reduced signal quality and changes to SSVEP harmonics (Szalowski and Picovici, 2015). In an experimental design incorporating constant-period stimuli as well as approximated stimuli, the two methods of SSVEP generation could be an important confound.

Despite limitations related to frame rate, computer monitors have some strong advantages over other methods of evoking SSVEPs. Checkerboards, concentric rings, text, and other complex stimulus patterns can be displayed using software such as Psychtoolbox or E-Prime. Testing various stimulus parameters can be quite simple with these implementations, allowing a convenient iterative experimental design process. Presentation through a computer monitor also facilitates stimulus consistency between recording sessions and particularly between site locations. Furthermore, stimulus presentation software and display devices are readily accessible to most researchers and do not require the construction of additional hardware.

Direct modulation of LEDs

Individual light sources, such as strobe lamps and LEDs, are another common method for the generation of SSVEPs. Strobe lamps offer some advantages over computer monitors, as they often can be adjusted continuously over a wide frequency range and can easily stimulate a subject's entire visual field. However, strobe lamps typically do not allow control over the stimulus waveform beyond the flicker frequency. Direct modulation of a light source provides

precise stimulus control, usually in the form of purpose-built electronic hardware driving an LED. The design of a custom electronic device requires some specialized knowledge and skill, but such a device can be constructed using inexpensive, off-the-shelf components. Unlike LCD displays, direct modulation of an LED does not restrict the frequency or the duty cycle of a rectangular wave. Additionally, sinusoidal and triangular stimulus waveforms can be generated with an LED, although these waveforms are somewhat nontrivial compared to rectangular waves (Teng et al, 2010). The presentation of complex stimulus patterns using custom hardware can be prohibitively challenging, but direct modulation of a light source offers unmatched precision and flexibility for simple stimuli.

Three of the experiments presented in this manuscript feature a custom electronic device for modulating LED stimuli. The device, pictured in Figure 1.1., consists of an Arduino UNO single-board microcontroller (http://arduino.cc) and supporting circuitry made from discrete components for driving the LED. The Arduino UNO board uses an ATmega328P microprocessor operating at 16 MHz, orders of magnitude faster than any SSVEP stimulus. Firmware for the device was written in the Arduino IDE (integrated development environment) using a special set of C/C++ functions, and MATLAB scripts were written to facilitate serial communication with the device from a personal computer over USB. Power was also supplied to the device via a USB. Additional connections were made between the device and the EEG recording system, allowing the transfer of timing signals used as event markers.

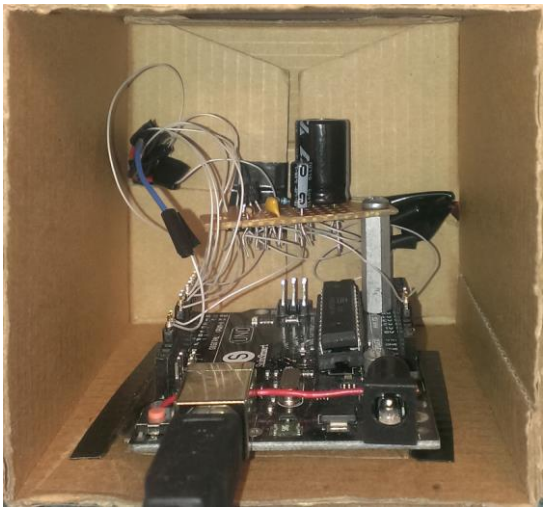

Figure 1.1. The custom stimulus device.

The device firmware handles serial communication over USB, modulates the stimulus LED, and sends timing information to the EEG system. Serial communication is used each time the device operates to establish parameters such as stimulus duration, flicker frequency, duty cycle, and luminance. The digital outputs of the Arduino board are not capable of directly providing the current necessary to power the LED; the supporting circuitry employs an additional transistor to supply current to the LED that is switched on and off by the device firmware. Event markers are inserted into the EEG recording using transistor-transistor logic via a hardware interface. Three versions of the firmware were made, with each version offering functionality specific to the requirements of each experiment. The appendix of this manuscript contains the source code for the three firmware versions.

Controlling the frequency and duty cycle of the stimulus waveform is rather straightforward, but changes to luminance pose a slight challenge. The current through an LED determines its brightness, and the current through an LED is a nonlinear function of the voltage across it (Sedra and Smith, 2004). These properties make it difficult to modulate the brightness of an LED directly, so the device controls stimulus luminance with pulse width modulation

(PWM) during the active phase of the stimulus waveform. The device uses a PWM switching frequency of 326.8 Hz with pulse width increments of 12 microseconds; the rapid PWM switching far exceeds the flicker fusion rate and appears as a steady stimulus (Parsons and Miller, 1957). The Arduino language includes PWM functionality through a high-level command, but this method lacks the precision and dynamic range needed for these experiments. The device's custom PWM implementation utilizes interrupt service routines triggered by the microcontroller's hardware timers, ensuring that transitions between the on and off states of the LED occur with maximum accuracy.

CHAPTER 2: PRELIMINARY EXPERIMENTAL RESULTS

Preliminary Study 1: A Pilot Experiment of SSVEP in Relation to Attention Disorders

Introduction

Individuals diagnosed with attention deficit hyperactivity disorder (ADHD) exhibit increased variability in performance during behavioral testing as compared to normal control subjects (Castellanos et al, 2005; Klein et al, 2006; Johnson et al, 2007; Vaurio et al, 2009). Identification of the neurophysiological bases of these behavioral differences would offer great benefit to the understanding, diagnosis, and treatment of ADHD. Research using fMRI has revealed relationships between performance variability and low-frequency oscillations in the so-called default mode network for individuals with ADHD and has implicated a role for slow fluctuations in other networks (Helps et al, 2007). As a non-invasive biomarker, low-frequency EEG oscillations exhibiting similar relationships with ADHD-linked behavioral characteristics would be useful in both clinical and research settings, particularly given the practical advantages of EEG over fMRI.

Attentional modulation of SSVEPs, namely the enhancement of covertly attended SSVEP targets, is a well-established phenomenon (Morgan et al, 1996; Müller et al, 1998; Russo et al, 2002; Kelly et al, 2005) that suggests that momentary fluctuations in SSVEP signals may be relevant to attention processes as well. The present EEG study investigates fluctuations in attended and ignored SSVEPs over the course of a continuous performance covert attention task. The analyses explore relationships between SSVEP low-frequency oscillations and behavioral performance measures, both within subjects and between ADHD and control groups, in search of SSVEP indicators of attention with potential applications for ADHD assessment.

Methods

Two adult subjects diagnosed with ADHD and two adult control subjects performed a covert visual attention task. All subjects had normal color vision. An Electrical Geodesics 256-channel EEG system recorded the subjects' neural activity while they performed the task described below. Recordings were taken using a 250 Hz sample rate in a room equipped with electromagnetic shielding to reduce external contamination of the EEG signal. All subjects provided informed written consent prior to their participation.

Stimuli were displayed on a 22 inch LCD computer monitor with a frame rate of 60 Hz using Psychtoolbox (Brainard, 1997; Pelli, 1997; Kleiner et al, 2007) in MATLAB. During the task, subjects viewed a centrally located plus sign and two stimulus regions made up of flickering concentric rings that appeared directly to the left and to the right of the plus sign. Figure 2.1 illustrates the arrangement and relative size of the flickering regions. The rings were centered 10.6 cm to the left and right of the middle of the screen. The largest rings were 15.2 cm in diameter; the thickness of each ring, and of each space between rings, was just over 1 cm. Subjects sat roughly 50 cm from the screen and were told to maintain that distance, but subjects were not held in place. At that distance, the flickering regions would be 17º in diameter at an eccentricity of 12º; deviations from the intended viewing distance by ± 10 cm would change the diameter and eccentricity of the stimuli by approximately ± 3º and ± 2º, respectively.

The left and right stimulus regions underwent rectangular wave oscillation at 13.5 Hz and 16.5 Hz respectively. Flickers alternated between black and white, against a grey background that was 50% of the maximum screen brightness. As the refresh rate of the monitor was not an integer multiple of either flicker stimulus frequency, the oscillations were generated via an approximation method using rectangular waves of varying duration to provide the intended

average frequency (Nakanishi et al, 2013). The duty cycle of each of these stimuli also varied throughout the task as a consequence of this approximation method.

Subjects received instructions to fixate on the central plus sign at all times throughout six 90-second task blocks. Prior to each task block, an audio message cued subjects to attend to either the left or the right flickering region without changing their gaze. Throughout the task, red circular probe stimuli briefly appeared superimposed on top of the flickering regions, as in Figure 2.1. Probes had a diameter of 9.1 cm, or about 10º. Probes occurred with a randomized inter-stimulus interval between 1-3 seconds independently in both flickering regions, and each probe remained visible for 250 ms. Subjects were instructed to respond with the keyboard to the appearance of each probe in the attended region while ignoring probes in opposite region. The attended region alternated across the six blocks. Subjects were told to respond as quickly as possible while retaining accuracy. Subject reaction times were monitored via Psychtoolbox in MATLAB, and event markers noting each response were inserted into in the EEG recording. The precise timings of the beginning and end of each stimulus block were also marked in the recording.

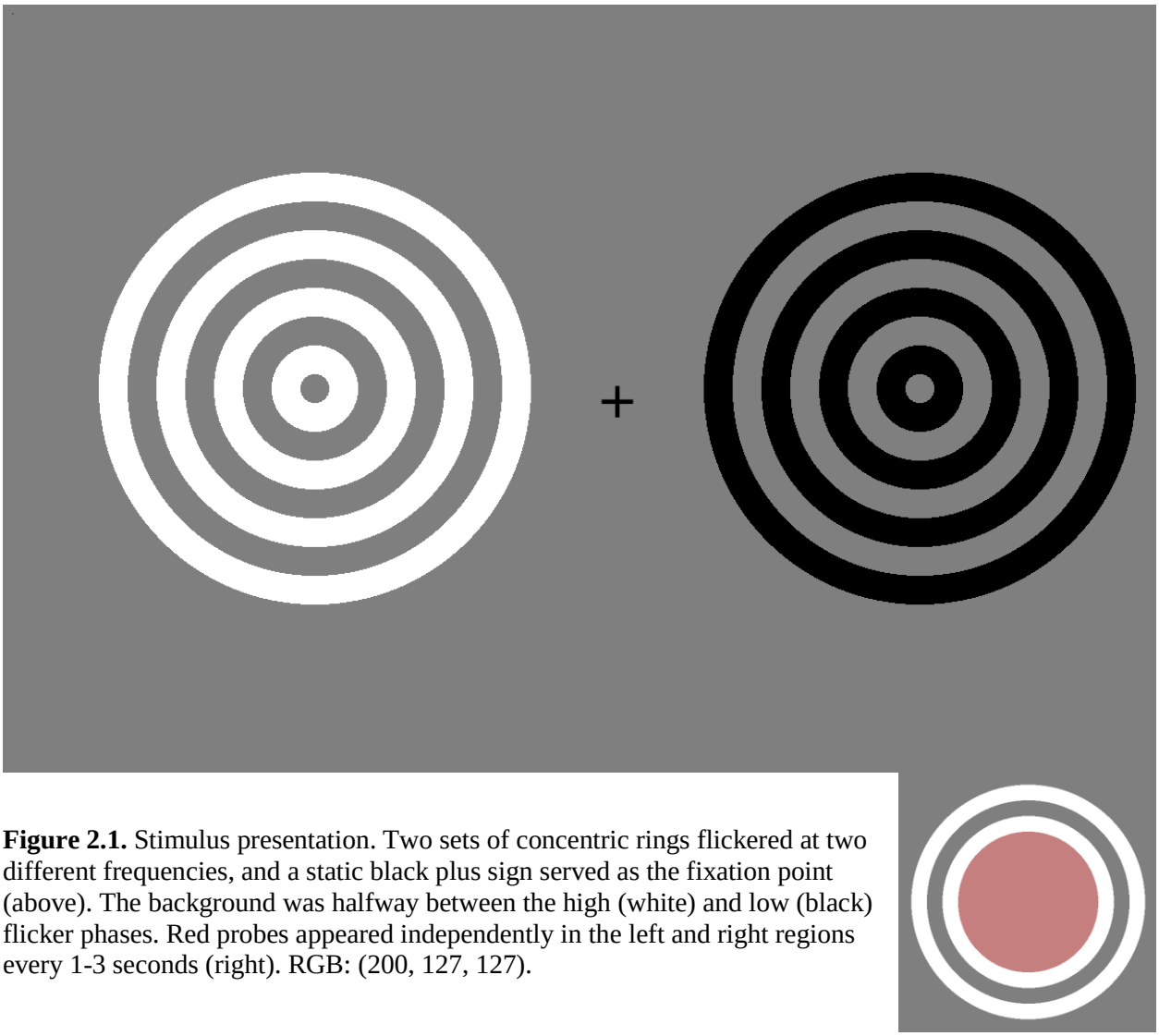

Figure 2.1. Stimulus presentation. Two sets of concentric rings flickered at two different frequencies, and a static black plus sign served as the fixation point (above). The background was halfway between the high (white) and low (black) flicker phases. Red probes appeared independently in the left and right regions every 1-3 seconds (right). RGB: (200, 127, 127).

Analyses

Spectral analyses on the EEG data were performed in MATLAB. The fast Fourier transform (FFT) was applied to each of the six task blocks to obtain the power spectrum for the O_Z electrode. The spectral power at the two stimulus frequencies were then selected for comparison of SSVEP strength across blocks. Block-wise attentional modulation was assessed within subjects for each frequency using a two-sample t-test on the SSVEP frequency components, to confirm whether SSVEP power increased in response to covert attention.

A second method of assessing attentional modulation was performed, in anticipation of possible interference via attention capture by distractor probes. Even with complete subject compliance, the appearance of distractor probes could redirect attention briefly away from the target SSVEP. As such, attentional modulation was also calculated after excluding 1.33 seconds of the EEG following each distractor, corresponding to approximately half of each block. After excluding distractor segments, power was calculated at the attended and ignored frequencies for each block, and a two-sample t-test was used to evaluate attentional modulation of each frequency for each subject.

To determine fluctuations in SSVEP magnitude over time within each block, a moving window FFT was applied to the raw EEG recording using 10-second Hanning windows at increments of 0.5 seconds. The changing power of the spectral components for the two stimulus frequencies in each window provided the time series of SSVEP fluctuations. The correlation coefficient between the power fluctuations at both frequencies was calculated per block, revealing the degree of covariance between the attended and ignored signals. Large positive correlation between the two signals would suggest that fluctuations in the SSVEPs arise from a single driving factor, likely unrelated to attention, whereas large *negative* correlation could suggest that subject efforts in covert attention simultaneously enhance the target SSVEP while diminishing the distractor. Weak correlation would imply that the fluctuations in the two signals are derived from separate processes, possibly distinct mechanisms for attending and ignoring.

Statistical measures were used to search for associations between characteristics of the neural signals and changes in performance of the task. The variance and coefficient of variation (CV) of the attended SSVEP fluctuations and the mean, variance, and CV of the reaction times were calculated for each block. Within each subject, the relationship between SSVEP

fluctuations and reaction time was explored via least squares linear regression, using the variance and CV of the attended fluctuations as explanatory variables and the mean, variance, and CV of reaction time as response variables.

Following the individual analyses, the processed data were used to evaluate the similarity of the two groups and to assess trends across all subjects. To test the hypotheses of greater measures of variability in ADHD subjects, the variability in SSVEP fluctuations and reaction time were assessed using two-sample t-tests comparing ADHD and control subjects. Additionally, the relationships between reaction time and SSVEP variability per block were assessed using least squares linear regression, to determine whether decreased SSVEP stability correlated with poor or variable reaction time. The models used for analyses within individuals were applied across all subjects without respect to the two groups.

Results

The recorded responses indicated that subjects complied with the task instructions; Table 2.1 lists the average reaction time and the number of false alarms (a subject response following a distractor probe) for each subject. Subjects did not demonstrate SSVEP attention effects across blocks for the either stimulus frequency, as indicated in Table 2.2. In control subjects overall, average power during attended blocks was slightly higher than that of ignored blocks, but t-tests revealed no statistically significant differences. ADHD subjects also lacked significant differences in SSVEP power between conditions, and power was reduced slightly during attended blocks in most cases. As presented in Table 2.3, evaluation of attentional modulation after excluding segments following each distractor also revealed no significant effects. These outcomes contradict previous findings and conflict with expectations about SSVEP indicators of attention and task performance.

Table 2.1
Behavioral Performance

Subject	Mean Reaction Time (ms)	Reaction Time Standard Deviation (ms)	False Alarms
ADHD1	408	111	31 (9.5 %)
ADHD2	473	97.5	18 (5.6 %)
Control 1	415	86.9	6 (1.8 %)
Control 2	426	82.5	18 (5.4 %)

Table 2.2
SSVEP Block-wise Attention Modulation

	13.5 Hz Power (μV^2)			16.5 Hz Power (μV^2)			Overall
Sbj.	**Mean Attend**	**Mean Ignore**	**p**	**Mean Attend**	**Mean Ignore**	**p**	**p**
ADHD 1	0.21 ± 0.067	0.14 ±0.0077	0.19	0.067 ± 0.027	0.11 ± 0.048	0.78	0.43
ADHD 2	0.070 ± 0.013	0.076 ± 0.014	0.64	0.016 ± 0.0035	0.024 ± 0.010	0.75	0.65
Control 1	0.10 ± 0.034	0.033 ± 0.0034	0.062	0.021 ± 0.013	0.022 ± 0.0034	0.57	0.096
Control 2	0.14 ± 0.0089	0.13 ± 0.023	0.42	0.025 ± 0.0072	0.022 ± 0.0029	0.35	0.46

Note. P-values based on two-sample t-tests of attend > ignore.

Table 2.3
SSVEP Block-wise Attention Modulation after Excluding Distractor Segments

	13.5 Hz Power (μV^2)			16.5 Hz Power (μV^2)			Overall
Sbj.	**Mean Attend**	**Mean Ignore**	**p**	**Mean Attend**	**Mean Ignore**	**p**	**p**
ADHD 1	0.034 ± 0.011	0.026 ± 0.019	0.36	0.0060 ± 0.0023	0.0071 ± 0.0045	0.58	0.39
ADHD 2	0.0072 ± 0.0021	0.037 ± 0.021	0.88	0.012 ± 0.0053	0.038 ± 0.027	0.81	0.95
Control 1	0.015 ± 0.0061	0.014 ± 0.011	0.48	0.0083 ± 0.0034	0.0062 ± 0.0020	0.31	0.41
Control 2	0.035 ± 0.019	0.074 ± 0.052	0.73	0.0072 ± 0.0030	0.014 ± 0.0073	0.78	0.76

Note. P-values based on two-sample t-tests of attend > ignore.

The moving window FFT revealed the presence of strong slow fluctuations in both SSVEP signals for each subject. Figure 2.2 illustrates the scale of these fluctuations, which surpassed that of the block-wise differences. Correlational analyses showed that the two signals varied independently; correlation coefficients ranged from -0.26 to 0.32 across subjects, with a mean of -0.0034 and a standard deviation of 0.18. The mean of the absolute value of the correlation coefficients was 0.15 across subjects with a standard deviation of 0.098. Correlation between the attended and ignored SSVEPs was significant in only 14 of the 24 blocks. Strong correlation between the two signals would have discredited the assumption of their independent modulation.

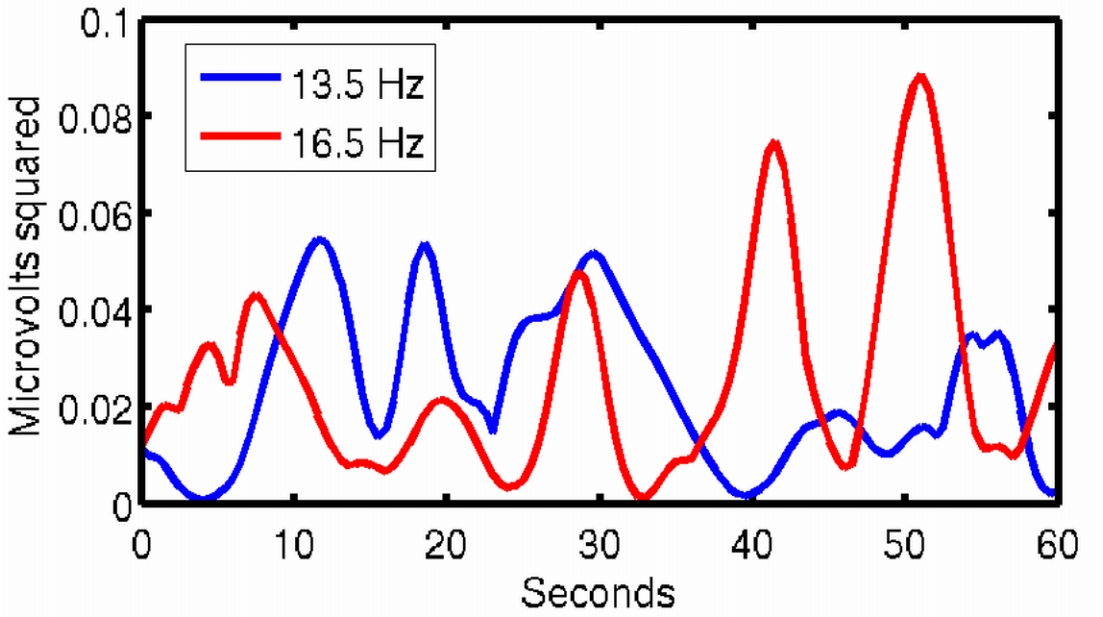

Figure 2.2. SSVEP fluctuations in attended (13.5 Hz) and ignored (16.5 Hz) signals did not covary. The magnitude of fluctuations exceeded the magnitude of attentional modulation.

Table 2.4 lists the statistical measures of SSVEP fluctuations and reaction time for the two groups. Relative to controls, ADHD subjects exhibited increased variability in both SSVEP fluctuations and reaction time as well as greater average reaction time, but only the difference in reaction time variance was statistically significant.

Table 2.4
SSVEP Fluctuations and Reaction Time in ADHD and Control Groups

	ADHD Group	**Control Group**	**ADHD − Control**	**p**
Fluctuation Variance (μV^2)	0.0037	0.0019	0.0018	0.16
Fluctuation CV	0.77	0.72	0.042	0.20
Reaction Time Mean (ms)	440	421	19	0.068
Reaction Time Variance (ms)	100	81	19	0.038
Reaction Time CV	0.23	0.19	0.037	0.073

Note. p-values from two-sample t-tests.

Through linear regression, several relationships were found between SSVEP fluctuations and measures of task performance. Table 2.5 presents the results of the regression analyses performed within each subject, which can be compared to the results across all subjects as shown in Table 2.6. Significant correlation was discovered in at least one individual for all but one of the regressor-regressand pairs, but analyses across subjects found only three significant relationships: SSVEP variance as a predictor of RT variance, SSVEP variance as a predictor of RT coefficient of variation, and SSVEP coefficient of variation as a predictor of RT variance.

Table 2.5

Regression within Subjects: SSVEP Variability as Block-wise Predictors of Reaction Time

SSVEP Regressor	**RT Regressand**	**β**	**R^2**	**p**
Variance (μV^4)	Mean (ms)	120 2900 410 3700	0 0 0 0.91	0.90 0.87 0.99 0.0031
Variance (μV^4)	Variance (ms^2)	4200 29000 2500 4500	0.78 0.44 0.61 0.73	0.020 0.15 0.068 0.030
Variance (μV^4)	CV	10 62 61 8.5	0.74 0.50 0.57 0.64	0.027 0.11 0.082 0.056
CV	Mean (ms)	-22 63 -22 71	0.041 0.093 0 0.38	0.70 0.56 0.88 0.19
CV	Variance (ms^2)	220 230 65 42	0.56 0.73 0.23 0.74	0.085 0.030 0.33 0.60
CV	CV	0.56 0.46 0.18 0.059	0.58 0.73 0.29 0.034	0.077 0.030 0.27 0.73

Note. Subject order: ADHD 1, ADHD 2, Control 1, Control 2. Highlighted values indicate significance.

Table 2.6
Regression across Subjects: SSVEP Variability as Block-wise Predictors of Reaction Time

SSVEP Regressor	**RT Regressand**	**β**	**R^2**	**p**
Variance (μV^4)	Mean (ms)	-620	0.0070	0.70
Variance (μV^4)	Variance (ms^2)	4300	0.50	< 0.001
Variance (μV^4)	CV	11	0.55	< 0.001
CV	Mean (ms)	100	0.14	0.069
CV	Variance (ms^2)	110	0.23	0.017
CV	CV	0.20	0.14	0.069

Note. Highlighted values indicate significance.

Linear regression across all subjects revealed that the variance of SSVEP fluctuations correlated significantly with reaction time variance; the same relationship was significant within individuals for two subjects, one ADHD and one control. The significant group result appears to be dominated by the two individuals, as seen in Figure 2.3. Analyses across subjects found the variance of SSVEP fluctuations to covary significantly with reaction time CV as well; this relationship was only significant within a single individual. Figure 2.4 shows that this second group result seems influenced heavily by the same two individuals. Linear regression also revealed a third significant correlation across groups between the CV of the SSVEP fluctuations and the reaction time variance. Within-subject analyses of this model found a significant relationship in only one subject, but Figure 2.5 illustrates that the third group result reflects data from all subjects with more consistency than do the other two models.

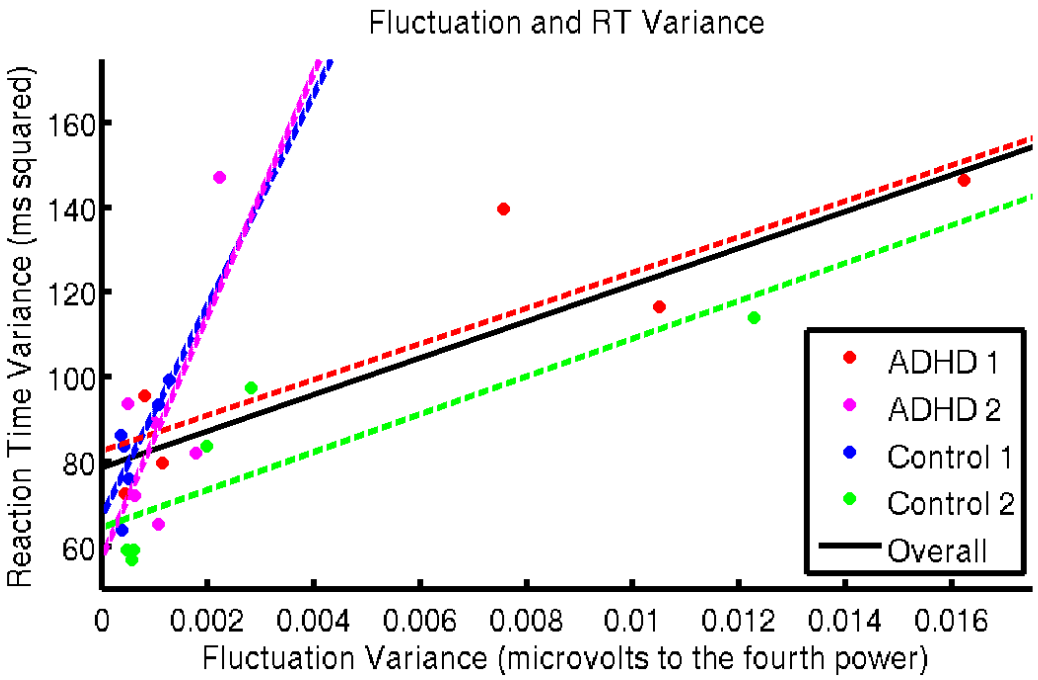

Figure 2.3. The variance of the attended SSVEP had significant positive correlation with reaction time variance across all subjects ($p < 0.001$, R-squared = 0.50). Correlations within subjects were positive but significant in only two individuals (ADHD 1 and Control 2).

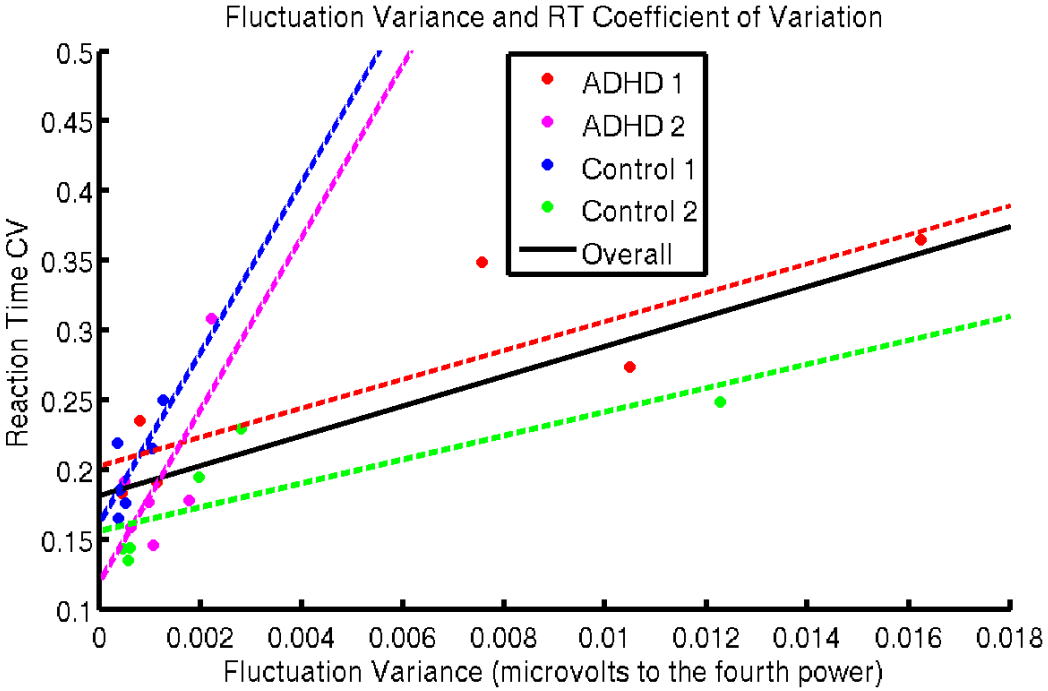

Figure 2.4. The variance of the attended SSVEP had significant positive correlation with reaction time coefficient of variation across all subjects ($p < 0.001$, R-squared = 0.55). Correlations within subjects were positive but significant in only one individual (ADHD 1).

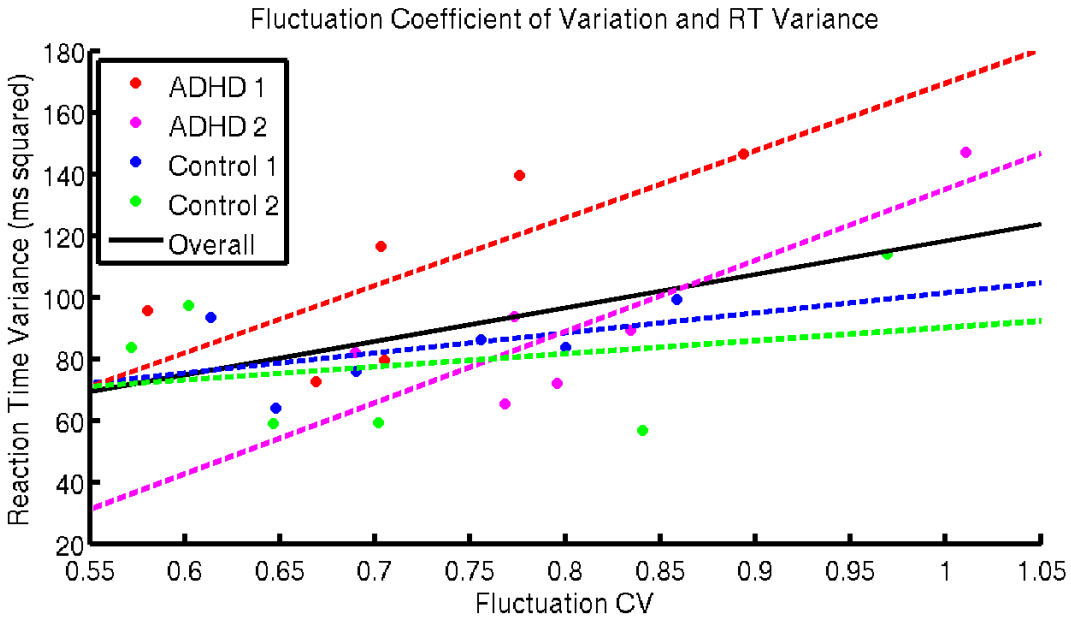

Figure 2.5. The coefficient of variation of the attended SSVEP had significant positive correlation with reaction time variance across all subjects ($p = 0.017$, R-squared = 0.23). Correlations within subjects were positive but significant in only one individual (ADHD 2).

Discussion

No subjects demonstrated significant differences in SSVEP power between attend and ignore conditions, which is troubling given the reported consistency of this effect in prior literature. The presence of distractor probes may have disrupted subjects' covert attention, but the exclusion of segments following distractors did not improve measured modulation. Consequently, attention capture by the distractor probes cannot explain the failure to replicate previous reports of SSVEP attentional modulation.

Regarding behavioral performance measures and variability in the EEG signal, only one significant difference was found between the two subject groups. The ADHD subjects exhibited significantly greater variance in reaction time, consistent with prior literature (Castellanos et al, 2005; Klein et al, 2006; Johnson et al, 2007; Vaurio et al, 2009). SSVEP fluctuations also appeared more variable in ADHD subjects, but these differences were not statistically

significant. The small sample size of both groups was a serious weakness of this study. Further experimentation using a greater number of subjects could determine if SSVEP variability is truly elevated in subjects with ADHD or could confirm that the results here arose by chance.

Fluctuations in the SSVEP power elicited by the two stimuli were shown to have low correlation with each other. If overall arousal or activation of the default mode network drove the large fluctuations in the SSVEP signals, then power at the two frequencies should covary. The observed low correlation may indicate that independent mechanisms control the enhancement and inhibition of attended and ignored visual stimuli. The correlation across blocks between variability in reaction time and variability in the SSVEP fluctuations supports the use of SSVEP measures as indicators of attention. However, while the small sample size in this experiment limits the ability to find meaningful effects, it also increased the likelihood of false positives (Button et al, 2013). Any relationship between SSVEP fluctuations and behavioral performance must be confirmed with more data. If successful, continued investigation into the relationship between neural phenomena in SSVEP and behavioral performance could lead to improved EEG classifiers of attentional state and to more quantitative descriptions of attentional disorders.

Preliminary Study 2: Studying Fluctuations of Attention Using SSVEP Variability

Introduction

The previous experiment produced encouraging results regarding the relationship between SSVEP fluctuations, behavioral task performance, and ADHD, but no definitive conclusions could be drawn. As the ADHD group and the control group both consisted of only two subjects, sample size was clearly a limiting factor. Additionally, greater intra-individual variability has been demonstrated in EEG recordings of subjects with ADHD (Ghajar and Ivry, 2009). Developing tools for assessing SSVEP fluctuations as predictors of performance may benefit from beginning with a population without ADHD.

Task-related enhancement of covertly attended SSVEP targets is a well-established phenomenon (Morgan et al, 1996; Müller et al, 1998; Russo et al, 2002; Kelly et al, 2005); prior literature has shown that SSVEP strength can increase or decrease when a stimulus is attended or ignored, respectively. It follows that momentary fluctuations in SSVEP signals may be relevant to attention processes even when attention conditions remain constant. This experiment investigates the association between reaction time in a continuous performance task and fluctuations in SSVEPs generated from attended and ignored stimuli. Linear regression was used to test the hypothesis that SSVEP variability would correlate with poor reaction time. The hypothesis that momentary increases in SSVEP power at the attended frequency would correlate with better performance was also tested with linear regression. The experiment was designed and conducted with the hope of identifying characteristics in SSVEP fluctuations preceding or concurrent with changes in task performance that could be used as indicators of attentional state.

In an effort to remove one possible source of extraneous variability, this study did not include any subjects with a known ADHD diagnosis. Stimulus methods used here largely

resemble the implementation of the previous pilot study, apart from a few changes to parameters such as block length and one flicker frequency.

Methods

Twenty-three adult subjects performed a covert visual attention task. An Electrical Geodesics 256-channel EEG system recorded the subjects' neural activity while they performed the task. Recordings were taken using a 250 Hz sample rate in a room equipped with electromagnetic shielding to reduce EEG artifact. All subjects provided informed written consent prior to their participation.

Stimuli were displayed on a 22 inch computer monitor with a refresh rate of 60 Hz using Psychtoolbox (Brainard, 1997; Pelli, 1997; Kleiner et al, 2007) in MATLAB. During the experiment, subjects viewed a centrally located plus sign and two flickering regions of concentric rings, as described in the previous section and as illustrated in prior Figure 2.1.

The stimulus regions underwent continuous rectangular wave oscillation at two different frequencies, 13.5 Hz and 15 Hz. As in the previous experiment, flickers alternated between black and white against a 50% grey background. The frame rate of the monitor was an integer multiple of the 15 Hz frequency, and therefore the period of this rectangular wave remained constant. Since each period of the 15 Hz stimulus consisted of four frames, this stimulus had a constant 50% duty cycle as well. Once again, the 13.5 Hz oscillations were generated via an approximation method using rectangular wave periods of varying duration to provide the intended average frequency (Nakanishi et al, 2013). The duty cycle of the 13.5 Hz stimulus also varied throughout the task as a consequence of the implementation of this approximation method.

The experiment consisted of a two-minute passive viewing block and multiple attention task blocks. Throughout the attention task blocks, red circular probe stimuli briefly appeared superimposed on top of the flickering regions (see prior Figure 2.1). Probes had a diameter of 9.1 cm or about 10º. Probes occurred with a randomized inter-stimulus interval between 1-5 seconds independently in both flickering regions, and each probe remained visible for 200 ms. Stimulus presentation began with the passive viewing block, which included flickering stimuli but did not include probe stimuli. Four 45-second "short" attention task blocks followed the passive block and included probe stimuli. The third portion of the experiment consisted of four 240-second "long" attention task blocks, which also featured attention probes. Prior to the passive block, subjects were instructed to keep their gaze on the central plus sign at all times throughout the entirety of the experiment.

After the passive block, subjects were given instructions on the behavioral task and reminded to look directly at the central plus sign at all times. Prior to each short block, an audio message cued subjects to attend either the left or the right flickering region without changing their gaze. Subjects were instructed to respond with the keyboard to the appearance of each probe in the attended region while ignoring probes in opposite region. The attended region alternated across the four short blocks. Short blocks were separated by periods of rest lasting 15 seconds. Subjects were told to respond as quickly as possible while remaining accurate. Subject reaction times were monitored via Psychtoolbox in MATLAB and were inserted as event markers in the EEG recording.

The long blocks followed the short blocks without any further instructions. As with the short blocks, an audio message preceded each long block, cuing the subjects to attend either the left or the right flickering region without changing their gaze. Long blocks were separated by

periods of rest lasting 30 seconds. The attended region did not alternate across the four long blocks, although the attended side was balanced across subjects. The frequencies of the left and right stimuli were also balanced across subjects, as was the initial attended side.

Analyses

Spectral and statistical analyses on the EEG data were performed in MATLAB. First, the unfiltered EEG time series were segmented into the nine blocks (one 120-second passive block, four 45-second short blocks, and four 240-second long blocks) in preparation for further analyses. The FFT was applied to each of the nine blocks to obtain the power spectra for the O_Z electrode. The spectral components at the two stimulus frequencies were then selected for comparison of SSVEP strength across blocks. Block-wise attentional modulation was calculated within each subject for each frequency after first finding the mean power during attended blocks and the mean power during ignored blocks. The attentional modulation contrast was calculated by dividing the attend - ignore difference by the attend + ignore sum. Significance of the SSVEP attentional modulation was assessed at the group level using a one-sample t-test of the contrast calculated per subject. Standard error estimates were generated with 1000 bootstrapped samples of the per-block SSVEP powers for individual subjects and of the per-subject mean contrast values for the across-subject average.

To determine fluctuations in SSVEP magnitude over time within each block, a moving window FFT was applied to the raw EEG recording using 10-second Hanning windows at increments of 0.5 seconds. The changing power of the spectral components at the two stimulus frequencies in each window provided the time series of SSVEP fluctuations.

Statistical measures were used to contrast SSVEP fluctuations according to task conditions and to search for connections between characteristics of the neural signals and

changes in performance outcomes. The variance and coefficient of variation (CV) of the SSVEP fluctuations were calculated for all nine blocks (one passive, four short, and four long). These two variability measures were used to assess attended and ignored fluctuations across task blocks, both within and across subjects. Two-sample t-tests compared variability between attended and ignored fluctuations during short blocks and compared variability between attended and ignored fluctuations during long blocks. Additionally, two-sample t-tests were used to compare passive blocks and long blocks across subjects in terms of variability in fluctuations at both frequencies. The hypotheses predicted increased variability in the attended SSVEPs compared to the ignored SSVEPs and throughout task blocks relative to passive blocks.

Subject reaction times were analyzed in conjunction with SSVEP fluctuations. The mean, variance, and CV of the reaction times were calculated for each short block. Least squares linear regression was used to assess the relationship between reaction time and SSVEP variability across short blocks from all subjects. The variance and CV of SSVEP fluctuations at the attended and ignored frequencies were tested independently as predictors of mean reaction time, of reaction time variance, and of reaction time CV. The interactions between behavioral performance and neural signals during long blocks also were assessed with linear regression across individual events, both within and across subjects. SSVEP power at the attended frequency and SSVEP power at the ignored frequency, as calculated with the moving window FFT, were evaluated as predictors of reaction time for each probe occurrence.

Results

Recorded responses indicated that subjects complied with the task instructions; Table 2.7 lists the average reaction time and the number of false alarms (a response following a distractor probe) for each subject. Spectral analyses of the short task blocks did not reveal an SSVEP

attention effect. Table 2.8 shows the mean and standard error of the attentional contrasts for the left and right stimuli. The attentional contrast was calculated by dividing the attend - ignore difference by the attend + ignore sum. This was done first for each frequency individually and then after averaging the attended power for both frequencies and the ignored power for both frequencies (rather than averaging directly the contrasts calculated per frequency). Attentional contrast was not consistent across subjects. Some subjects demonstrated robust increases in SSVEP power accordant with task conditions, while others exhibited striking differences in attentional contrast between the two stimulus targets. Only a single subject had consistent negative attentional contrast. Overall, mean attentional contrast was not significantly different from 0 ($p = 0.11$).

Table 2.7
Behavioral Performance

Subject	Reaction Time (mean, standard deviation in ms)		False Alarms
1	485	105	4 (1.3%)
2	457	124	2 (0.71%)
3	462	308	1 (0.39%)
4	474	104	9 (2.5%)
5	400	92	3 (0.9%)
6	490	67.5	4 (1.4%)
7	428	102	7 (2.4%)
8	388	56.4	4 (1.2%)
9	384	47	0 (0%)
10	389	63.9	2 (0.68%)
11	548	131	10 (2.7%)
12	436	70.2	3 (0.84%)
13	470	102	15 (5.2%)
14	438	84	0 (0%)
15	411	67.1	1 (0.28%)
16	455	109	22 (6%)
17	432	61.3	0 (0%)
18	414	64.9	3 (0.95%)
19	487	95.9	6 (1.7%)
20	452	99.4	18 (4.5%)
21	365	49.3	7 (2.4%)
22	445	82.8	0 (0%)
23	443	74.5	2 (0.53%)
Average	441	94.0	5 (1.6%)

Table 2.8
SSVEP Attentional Contrast Per Frequency and Overall (with Standard Error)

Sbj.	Left Stimulus	Right Stimulus	Mean
1	0.16 ±0.17	0.0064 ±0.27	0.10 ±0.13
2	0.28 ±0.059	0.20 ±0.016	0.22 ±0.030
3	-0.0083 ±0.18	-0.27 ±0.053	-0.11 ±0.12
4	-0.45 ±0.19	0.53 ±0.069	0.12 ±0.28
5	0.052 ±0.30	0.45 ±0.18	0.12 ±0.26
6	0.23 ±0.076	-0.13 ±0.41	-0.011 ±0.25
7	0.15 ±0.11	-0.65 ±0.37	-0.44 ±0.33
8	0.24 ±0.27	-0.42 ±0.37	0.16 ±0.28
9	0.77 ±0.0063	0.86 ±0.0087	0.79 ±0.025
10	0.33 ±0.40	0.20 ±0.052	0.23 ±0.13
11	-0.21 ±0.044	-0.37 ±0.16	-0.27 ±0.081
12	0.0038 ±0.14	-0.40 ±0.24	-0.29 ±0.20
13	-0.46 ±0.13	0.14 ±0.24	-0.12 ±0.21
14	-0.034 ±0.059	-0.078 ±0.17	-0.060 ±0.086
15	0.25 ±0.41	0.041 ±0.24	0.15 ±0.23
16	-0.39 ±0.22	0.037 ±0.094	-0.087 ±0.14
17	0.60 ±0.12	0.43 ±0.18	0.52 ±0.11
18	0.082 ±0.21	-0.15 ±0.098	-0.028 ±0.093
19	0.62 ±0.046	0.48 ±0.048	0.55 ±0.049
20	-0.095 ±0.25	0.58 ±0.029	0.44 ±0.18
21	0.021 ±0.21	-0.67 ±0.20	-0.51 ±0.25
22	0.36 ±0.17	-0.039 ±0.30	0.13 ±0.21
23	0.23 ±0.27	0.40 ±0.035	0.28 ±0.20
Group	p = 0.11		0.082 ±0.065

Note. A single group average was calculated because the frequencies of the left and right stimuli varied across subjects.

Prior to the investigation of SSVEP fluctuations with respect to behavioral task performance, SSVEP variability was compared between blocks of differing task conditions. However, statistical analyses of the variability in SSVEP fluctuations were not successful in identifying effects of attention or task conditions: results are summarized in Table 2.9. Two-

sample t-tests of the variability during short blocks revealed very few significant differences between the attended and ignored signals within subjects, and these comparisons were not significant at the group level. Two-sample t-tests of variability in the attended and ignored signals during long blocks also exhibited little significance within subjects and no significance across subjects. Lastly, two-sample t-tests at the group level of differences in SSVEP variability between passive blocks and long task blocks returned a single significant finding: fluctuations from long task blocks had greater CV values than those from passive blocks. However, this result was barely significant.

Table 2.9
Assessments of Differences in SSVEP Fluctuation Variability between Conditions

Comparisons	**Number of Subjects with Individual Significance**	**p-values Across All Subjects**
Short: Attend vs Ignore Variance	3	0.15
Short: Attend vs Ignore CV	2	0.95
Long: Attend vs Ignore Variance	1	0.96
Long: Attend vs Ignore CV	4	0.68
Passive vs Long Variance	N/A	0.13
Passive vs Long CV	N/A	0.041

Note. Highlighted value indicates significance.

The first main hypothesis predicted that SSVEP variability would correlate with behavioral performance, measured by the average and the consistency of reaction times. Least-squares linear regression detected no statistically significant relationships across blocks between reaction time statistics and SSVEP variability. As Table 2.10 reports, the regression coefficients and R^2 values for these models were very low and failed to support this hypothesis.

Table 2.10
Linear Regression across Subjects: SSVEP Variability as Block-wise Predictors of Reaction Time

SSVEP Regressor	**Reaction Time Regressand**	**β**	**R^2**	**p**
Attended Variance	Reaction Time Mean	0.44	0.0048	0.51
Attended Variance	Reaction Time Variance	0.050	0.0036	0.57
Attended Variance	Reaction Time CV	0.45	0.0018	0.69
Attended CV	Reaction Time Mean	0.0049	0.00028	0.87
Attended CV	Reaction Time Variance	-0.0028	0.0052	0.50
Attended CV	Reaction Time CV	-0.044	0.0080	.040
Ignored Variance	Reaction Time Mean	0.53	0.0035	0.58
Ignored Variance	Reaction Time Variance	0.087	0.0052	0.49
Ignored Variance	Reaction Time CV	1.4	0.0086	0.38
Ignored CV	Reaction Time Mean	-0.0058	0.00045	0.84
Ignored CV	Reaction Time Variance	0.0027	0.0053	0.49
Ignored CV	Reaction Time CV	0.047	0.010	0.34

The second main hypothesis predicted that reaction time at individual events would correlate positively with momentary SSVEP power at the attended frequency and negatively with momentary power at the ignored frequency. Linear regression did not reveal strong interactions between reaction time and SSVEP power at the moment that each probe occurred. Across subjects, neither power at the attended frequency nor power at the ignored frequency were significant predictors of reaction time using simple linear regression or multiple regression. Significant effects within subjects were found only in a handful of individuals, as presented in Table 2.11.

Table 2.11
Linear Regression between SSVEP Power and Reaction Time across Individual Events

SSVEP Regressors	Effects across Subjects			Number of Subjects with Individual Significance
	β	R^2	p	
Simple Regression: Attended Power	-0.0090	0.00044	0.13	5
Simple Regression: Ignored Power	-0.0076	0.00021	0.29	4
Multiple Regression: Attended Power	-0.012	0.00046	0.30	5
Multiple Regression: Ignored Power	0.0043			

Discussion

Attentional modulation of SSVEP signals is a reportedly robust phenomenon (Morgan et al, 1996; Müller et al, 1998; Russo et al, 2002; Kelly et al, 2005), so the lack of a statistically significant attention effect in these data is troublesome. Demonstrated SSVEP paradigms influenced the design of this stimulus procedure, but this experiment did not perfectly replicate any previously proven setup. Perhaps aspects of the implementation introduced unwanted sources of variability in the SSVEP signal or in its modulation from covert attention. One possible confounding factor was the inclusion of two stimulus frequencies that are generated by different methods. Since this experiment was conducted, the approximation method used in generating the 13.5 Hz stimulus frequency has been shown to degrade signal quality (Szalowski and Picovici, 2015). Other design choices, such as the pattern of the flickering stimuli or the parameters of the attention probes, also may have clouded the SSVEP signals and their attentional modulation.

In addition to the difficulty in replicating attentional modulation seen in prior literature, outcomes with respect to SSVEP variability did not meet expectations. Fluctuations in SSVEP power were not statistically distinguishable between attended or ignored signals or between passive and task blocks, with one exception (CV in passive vs long task blocks), and subject

reaction time was not found to be significantly related to SSVEP variability or momentary power. Without confirmation of an attention effect across task blocks, it would be difficult to make definitive interpretations of the fluctuations of SSVEPs within blocks or to form conclusions about the ability of SSVEPs to predict task performance. Unfortunately, the failure to replicate block-wise attentional modulation was followed by a failure to provide evidence supporting the main hypotheses. The coefficients of variation of SSVEP fluctuations were greater for long task blocks than for passive blocks with low statistical significance, but the scientific significance of this result is questionable in light of the other outcomes. Furthermore, the number of blocks and the block lengths were not identical for the passive and long task conditions. It is unknown whether the inadvertent introduction of additional sources of variability contributed to the sole positive result.

CHAPTER 3: DEVELOPING AN IMPROVED SSVEP ATTENTION STUDY

Overview

The limited success of the previous research revealed unforeseen challenges in the application of SSVEPs to the assessment of attention. Failure to replicate the attentional modulation of SSVEP signals, which had been reported by multiple groups (Morgan et al, 1996; Müller et al, 1998; Russo et al, 2002; Kelly et al, 2005), suggested that the methodologies of the first two experiments may have been deficient. Subsequently, several small exploratory studies were conducted to inform the development of an improved implementation. This chapter describes the process of pilot testing used to optimize the SSVEP stimuli and concludes with the details of the revised experimental design for assessing attention with SSVEPs.

Variations in multiple aspects of the experimental methods were investigated as possible ways to boost the SSVEP signal quality, to strengthen the SSVEP attentional modulation, or to improve the efficacy of the behavioral task. The iterative process included evaluation of the different stimulus arrangements within the visual field, assessment of the effects of inconsistent subject gaze, consideration of stimulus and background contrast, and alteration of the target and distractor probes. These ranging experiments contributed to the success of the final design for studying attention described at the end of this chapter as well as to the designs employed in Chapter 4.

Consistent Methodologies

While several experimental design iterations were employed, many components of the stimulus implementations remained consistent across some or all of the pilot testing.

Commonalities of the methods are described here; later sections of this chapter specify any deviations from these general parameters.

Adult subjects performed one of several iterations of a covert visual attention task while an Electrical Geodesics 256-channel EEG system recorded neural activity at a sample rate of 250 Hz. Data collection took place in a room equipped with electromagnetic shielding to reduce external contamination of the EEG signal. Stimulus presentation and the recording of subject responses were implemented through Psychtoolbox (Brainard, 1997; Pelli, 1997; Kleiner et al, 2007) in MATLAB. Stimuli were displayed on a 22 inch LCD monitor with a frame rate of 60 Hz for the majority of the testing in this chapter, excluding the last pilot experiment and the final revision of the attention design, which used a 24 inch LCD monitor with a 120 Hz frame rate.

Subjects viewed a centrally located plus sign and two stimulus regions flickering at different frequencies that appeared directly to the left and to the right of the plus sign. Each experiment used one of two stimulus arrangements. In the first stimulus arrangement, shown in Figure 3.1, two regions made of concentric rings underwent continuous rectangular wave oscillation, one at 13.5 Hz and the other at 15 Hz. Flickers alternated between high and low, against a grey background with a brightness halfway between those of the two flicker phases. The rings were centered 10.6 cm to the left and right of the middle of the screen. The largest rings were 15.2 cm in diameter; the thickness of each ring, and of each space between rings, was 1 cm. Subjects sat roughly 50 cm from the screen and were told to maintain that distance, but subjects were not held in place. At that distance, the flickering regions would be 17º in diameter at an eccentricity of 12º; deviations from the intended viewing distance by ± 10 cm would change the diameter and eccentricity of the stimuli by approximately ± 3º and ± 2º, respectively.

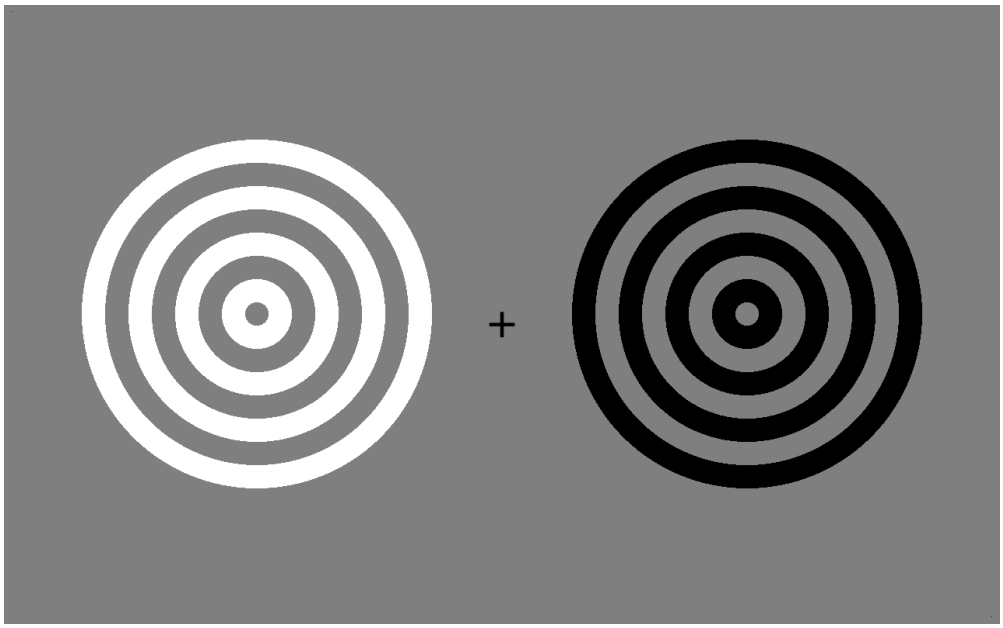

Figure 3.1. First stimulus iteration. Two sets of concentric rings flickered at two different frequencies, and a static black plus sign served as the fixation point (above). The background was halfway between the high (white) and low (black) flicker phases.

The 60 Hz monitor was used along with the first stimulus arrangement, so the frame rate of the monitor was an integer multiple of the 15 Hz frequency. Therefore the period of the 15 Hz rectangular wave remained constant. Since each period of the 15 Hz stimulus consisted of four frames, this stimulus had a constant 50% duty cycle as well. As the refresh rate was not an integer multiple of the 13.5 Hz frequency, the oscillations in the corresponding pattern were generated via an approximation method using rectangular wave periods of varying duration to provide the intended average frequency (Nakanishi et al, 2013). The duty cycle of the 13.5 Hz stimulus also varied throughout the task as a consequence of the implementation of this approximation method.

Later pilot testing was performed using a second stimulus arrangement and with the 120 Hz monitor. Stimulus frequencies of 15 Hz and 17.14 Hz (120/7) were used with the second monitor and were chosen to avoid the previously mentioned approximation method. As illustrated in Figure 3.2, the second stimulus arrangement made use of flickering circular regions

instead of concentric rings, and the central plus sign also flickered at a third unique frequency of 20 Hz. Flickering regions alternated between off and on, against a black background indistinguishable from the off flicker phase. The monitor was positioned 76 centimeters from the subjects' eyes to ensure consistency in the size of the stimuli. Subjects were told to maintain that distance, but their motion was not restrained. Both circular regions had diameters of 5.8º visual angle and were centered 6.8º from the middle of the screen. The central plus sign was formed by two rectangles with side lengths of 0.2º and 0.8º visual angle; the rectangles did not flicker but were surrounded by a flickering circle with a diameter of 1º visual angle.

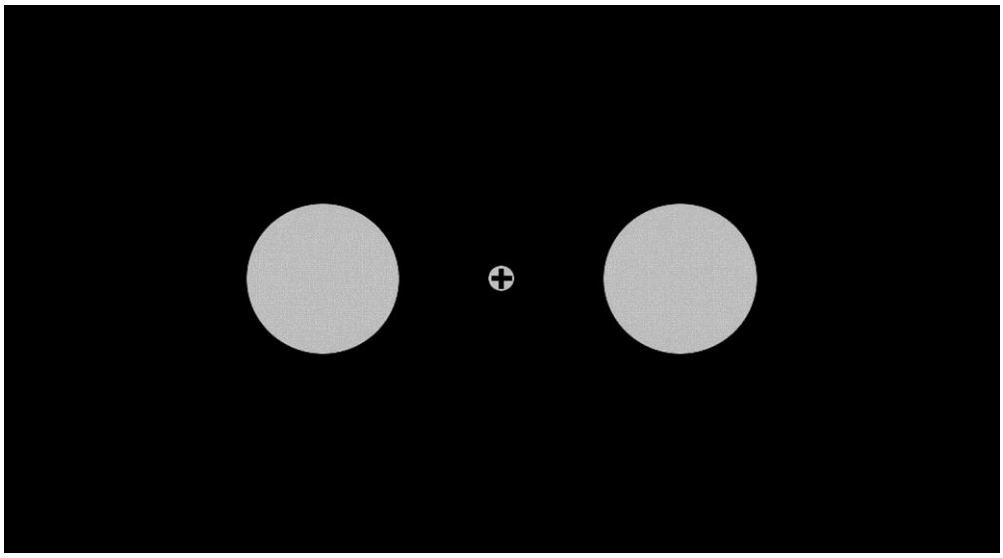

Figure 3.2. Second stimulus iteration. Three circular regions flicker at three unique frequencies. A black plus sign remains on top of the central region and serves at the fixation target.

Each design iteration consisted of multiple stimulus blocks lasting one or two minutes. The precise timings of the beginning and end of each stimulus block were stored as event markers in the EEG recording. Two types of stimulus blocks were used. Some experiments used passive viewing blocks, in which subjects simply observed the peripheral flickering stimuli while fixating at the central plus sign. Other designs included active task blocks, before which subjects were instructed to maintain fixation on the central plus sign while attending covertly to one of

the two flickering regions. Throughout the task blocks, probe stimuli briefly appeared superimposed on top of the flickering regions, as in Figure 3.3. Subjects responded with the keyboard to probes in the attended flicker region while ignoring probes in the opposite region. Subject reaction times also were noted as event markers in the EEG recording. Most implementations used probes with 200 ms durations and 1-5 second ISIs independently in each flickering region (continuous uniform distributions).

Figure 3.3. Target/distractor attention probes. During task blocks, red probes appeared independently in the left and right flicker regions every 1-5 seconds. Each probe remained visible for 200 ms. RGB: (200, 127, 127).

Consistent Analyses

Several data processing steps were common to the analyses of each experiment. As the pilot testing included few subjects, all analyses were performed at the individual level. Temporal and spectral analyses of the EEG recordings were performed in MATLAB with the use of the EEGLAB toolbox (Delorme and Makeig, 2004). Electrodes with impedances above 50 kilohms as measured at the time of the recording were immediately excluded from processing. The remaining EEG time series were band-pass filtered between 0.5 Hz and 55 Hz for the purpose of artifact detection, using a finite impulse response filter included in EEGLAB. Additional noise-contaminated channels were identified in the filtered data using automated channel rejection implemented in EEGLAB, based on abnormally low correlation between neural signals and artifact (Delorme et al, 2011). The band-pass filtered data were used only for identification of contaminated channels; subsequent processing steps were performed on the unfiltered data.

Next, the unfiltered EEG time series of non-rejected channels were segmented into the individual stimulus blocks using the stimulus onset and offset event markers (onset and offset of the continuously flickering stimulus, not individual flashes). Blocks lasted 60 to 120 seconds depending on the design iteration. The FFT was applied to each of the blocks to obtain the power spectra for all remaining electrodes. The spectral components at the SSVEP stimulus frequencies were then selected for comparison of SSVEP strength across blocks. For design iterations including active task blocks, block-wise attentional modulation was calculated within each subject after first finding the mean power during attended blocks and the mean power during ignored blocks. The attentional modulation contrast was calculated by dividing the attend - ignore difference by the attend + ignore sum.

Further analyses explored changes to the SSVEPs or to attentional modulation as a result of design choices specific to each pilot experiment. Excluding the creation of topographic maps, these analyses were made using data from the O_Z electrode only. The small number of subjects involved in these exploratory tests limited the scope of the analyses. As such, the outcomes were used to inform design choices for successive iterations rather than to make inferences regarding neural mechanisms.

Design Variations

Four pilot experiments were conducted to test potential improvements to methodologies, and a fifth design was created and implemented in a large attention study involving adults with ADHD. The first experiment compared the original stimulus arrangement against an alternative consisting of four flickering regions, one in each quadrant of the visual field. The second experiment contrasted covert shifts of attention with overt changes in subject gaze, using a modified version of the first stimulus arrangement that featured an additional flickering region at

the center of the screen. A third pilot assessed the use of on/off flickers against a black background as opposed to the original high/low flickers against neutral grey. The fourth study explored the influence of stimulus contrast on SSVEP strength, attentional modulation, and subject comfort. Finally, a revised attention study was designed based on outcomes from the pilot testing. Table 3.1 summarizes the variations in each implementation.

Table 3.1
Design Changes during Iterative Pilot Testing

	Pilot 1	**Pilot 2**	**Pilot 3**	**Pilot 4**	**Final Design**
Purpose	Stimulus arrangement	Gaze shifts	Background contrast	Flicker contrast	ADHD study
Monitor	22 in, 60 Hz	22 in, 60 Hz	22 in, 60 Hz	24 in, 120 Hz	24 in, 120 Hz
Flicker Pattern	Rings	Rings	Rings	Solid circles	Solid circles
Flicker Frequencies	13.5 & 15 Hz	13.5 & 15 Hz	13.5 & 15 Hz	15 & 17.14 Hz	15 & 17.14 Hz
Fixation Frequency	N/A	20 Hz	N/A	20 Hz	20 Hz
Background	Grey	Grey	Grey, black	Black	Black
Flicker Contrast	100%	100%	100%	15%, 55%, 75%	75 %
Probe Type	Red dots	N/A	Red dots	Red dots	Checkerboard
Probe ISI	1-3 seconds	N/A	1-5 seconds	1-5 seconds	1-5 seconds
Probe Duration	200 ms	N/A	200 ms	200 ms	100 ms
Number of Blocks	4	12	12	18	2 passive, 8 task
Block Duration	120 seconds	60 seconds	60 seconds	60 seconds	60, 120 seconds

Note. Flicker contrast reflects percent of full monitor contrast.

Eliciting SSVEPs in Four Quadrants of the Visual Field

Introduction

The first stage of pilot testing addressed a potential confound present in the stimulus arrangement used in the experiments described in Chapter 2. While subjects were instructed to fixate continuously on the central plus sign, the covert attention task created an inherent asymmetry in salience between the left and right visual hemifields. As such, there was concern that subject gaze may have tended to drift toward the target stimulus. Alternative stimulus configurations were considered that would remove the task asymmetry by presenting subjects with simultaneously attended stimuli on either side of the fixation point.

One concept was evaluated against the previous implementation: the use of four driving stimuli positioned in the four quadrants of the visual field. In this new design, one pair of stimuli in diagonally opposing quadrants was attended simultaneously while the other diagonal pair of stimuli was ignored. The following pilot compared these two implementations in terms of the elicited SSVEPs.

Methods

Two adult subjects performed the covert attention task as described at the beginning of this chapter. Stimulus presentation alternated across four 120-second blocks between the original arrangement (in prior Figure 3.1) and an alternative design. In the new "quadrant" configuration illustrated by Figure 3.4, one set of concentric rings was located in each of the four quadrants of the screen, equidistant from the central plus sign. The top-left and bottom-right stimuli flickered at 13.5 Hz, and the top-right and bottom-left stimuli flickered at 15 Hz. For a subject sitting 50 cm from the screen, the flickering regions were 12.75º in diameter, with vertical eccentricities of

9º and horizontal eccentricities of 13.5º. The thickness of each ring was 0.6º, as was that of each space between rings.

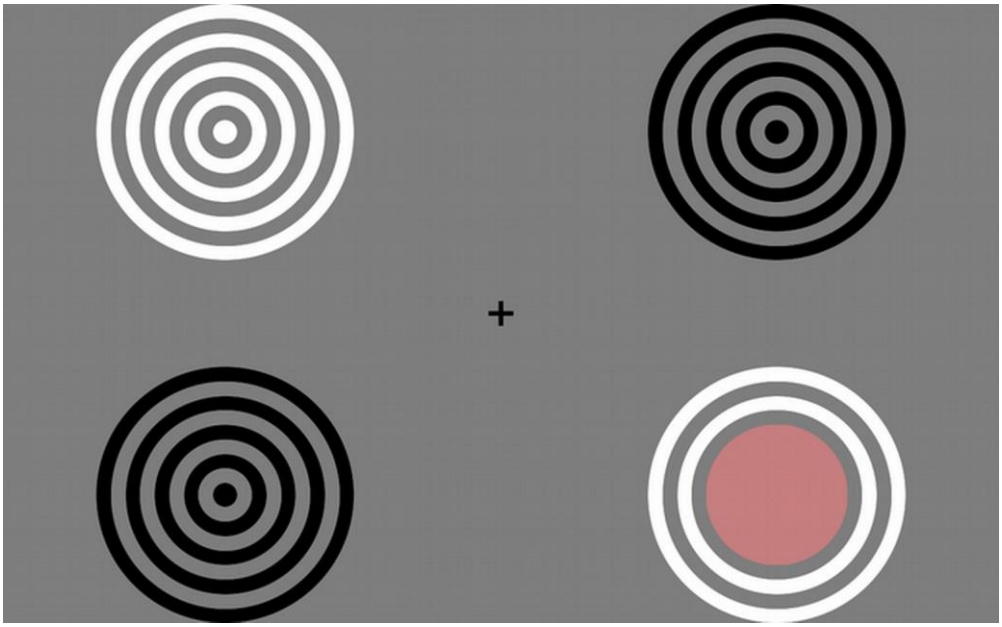

Figure 3.4. Stimulus presentation in the quadrant configuration. Diagonally opposed stimuli oscillated at the same frequency. Red probes appeared independently in the two diagonal pairs every 1-3 seconds, RGB: (200, 127, 127). Only one flicker per diagonal pair displayed a probe at each occurrence, and probes remained visible for 200 ms.

Two task blocks were presented using each configuration, and configurations alternated across the four blocks. In the quadrant configuration, subjects attended both stimulus regions of a diagonal pair. The frequency of the probes was shared between the two regions in diagonally opposing quadrants and was independent between the two diagonal pairs, such that probes occurred in one of the two regions for a given diagonal pair every 1-3 seconds. Probe occurrences were equally likely between the two regions in either pair. In both configurations, probes were centered over their respective flicker regions, and each probe remained visible for 200 ms.

Analyses & Results

The EEG data were analyzed in MATLAB according to the standard processing pipeline outlined at the beginning of the chapter. The two stimulus configurations were compared in terms of SSVEP power and attentional modulation contrast, listed in Table 3.2. SSVEPs elicited in the quadrant condition were lower in power than those elicited in the hemifield configuration, with no indication that attentional modulation was improved by removing the task asymmetry. Topographic maps of SSVEP power during the quadrant configuration unsurprisingly exhibited wider spatial distributions and increased variability, a likely consequence of the stimulus complexity. Examples of the disparate topographies can be seen in Figure 3.5.

Table 3.2
SSVEP Power and Attentional Modulation (Attend – Ignore) / (Attend + Ignore) at O_Z

	Hemifield			**Quadrant**		
	Attend	**Ignore**	**Modulation**	**Attend**	**Ignore**	**Modulation**
Subject 1 13.5 Hz	0.39	0.31	0.11	0.15	0.19	-0.12
Subject 1 15 Hz	0.49	0.39	0.11	0.22	0.19	0.073
Subject 2 13.5 Hz	0.42	0.40	0.024	0.18	0.18	-0.0019
Subject 2 15 Hz	0.34	0.26	0.13	0.12	0.15	-0.11

Note. Values in microvolts squared. Each condition was presented for a single block, so standard error values do not exist.

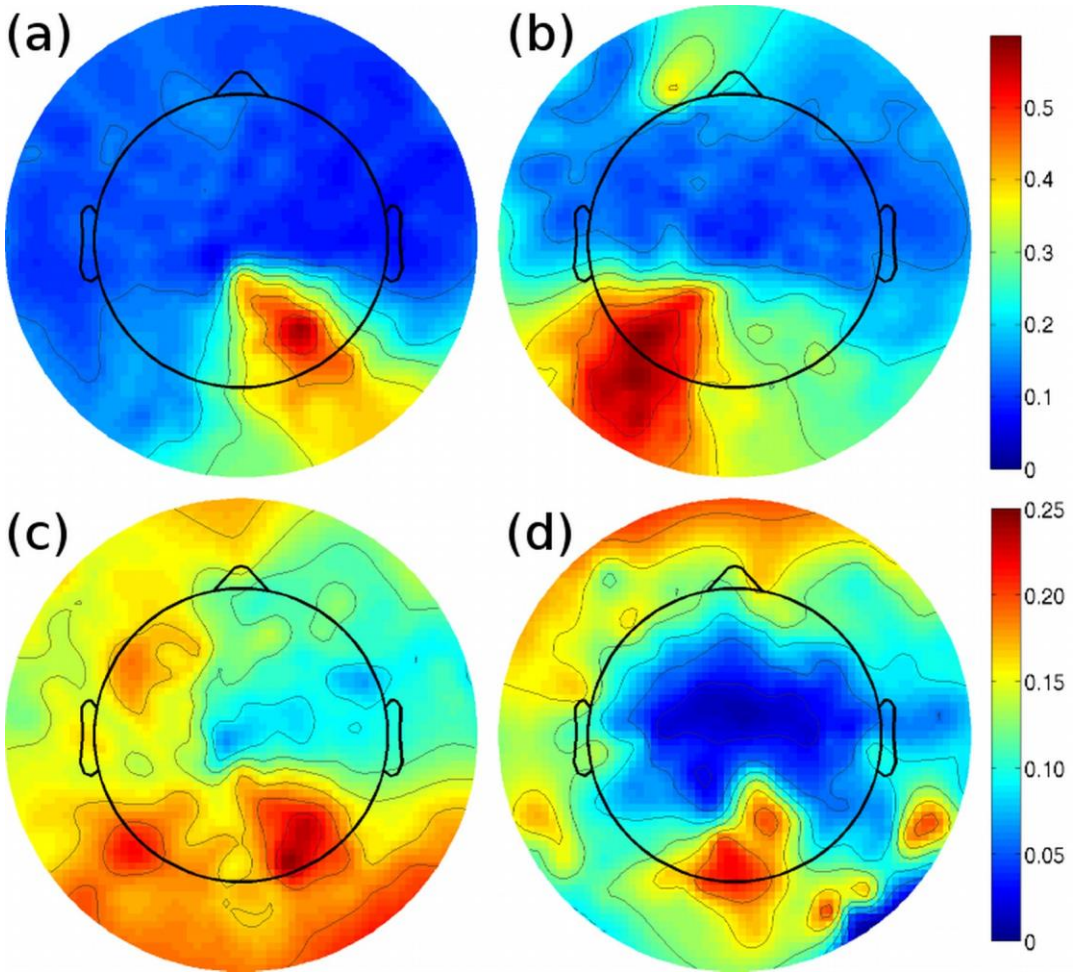

Figure 3.5. Sample SSVEP Topography. Topographies of SSVEP power have distinct characteristics under different stimulus configurations. The hemifield configuration (top) exhibits expected spatial distributions for 13.5 Hz (a) and 15 Hz (b). SSVEP power is lower in the quadrant configuration (bottom) at both 13.5 Hz (c) and 15 Hz (d), with less apparent structure. Data from Subject 1 with 13.5 Hz stimulus attended.

Discussion

The quadrant stimulus configuration was not chosen to be incorporated into future designs, as these pilot data did not indicate that the new configuration offered any advantage over the original version. In the hemifield method, each stimulus frequency projects primarily onto only a single cerebral hemisphere (Kandel et al, 2000). However, the quadrant condition drives both cerebral hemispheres at both stimulus frequencies: the reduced quality of the SSVEP signals could be a consequence of competition between the two evoked responses. While

previous studies have reported attention effects using somewhat complex target regions (Müller and Hübner, 2002), the added complexity seems ill suited for this design.

Contrasting Effects of Attention to Changes in Fixation

Introduction

One possible confound of the research presented in Chapter 2 is the difficulty in discriminating between fluctuations in SSVEP power due to attentional modulation and fluctuations caused by other factors, such as deviations of subject gaze. The low correlation between power oscillations at the two SSVEP frequencies suggests that subject gaze was not a primary driving factor of the fluctuations, because alternating gaze between the two flickering regions should introduce considerable negative covariance (Silberstein et al, 1990). However, this possibility cannot be dismissed definitively without evidence specific to this implementation.

The following pilot explored the effects of overt shifts of fixation in contrast with SSVEP modulation caused by covert redirection of attention. The experimental design was modified to include a flickering stimulus at a third frequency used as the central fixation target. Indicators of changing gaze based on the central fixation flicker could aid the assessment of task compliance in future studies and strengthen the ability to interpret SSVEP fluctuations in the context of attention paradigms.

Methods

A single subject viewed three flickering patterns, including a centrally located plus sign and two sets of concentric rings appearing directly to the left and to the right of the plus sign. Figure 3.6 presents the configuration, which differed from the first general arrangement (see prior Figure 3.1) only in the use of the third flickering region. The central plus sign was formed by rectangles with side lengths of 0.4º and 1.2º visual angle; the rectangles did not flicker but were surrounded by a flickering circle with a diameter of 2º. The plus sign oscillated at 20 Hz, which allowed the period of the rectangular wave to remain constant, with a 2/3 duty cycle.

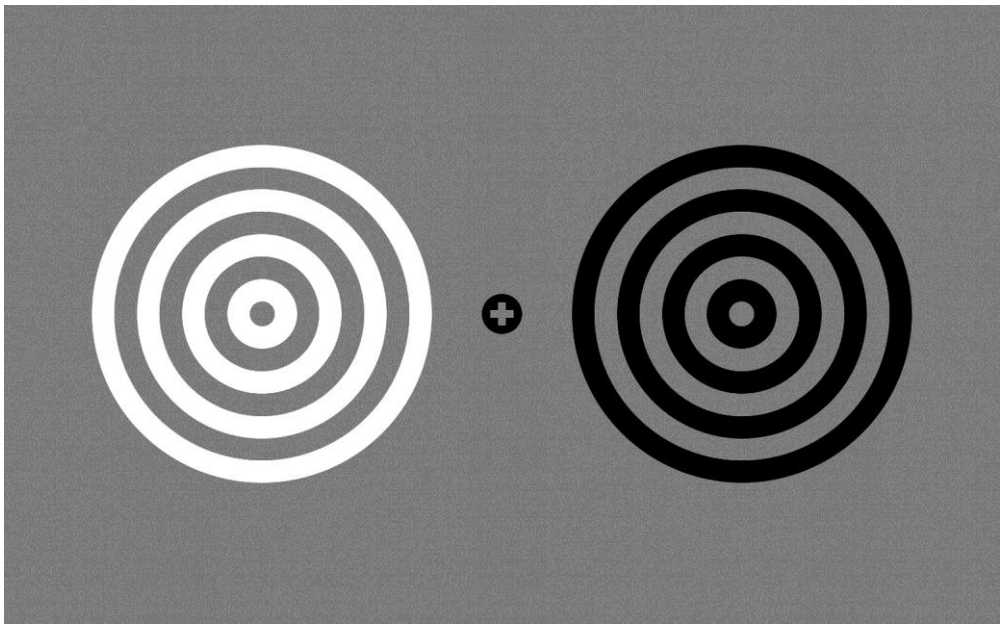

Figure 3.6. Stimulus presentation for Pilot 2. The central plus sign flickered at a third driving frequency.

Stimulus presentation occurred over twelve 60-second blocks, which included both covert attention and overt changes of gaze. Prior to each of the blocks, the subject received instructions on where to fixate their gaze and whether to attend to any of the stimuli. In six of the blocks, the subject fixated on one of the three patterns without attending to any of the patterns in particular. In the other six blocks, the subject fixated on the central plus sign at all times while either covertly attending to one of the adjacent sets of concentric rings or overtly attending to the central plus sign. For each attention block, the subject was instructed to ignore the other two patterns. Each pattern was the passive fixation target for two blocks and the covert (for the concentric rings) or overt (for the central plus sign) attention target for two blocks. No probe stimuli were used.

Analyses

Analyses of the EEG data were performed according to the steps outlined at the beginning of this chapter to determine SSVEP strength during each block. Modulation of SSVEP

power in response to gaze shifts was calculated for comparison with covert attentional modulation, and topographic plots of SSVEP power were created using EEGLAB to visualize the effect of gaze and of attention on the SSVEP cortical foci. Despite the knowledge that changing gaze would affect the location of SSVEP activity, modulation of SSVEP power was calculated using the O_Z electrode in both cases. Changes in gaze would not be an intended aspect of a standard SSVEP covert attention study, so the characteristics of changing gaze within a single electrode are most relevant.

Results

SSVEP power at the three stimulus frequencies for each block is presented in Table 3.3. Covert attentional modulation was inconsistent across the three frequencies, as only the 13.5 Hz signal exhibited greater mean power during attended blocks. Attentional modulation was considerably smaller in magnitude than modulation from changing gaze, which was positive for all frequencies. A paired t-test confirmed that the gaze modulation was significantly greater than the attentional modulation with a p-value of 0.0041.

Table 3.3
SSVEP Power (microvolts squared) per Block for Three Stimulus Frequencies

Condition	13.5 Hz (Left)	20 Hz (Center)	15 Hz (Right)
Attend Left 1	0.30	0.35	0.33
Attend Left 2	0.11	0.44	0.13
Attend Center 1	0.19	0.46	0.55
Attend Center 2	0.040	0.21	0.11
Attend Right 1	0.22	0.29	0.34
Attend Right 2	0.034	0.34	0.12
Gaze Left 1	2.3	0.021	0.023
Gaze Left 2	1.1	0.023	0.054
Gaze Center 1	0.14	0.25	0.27
Gaze Center 2	0.15	0.24	0.64
Gaze Right 1	0.062	0.045	2.4
Gaze Right 2	0.028	0.066	1.2
Attentional Modulation	0.26	-0.033	-0.11
Gaze Modulation	0.89	0.73	0.76

Note. Blocks arranged here for convenience. Blocks alternated between condition types during recording. Two blocks occurred for each condition (e.g. Attend Left 1 and Attend Left 2) but did not differ in task or stimulus parameters. Data from each block are presented in lieu of standard error values, as only two values existed per condition.

Topographic maps of the spectral power at each stimulus frequency illustrated that different attention conditions with the same fixation target resulted in similar spatial distributions even when SSVEP strength varied across blocks. In contrast, the topographies under different fixation conditions were less similar, reflecting the relocation of the SSVEP foci. Sample topographic maps are presented in Figure 3.7. The larger changes in topography resulting from redirected gaze are coherent with the greater modulation due to fixation compared to covert attentional modulation.

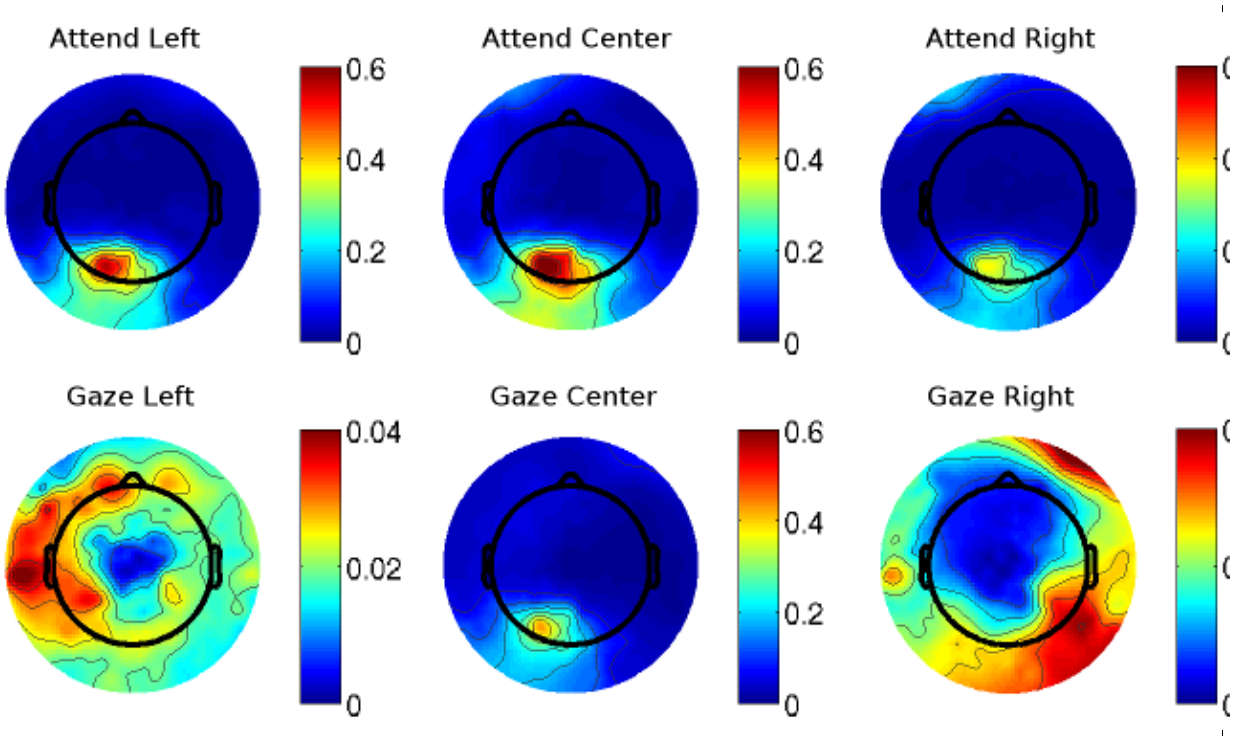

Figure 3.7. Contrasting covert attention and gaze changes. Topographic maps illustrate the spatial stability of SSVEPs throughout changes in covert attention (top) and the noticeable shifts with changing gaze (bottom). The figure presents the power at 20 Hz, corresponding to the central stimulus.

Discussion

This experiment assessed whether an SSVEP driven by a central stimulus could be used to confirm subject compliance with the fixation target. Changes to the topographic maps under varying fixation conditions in contrast to the consistency of the topographic maps under varying attention conditions revealed that this implementation could be useful to future designs. Enhancement of the attended frequencies and inhibition of the ignored frequencies occurred without the large topographic changes that are seen for different fixation targets. Future SSVEP paradigms could benefit from including analysis of changes in EEG topography as a confirmation of subject task compliance. A stimulus region flickering at a distinct frequency could serve as a fixation target specifically for the purpose of monitoring changes in gaze. In this pilot, the subject made complete redirections of gaze to the various driving stimuli for the

entirety of each block; further research would be necessary to determine the limits of detection for subtle eye movements with shorter duration or lesser magnitude.

Optimizing Background Contrast

Introduction

Each of the previous experiments described in this manuscript consisted of stimuli that alternated between black and white against a grey background. The third stage of the iterative testing process investigated one possible method of improving the signal quality of elicited SSVEPs and the magnitude of attentional modulation. The following study compares the previous implementation to an alternate design using a black background, providing increased contrast during the high phase of the stimulus waveform and rendering the stimuli indistinct from the background in the low phase. This implementation was contrasted with the prior method in terms of the power and attentional modulation of the SSVEPs as well as by feedback regarding subject comfort.

Methods

A single subject performed the standard covert visual attention task described at the beginning of this chapter. Stimulus presentation alternated between the previously used "high/low" condition and a new "on/off" condition across twelve 60-second blocks. In the high/low condition, the flickering stimuli alternated between black and white over a grey background halfway between the two stimulus phases. In the on/off condition, a black background was used with the same stimuli, such that only the stimulus "on" phase was distinguishable. Figure 3.8 illustrates the two flicker phases under both conditions.

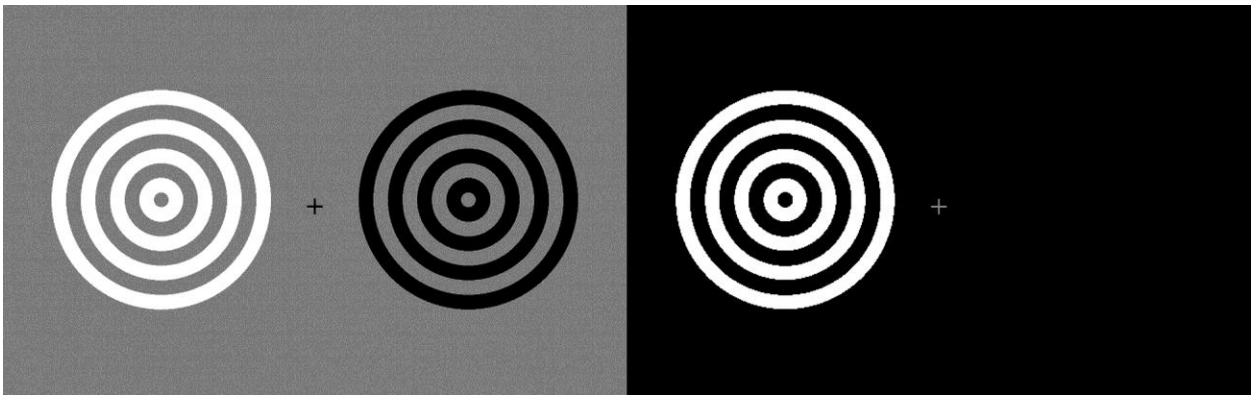

Figure 3.8. Stimulus presentation in the high/low condition (left) and the on/off condition (right).

Throughout each block, red circular probe occurred with a randomized inter-stimulus interval between 1-5 seconds independently in both flickering regions, and each probe remained visible for 200 ms. After the session, the subject was asked whether the difference in background color affected eyestrain or the difficulty of the task. The subject was not naïve to this aspect of the task.

Analyses & Results

Analyses of the EEG data were performed according to the standard processing steps outlined at the beginning of this chapter. Table 3.4 compares SSVEP power and attentional modulation between the two conditions. The limited data suggest that on/off flickers against a black background elicit stronger SSVEPs than high/low flickers against a grey background. However, attentional modulation was higher under the grey background condition for the 15 Hz signal. Attentional modulation of the 13.5 Hz signal was comparable between the two conditions. After performing the experiment, the subject reported that the on/off condition was less aversive than the high/low condition.

Table 3.4
Mean and Standard Error of SSVEP Power and Attentional Modulation in Each Condition

Block Type	Grey Background	Black Background
13.5 Hz All Blocks	0.11 ± 0.031	0.15 ± 0.042
13.5 Hz Attended	0.12 ± 0.032	0.17 ± 0.036
13.5 Hz Ignored	0.11 ± 0.037	0.12 ± 0.048
13.5 Hz Attentional Modulation	0.045 ± 0.20	0.17 ± 0.18
15 Hz All Blocks	0.27 ± 0.15	0.34 ± 0.092
15 Hz Attended	0.35 ± 0.050	0.43 ± 0.092
15 Hz Ignored	0.19 ± 0.064	0.25 ± 0.058
15 Hz Attentional Modulation	0.30 ± 0.21	0.26 ± 0.12

Note. All values in microvolts squared. Standard error calculated with bootstrapping over 1000 iterations.

Discussion

Both stimulus conditions used in this experiment succeeded in generating SSVEPs of acceptable quality, but the black background produced greater power at both frequencies. SSVEP modulation at 15 Hz was lower using the black background, although the absolute increase was larger. The subject also expressed a preference for the black background. Subject compliance is essential to the SSVEP attention paradigm, and ensuring subject comfort is one method of improving motivation. In accordance with the subject feedback and the assessment of SSVEP strength, the on/off configuration favored by the subject was chosen to be incorporated into future designs. This choice may have reduced SSVEP attentional modulation in terms of contrast.

Optimizing Stimulus Contrast

Introduction

In the fourth pilot experiment, different levels of contrast between the stimulus on and off phases were tested to determine possible effects on the SSVEP signals, attentional modulation, or subject comfort. Following the collection of the previous data, a new LCD monitor with a faster frame rate was purchased. The capabilities of the new monitor allowed precise generation of a greater number of stimulus frequencies. This experiment served also as the first test of the new monitor, taking advantage of the increased frame rate by changing one of the stimulus frequencies.

Methods

Three subjects performed the attention task described at the beginning of this chapter while viewing the second general stimulus design (see prior Figure 3.2). SSVEPs were generated at 15 Hz and 17.14 Hz (120/7). Stimulus presentation alternated between three conditions over eighteen 60-second blocks. The contrast between the on and off flicker phases varied between the three conditions, as illustrated in Figure 3.9. The "off" phases were indistinguishable from the black background in all three conditions, while different levels of grey were used for the "on" phases. The low, medium, and high contrast conditions used 15%, 55%, and 75% luminance, relative to the maximum brightness of the monitor.

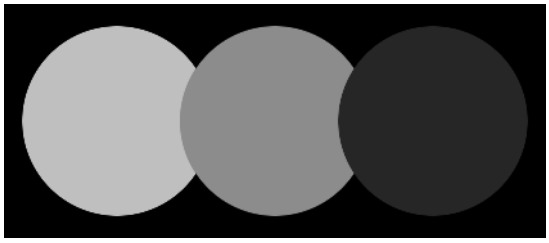

Figure 3.9. Three contrast conditions. Flickers oscillated between black and grey with three levels of contrast.

Throughout each block, subjects responded to attention probes identical to those used in the third pilot. At the end of the experiment, the subjects were asked whether the changes in contrast had any noticeable effect on eye fatigue, comfort, or their ability to perform the task.

Analyses & Results

The EEG data were analyzed in MATLAB according to the standard processing pipeline outlined at the beginning of the chapter. The three stimulus contrast conditions were compared in terms of average SSVEP power across subjects, presented in Table 3.5. SSVEP power varied appreciably across blocks and subjects, but higher SSVEP power seemed to be elicited during blocks with higher stimulus contrast. Attentional modulation also varied, with the low contrast stimulus resulting in the highest modulation.

Table 3.5
Mean and Standard Error of SSVEP Power Across Subjects, Per Condition

Block Type	**Low Contrast**	**Medium Contrast**	**High Contrast**
15 Hz All Blocks	0.14 ± 0.075	0.15 ± 0.026	0.18 ± 0.025
15 Hz Attended	0.16 ± 0.029	0.16 ± 0.041	0.17 ± 0.030
15 Hz Ignored	0.11 ± 0.019	0.14 ± 0.034	0.20 ± 0.042
15 Hz Attentional Modulation	0.18 ± 0.084	0.096 ± 0.20	-0.071 ± 0.10
17.14 Hz All Blocks	0.11 ± 0.018	0.15 ± 0.020	0.16 ± 0.021
17.14 Hz Attended	0.12 ± 0.027	0.14 ± 0.030	0.18 ± 0.025
17.14 Hz Ignored	0.095 ± 0.026	0.16 ± 0.027	0.14 ± 0.034
17.14 Hz Attentional Modulation	0.11 ± 0.17	-0.063 ± 0.078	0.10 ± 0.15

Note. All values in microvolts squared. Standard error calculated with bootstrapping over 1000 iterations.

Subject feedback was not unanimous with respect to the most comfortable stimulus condition. One subject reported that the highest contrast condition was tolerable but slightly more aversive than the other conditions. Another subject stated that the low contrast condition was too dim, and the third subject expressed no preference for any condition.

Discussion

The high contrast stimulus was selected for the next stimulus design, as there was no consensus among the subjects indicating that this implementation would cause substantial discomfort or impede task performance, and SSVEPs with the highest power were elicited during the high contrast condition. However, the low contrast stimulus seemed to produce the best attentional modulation, so this choice may improve SSVEP detectability at the expense of sensitivity to changes in attention. The limited scope of this pilot prevented confidence that either of these observations were true effects, but the data were deemed sufficient for informing the design of the next stimulus iteration.

A Revised Experimental Design for the Study of Attention via SSVEP

Introduction

Many cognitive and clinical neuroscience studies as well as biomedical engineering applications have featured SSVEPs as tools through which to investigate other neural processes (Vialatte et al, 2010; Amiri et al, 2013). SSVEPs offer resilience to common sources of EEG noise (Gray et al, 2003; Perlstein et al, 2003), and the ability to distinguish between responses to multiple stimuli via attentional modulation is widely reported (Morgan et al, 1996; Müller et al, 1998). Unfortunately, the initial experiments presented in Chapter 2 of this manuscript struggled to reproduce the SSVEP stability and the effects of attentional modulation found in the literature. Subsequently, deficient aspects of the original stimulus methods were revised through an iterative testing process, as described throughout the preceding sections of this chapter, and a new experimental design was produced for the assessment of attention using SSVEPs.

The new implementation employs an additional stimulus at a third frequency as the central fixation marker. A flickering fixation target provides an SSVEP signal that is not coupled directly to the attention task and that has the potential to serve as an indicator of arousal or other factors that may influence both of the task-modulated signals. Shifts in the topography of the SSVEP power at the third frequency could suggest that a subject failed to maintain proper fixation. The supplementary SSVEP expands the ability to assess variability within and across recordings.

Parameters such as background color and flicker contrast were optimized for data quality and subject comfort using pilot testing, as previously discussed. Other updates include changes to the probe stimuli acting as targets and distractors in the response task. Red circular probes were replaced with greyscale checkerboards to avoid the involvement of color-specific visual

pathways. Probe duration was also shortened to reduce inadvertent eye movements.

Early stages of this project implemented an approximation method to elicit SSVEPs at frequencies that could not be displayed accurately on a 60 Hz monitor (Nakanishi et al, 2013), but nonidealities in the waveforms generated by this approach may compromise data quality (Szalowski and Picovici, 2015). The acquisition of a monitor with a faster frame rate of 120 Hz allows a greater number of stimulus frequencies that do not require approximation. The new experimental design capitalizes on this capability: the period and duty cycle of each driving waveform remain stable throughout the duration of the stimulation. Frame rate limitations still demand consideration, as the stimuli cannot be displayed using the same duty cycle for each frequency. Duty cycle differences are compensated by adjustments to luminance, ensuring equal average luminance and perception of brightness for all stimuli.

The new implementation addresses potential interactions between the frequency of a stimulus and its location within the visual field by beginning with two passive blocks using alternate conditions that are immediately analyzed for comparison by SSVEP strength. The intermediate processing step ensures that the attention task utilizes the stimulus configuration that produces the optimal response.

The details of the new experimental design are presented here, but the projects using the implementation are still underway. Preliminary data analyses indicate that the revised methods have successfully improved the quality of the elicited SSVEPs and the attentional outcomes. Colleagues intend to incorporate this design into a commercial system for ADHD assessment.

Methods

Subjects perform passive viewing and covert visual attention tasks while an EEG system records neural activity. Stimuli are displayed on a 24 inch LCD computer monitor with a frame

rate of 120 Hz using Psychtoolbox (Brainard, 1997; Pelli, 1997; Kleiner et al, 2007) in MATLAB. The monitor is positioned 76 centimeters from the subjects' eyes to ensure consistency in the size of the stimuli. During the task, subjects view three flickering patterns, including a centrally located plus sign and two circular regions appearing directly to the left and to the right of the plus sign. The left and right circular regions have diameters of 5.8º visual angle and are centered 6.8º from the middle of the screen. The central plus sign is formed by two rectangles with side lengths of 0.2º and 0.8º visual angle; the rectangles do not flicker but are surrounded by a flickering circle with a diameter of 1º visual angle. The positioning of the flickering patterns can be seen in Figure 3.2 at the beginning of this chapter.

Each of the three patterns undergoes continuous rectangular wave oscillation at a unique frequency throughout the duration of the each block. The central plus sign oscillates at 20 Hz, while the two flanking regions oscillate at 15 Hz and 17.14 Hz. The stimuli alternate in an on/off cycle on top of a black background. The flicker frequencies were chosen such that the duration of a single period of any stimulus matches an integer number of frames (8 frames, 7 frames, and 6 frames corresponding to 15 Hz, 17.14 Hz, and 20 Hz). The period and duty cycle of each rectangular wave remain constant over the course of each block. The 15 Hz and 20 Hz stimuli both have a 50% duty cycle, and the 17.14 Hz stimulus has a 57.14% duty cycle as a consequence of consisting of an odd number of frames. During “off” phases, all three stimuli are black and indistinguishable from the background. During the “on” phases, the 15 Hz and 20 Hz stimuli are displayed as light grey, 75% of the maximum screen brightness. Average luminance is kept equal for all three regions by compensating the longer duty cycle stimulus with a slight reduction in brightness during the “on” phase: the 17.14 Hz stimulus is displayed at 65% of the maximum screen brightness.

The experiment includes passive viewing blocks as well as attention task blocks. Throughout the attention task blocks, checkerboard probe stimuli briefly appear superimposed on top of the left and right flickering regions, as shown in Figure 3.10. The probes are square, 3.9º in both width and height, and divided into four quadrants. Probes appear independently in both regions with a randomized inter-stimulus interval between 1-5 seconds per region; each probe remains visible for 100 ms. The checkerboard pattern ensures that probe visibility does not depend on the flicker phase: the grey and black quadrants respectively contrast with the black background and grey stimuli.

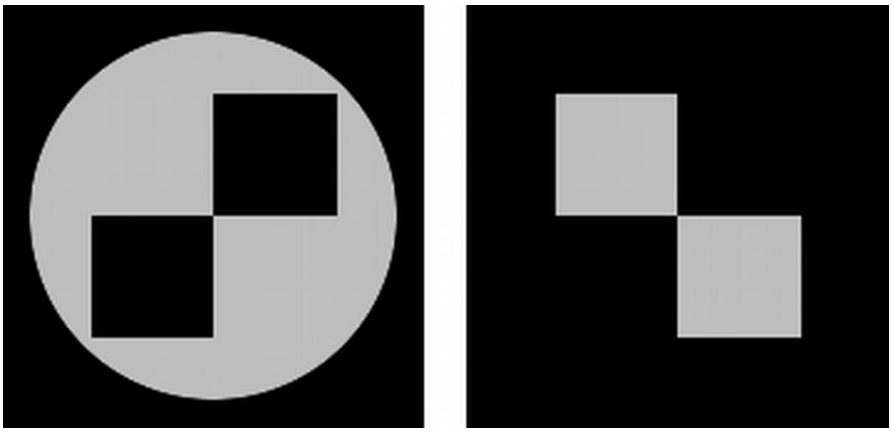

Figure 3.10. Target and distractor probes for the attention task. The checkerboard pattern is visible against the flicker on phase (left) and the background (right). Probes appeared independently in the left and right regions every 1-5 seconds.

Prior to stimulus presentation, subjects are instructed to fixate on the central plus sign at all times. The experiment begins with two 60-second passive viewing blocks, and the frequencies of the two flanking stimuli are exchanged between blocks. For example, if the first block presents the 15 Hz stimulus on the left and the 17.14 Hz stimulus on the right, then the second block presents 17.14 Hz on the left and 15 Hz on the right. Once completed, these passive blocks are processed in MATLAB using an automated script while the subject receives instructions on the attention task. The processing script identifies the electrodes with the strongest SSVEPs for each frequency in each location, allowing the researcher to determine the

optimal stimulus configuration for each subject, with respect to which frequencies are presented in the left and right regions. This step is somewhat subjective, and the two conditions do not vary substantially for every subject. However, some subjects exhibit responses that depend greatly on the frequency-location pairings, such that one frequency may evoke strong SSVEPs in only one hemisphere while a different frequency may evoke comparable SSVEPs in either hemisphere. As such, this step avoids inadvertently collecting fruitless data.

After the passive blocks, subjects receive instructions about the behavioral portion of the experiment and are reminded to look directly at the central plus sign at all times. The behavioral task occurs over eight two-minute blocks. Prior to each block, an audio cue informs subjects to attend either the left or right flickering region without changing gaze. Subjects respond with the keyboard to the appearance of each probe in the attended region while ignoring probes in the opposite region. Subjects are told to respond as quickly as possible while maintaining accuracy. The attended region alternates across blocks. A researcher checks on the subjects after every other block to provide encouraging feedback and to offer an opportunity to rest. Two five-minute resting EEG recordings, eyes-open and eyes-closed, follow the task and conclude the experiment.

CHAPTER 4: EXPLORING SOURCES OF SSVEP VARIABILITY

Simultaneous Attention of Multiple SSVEP Targets

Introduction

The first two studies presented in this manuscript were not successful in generating robust SSVEP signals across subjects or in replicating attention effects reported by multiple sources (Morgan et al, 1996; Müller et al, 1998; Russo et al, 2002; Kelly et al, 2005). Analyses of the collected data suggested that variability in the SSVEP signals within and between subjects may have been obscuring the intended investigations. As described throughout Chapter 3, subsequent exploratory research and pilot testing were conducted to develop an improved SSVEP attention study with an updated experimental design. These efforts produced an enhanced implementation that is currently being used in ongoing studies with anticipated publications and commercialization. However, many questions remain unanswered concerning the fundamental principles of SSVEP generation and the mechanisms of SSVEP attentional modulation.

The experiments presented in Chapter 2 investigated fluctuations in SSVEPs with respect to behavioral performance. Low correlation was discovered between SSVEP fluctuations at attended and ignored frequencies, possibly indicating that enhancement of the target and inhibition of distractor were modulating the two SSVEPs independently, but the difficulty that these studies faced in achieving stable and reproducible effects undermines any definitive interpretations. Momentary changes in detected SSVEP power most likely originate from the combination of many neural and external influences. Factors such as shifts in overall arousal have the potential to impact each simultaneously presented SSVEP to a similar extent, while other contributions, like noise contained in a narrow frequency band, may be limited to a single

signal. Differentiating between these multiple sources of variance may be facilitated by target and distractor stimuli each consisting of two SSVEPs, as the effects of attention should be shared. This experiment tests the hypothesis that two attended SSVEP signals should covary to a greater extent than one attended SSVEP and one ignored SSVEP. A demonstration of higher correlation between two SSVEP signals that are simultaneously attended would confirm attention regulation as a significant determinant in SSVEP fluctuations.

Methods

Two adult subjects performed a covert visual attention task while an Electrical Geodesics 256-channel EEG system recorded the subjects' neural activity. Recordings were taken using a 250 Hz sample rate in a room equipped with electromagnetic shielding to reduce EEG artifact. All subjects provided informed written consent prior to their participation.

Stimuli were displayed on a 24 inch computer monitor with a refresh rate of 120 Hz using Psychtoolbox (Brainard, 1997; Pelli, 1997; Kleiner et al, 2007) in MATLAB. Subjects were positioned with their eyes 76 centimeters from the screen for consistency in the size of the stimuli. Subjects were instructed to maintain that distance from the screen, but were not held in place. During each block, subjects viewed a centrally located plus sign and four rectangular flickering stimulus regions in the shape of vertical bars, illustrated by Figure 4.1. Each stimulus region had a height of 14º visual angle and a width of 3º visual angle. The four bars were centered 5.5º and 14.5º to the left and right of the central plus sign. Each of the stimulus regions underwent continuous rectangular wave oscillation at a unique frequency, either 13.33 Hz, 15 Hz, 17.14 Hz, or 20 Hz. Oscillation frequencies for the stimulus regions were chosen such that the refresh rate of the monitor was an integer multiple of each. As such, the period of each rectangular wave remained constant throughout the duration of the task. The 15 Hz and 20 Hz

stimuli both had a 50% duty cycle, while the 13.33 Hz and 17.14 Hz stimuli respectively had 55.56% and 57.14% duty cycles, because they both consisted of an odd number of refresh frames. During "off" phases, all four stimuli were black and indistinguishable from the background. During the "on" phases, the 15 Hz and 20 Hz stimuli were displayed as light grey, 75% of the maximum screen brightness. Average luminance was kept equal for all four regions by compensating the longer duty cycle stimuli with slight reductions in brightness during the "on" phases: the 13.33 and 17.14 Hz stimuli were displayed at 67% and 65% of the maximum screen brightness, respectively.

The experiment included passive viewing blocks as well as attention task blocks. Throughout the attention task blocks, red rectangular probe stimuli briefly appeared superimposed on top of the flickering regions, as in Figure 4.1. The frequency of these probes was shared between the two flickering regions on the same side of the central plus sign and was independent between the left side and the right side, such that probes occurred in one of the two stimulus regions for a given side with a uniformly randomized inter-stimulus interval between 1-5 seconds. Probe occurrences were equally likely between the two stimulus regions for either side. Probes had a width of 1º visual angle and a height of 4º visual angle. Probes were horizontally aligned with the center of the stimulus region above which they appeared, and probe position was randomized vertically, uniformly and continuously across pixels, such that the center of each probe was within 4º of the center of the stimulus region. Each probe remained visible for 100 ms.

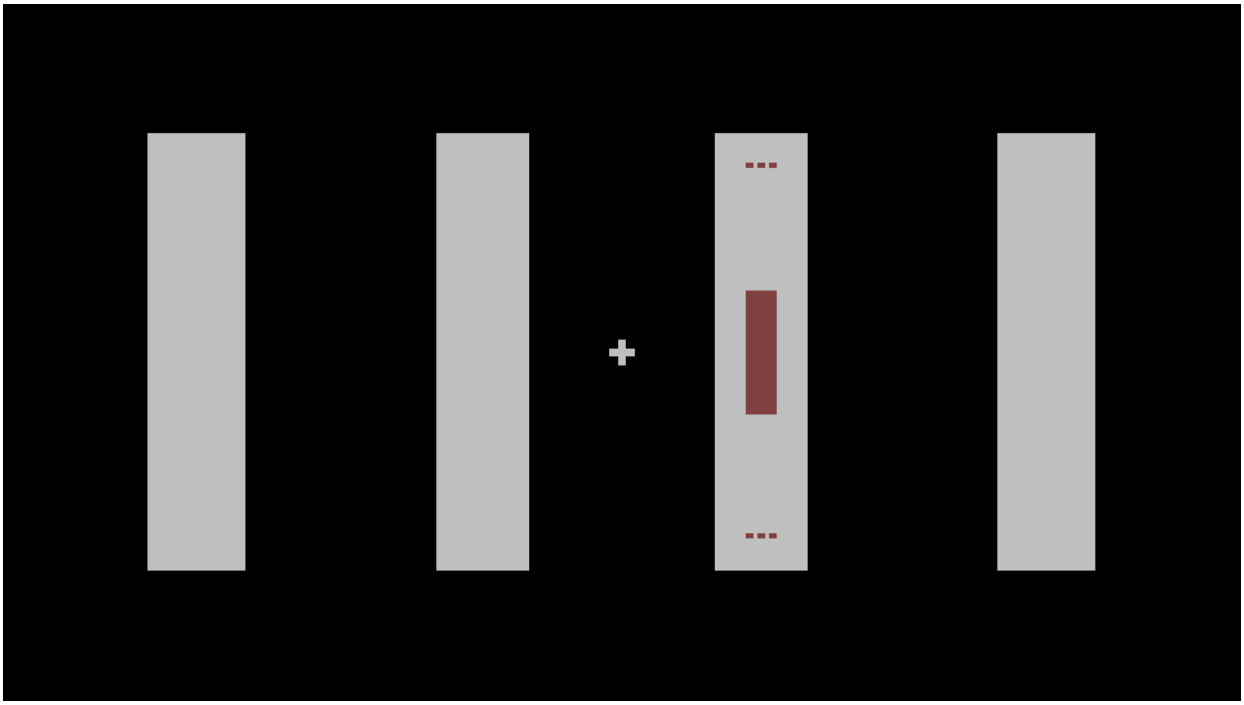

Figure 4.1. Four vertical bars flickered at unique frequencies. Subjects fixated on the static plus sign. During task blocks, red probes appeared over the flickering bars at randomized intervals. Probes occurred in the left pair of bars independently from the right pair (1-5 seconds per pair), and only one bar per pair displayed a probe at each occurrence. Probe positioning varied vertically: broken lines indicate the bounds of the upper and lower edges. RGB: (128, 64, 64).

Subjects received instructions to fixate on the central plus sign at all times throughout two 120-second passive viewing blocks followed by four 120-second attention task blocks. The frequencies of the four stimuli from left to right were 13.33 Hz, 17.14 Hz, 20 Hz, and 15 Hz in the first passive block and in the first and fourth task blocks. The order from left to right was 20 Hz, 15 Hz, 13.33 Hz, and 17.14 Hz in the second passive block and in the second and third task blocks, creating two configurations of four frequency-location pairs. Prior to each task block, an audio message cued subjects to attend either the left pair or the right pair of flickering regions without changing their gaze. Subjects were instructed to respond with the keyboard to the appearance of each probe in the attended regions while ignoring probes in opposite regions. The attended side alternated across the four task blocks, such that each frequency-location pair was attended once and ignored once. Subjects were told to respond as quickly as possible while

remaining accurate. Subject response times were monitored via Psychtoolbox in MATLAB and were inserted as event markers in the EEG recording.

Analyses

Temporal and spectral analyses on the EEG data were performed in MATLAB. First, the raw EEG data were segmented into the six blocks to allow further processing. The FFT was applied to the data from both of the passive blocks and from each of the four task blocks to obtain the power spectra at the O_Z electrode. The spectra from each block were inspected to assess the presence of SSVEP signals at each stimulus frequency. The spectral components at the four stimulus frequencies were then selected for comparison of SSVEP strength across blocks. Attentional modulation was calculated using the contrast between the attended and ignored blocks for each frequency-location pair, by dividing the difference of the two blocks by their sum. The average attentional contrast was calculated for each subject with error estimates generated through 1000 bootstrapped samples. Significance of the attention contrast values was assessed within each subject with a one-sample t-test.

To determine fluctuations in SSVEP magnitude over time within each block, a moving window FFT was applied to the raw EEG recording using 5-second Hanning windows at increments of 0.5 seconds. The changing power of the spectral components for the four stimulus frequencies in each window provided the four time series of SSVEP fluctuations. The correlation coefficients between the fluctuations in the four frequencies were calculated for passive and task blocks.

Correlation coefficients from the task blocks of both subjects were sorted into three groups to evaluate the similarity of fluctuations under shared conditions. An attend group and an ignore group were created using correlation coefficients calculated between fluctuations in the

two attended signals and between fluctuations in the two ignored signals; correlation coefficients calculated between one attended fluctuation and one ignored fluctuation were placed into the cross-condition group. The three groups of correlation coefficients were compared using two-sample t-tests to test the hypotheses that two attended signals or two ignored signals would show greater covariance than cross-condition pairs. The attend and ignore groups were compared directly to test for greater covariance between attended signals than between ignored signals.

Covariation also was compared between passive and task blocks with two-sample t-tests. The correlation coefficients from the passive blocks were divided into two groups. Correlations between both of the left fluctuations or both of the right fluctuations were placed into the same-side group, and correlation coefficients between one left fluctuation and one right fluctuation were sorted into the opposite-side group, analogous to the task cross-condition group. The task attend and ignore groups collectively were compared to the passive same-side group to test the hypothesis that the task same-condition group would show greater covariance than the passive same-side group. The task cross-condition group was compared to the passive opposite-side group to test the hypothesis that the task cross-condition group would show less covariance than the passive opposite-side group. Additionally, all of the correlation coefficients from the task blocks were compared to those of the passive blocks with a two-tailed two-sample t-test to determine whether the conditions varied at all.

Results

Spectral and topographic plots revealed prominent SSVEPs for the majority of frequencies and blocks, but signal strength varied substantially between blocks and subjects. The 17.14 Hz and 20 Hz signals were not at all discernible in two blocks from the second subject, and the first subject was missing a 20 Hz SSVEP in a single block. Figure 4.2 presents topographies

and spectra from several blocks as an indication of the range of signal quality. Table 4.1 lists the spectral power at the four stimulus frequencies in each block as well as the attentional contrast during the task blocks. Mean attentional contrast for subject 1 was 0.036 with a standard error of 0.060. Mean attentional contrast for subject 2 was -0.070 with a standard error of 0.12. Contrast was not found to be significantly greater than zero for either subject ($p = 0.30$ and $p = 0.69$ respectively). The variability in SSVEP quality may have contributed to the lack of attentional modulation.

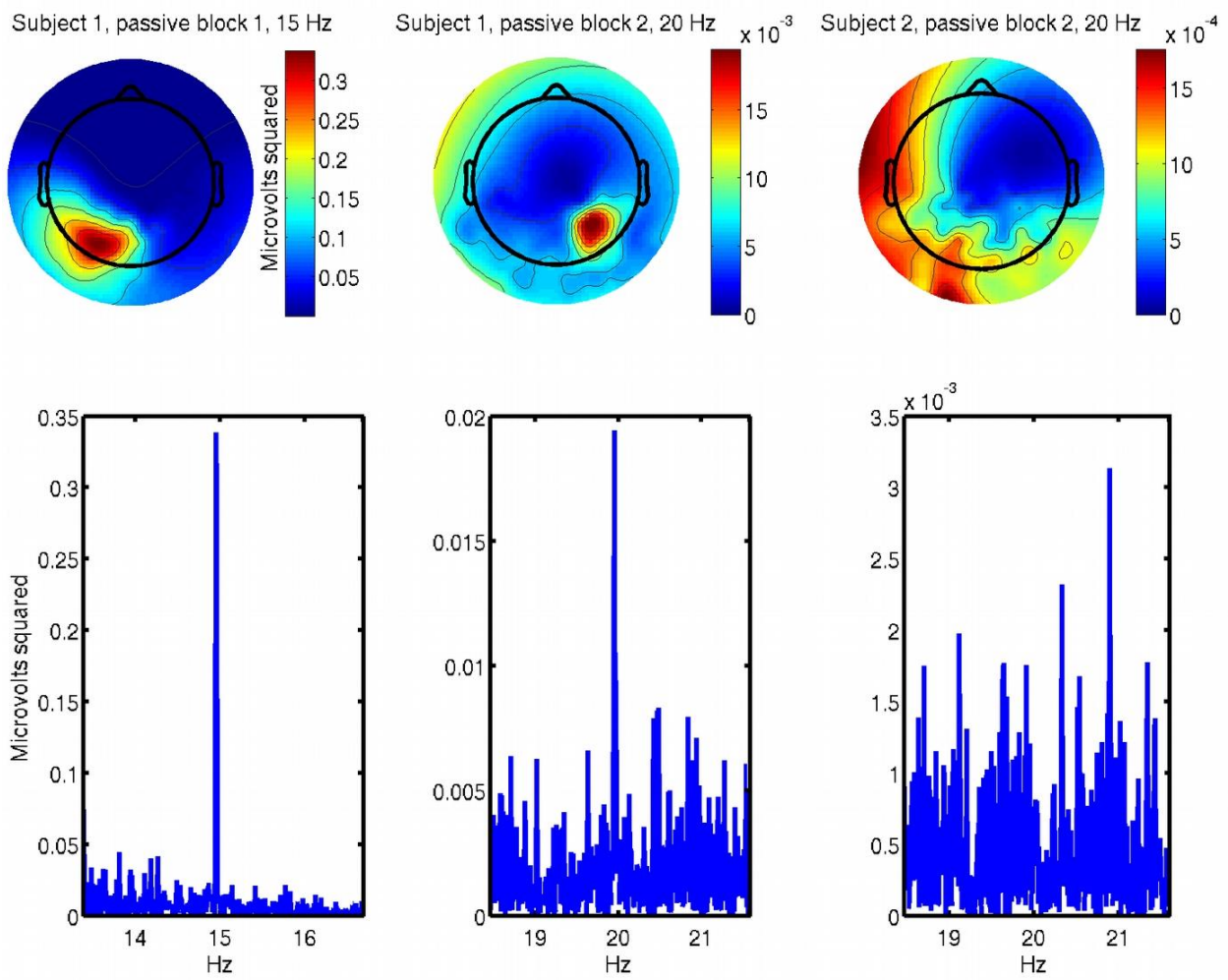

Figure 4.2. Topographic maps of SSVEP power and spectral plots illustrate the wide range of signal strength and quality. Most SSVEPs exhibited high SNR (left). Some SSVEPs, particularly those at higher frequencies, were reduced in magnitude but still quite evident (center). A small number of blocks had no apparent SSVEPs at one or both of the two highest frequencies (right)

Table 4.1
SSVEP Power (in microvolts squared) and Attention Contrast at Four Stimulus Frequencies

	Configuration 1				**Configuration 2**			
Subject 1	**13.33 Hz**	**17.14 Hz**	**20 Hz**	**15 Hz**	**20 Hz**	**15 Hz**	**13.33 Hz**	**17.14 Hz**
Passive	0.12	0.040	0.036	0.13	0.0063	0.25	1.1	0.02
Attend Left	0.073	0.14	0.066	0.11	0.0068	0.32	0.64	0.0094
Attend Right	0.11	0.11	0.074	0.14	0.0039	0.19	0.43	0.0074
Contrast	-0.19	0.11	0.053	0.096	0.27	0.26	-0.20	-0.12
	Configuration 1				**Configuration 2**			
Subject 2	**13.33 Hz**	**17.14 Hz**	**20 Hz**	**15 Hz**	**20 Hz**	**15 Hz**	**13.33 Hz**	**17.14 Hz**
Passive	0.043	0.098	0.0054	0.0013	0.00099	0.14	0.034	0.00098
Attend Left	0.017	0.045	0.0046	0.0064	0.0015	0.033	0.0056	0.00085
Attend Right	0.011	0.021	0.00085	0.0023	0.0017	0.061	0.012	0.00096
Contrast	0.19	0.36	-0.69	-0.47	-0.064	-0.29	0.35	0.061

Note. Each condition was presented for a single block, so standard error values do not exist.

Fluctuations in SSVEP power were substantial at all frequencies throughout both passive and task blocks, as illustrated in Figure 4.3, but the signals did not covary according to any aspect of the task. Comparisons between the three groups of correlation coefficients from the task blocks did not reveal any significant differences between the attend, ignore, or cross-condition groups, regardless of the groups compared or the electrodes chosen for assessment. Comparisons between the correlation coefficients of the task blocks and the values from the passive blocks also found no significant differences in all cases. The p-values of these tests are listed in Table 4.2. These results fail to identify attentional modulation as an important source of SSVEP fluctuations.

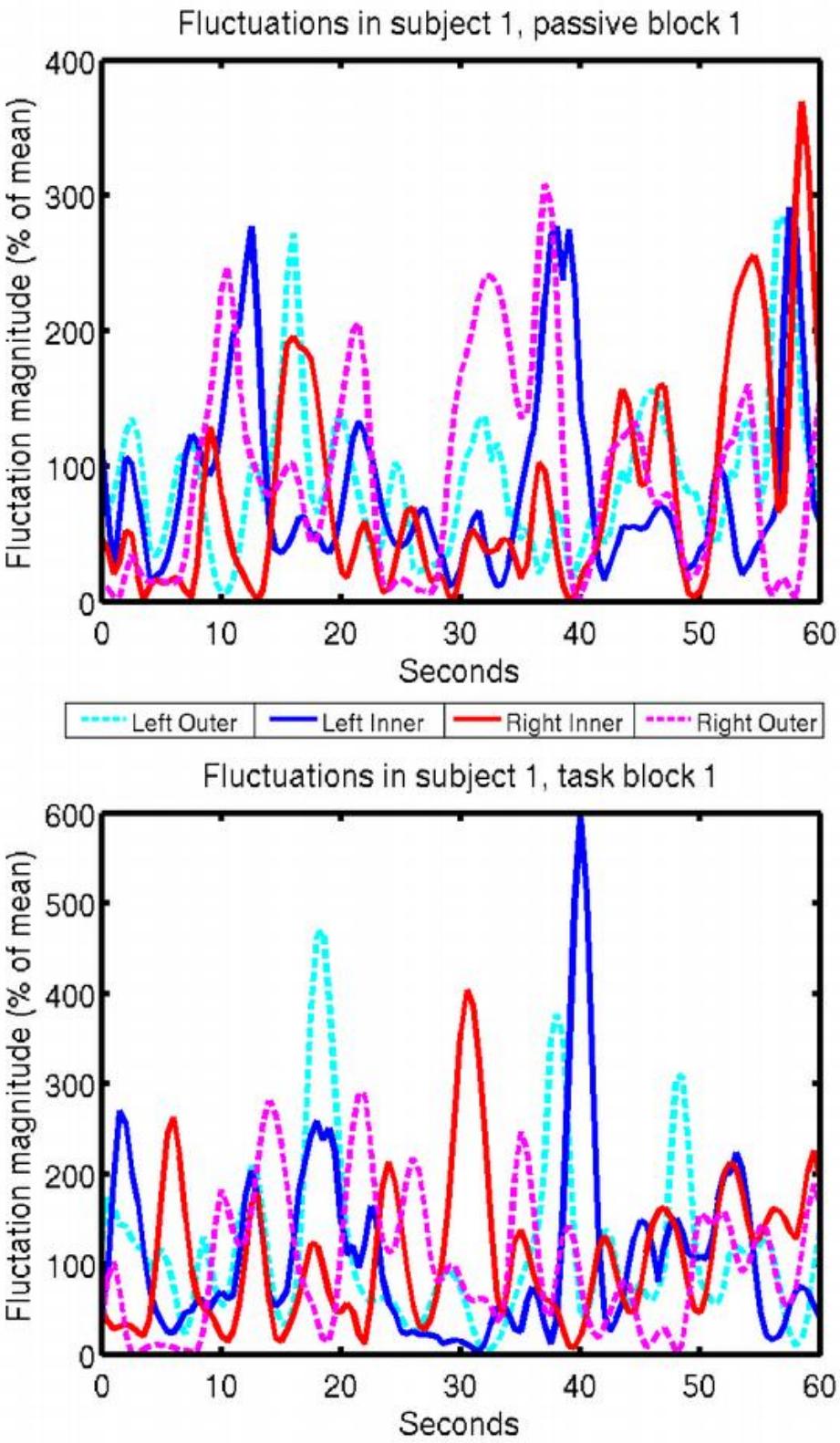

Figure 4.3. Fluctuations in four simultaneous SSVEPs. Fluctuations were comparable in passive blocks (top) and task blocks (bottom). Correlation between fluctuations was not greater during task blocks or in attended signals.

Table 4.2
p-values from Comparisons of Correlations between SSVEP Fluctuations

Comparison	p
Within-task: Attend vs Cross-condition	0.40
Within-task: Ignore vs Cross-condition	0.57
Within-task: Attend vs Ignore	0.80
Within-task: Attend and Ignore vs Cross-condition	0.34
Task Same-condition vs Passive Same-side	0.65
Task Cross-condition vs Passive Opposite-side	0.44
Task vs Passive Overall	0.63

Discussion

The lack of statistically significant SSVEP attentional modulation could suggest that the visual system may not be capable of enhancing multiple target regions simultaneously or of enhancing such a large portion of the visual field with the same degree of success as occurs in experiments with only a single attended stimulus region. Competition between the cortical activity driven by the two different attended stimulus frequencies could also diminish the entrainment at either frequency and therefore interfere with the SSVEP attention effect. Other researchers have reported difficulty in eliciting SSVEPs at more than two frequencies (Teng et al, 2010), although some BCI systems have been successful in distinguishing between 40 SSVEP targets of eight frequencies and five phase shifts using canonical correlation analysis applied to data from nine electrodes (Chen et al, 2014). Additionally, the presence of ignored distractor stimuli oscillating at somewhat similar frequencies may cause interference, especially from the ignored stimulus with a frequency between the two attended stimulus frequencies (for example, the 17.14 Hz signal when the 15 Hz and 20 Hz stimuli are being attended).

Failure to find any statistically significant differences between the attended, ignored, and cross-condition groups of correlation coefficients provides further evidence that generating an

SSVEP attention effect simultaneously in multiple attended and multiple ignored stimuli may not be possible, at least not with the effect size demonstrated in the enhancement and inhibition of individual SSVEP stimuli. Unfortunately, these null results could also indicate that attentional modulation simply does not have a strong influence on SSVEP fluctuations. The complete lack of significant differences between the correlation coefficients calculated in the task blocks and those from the passive blocks further demonstrates that attentional modulation of so many stimuli may exceed the capabilities of whatever mechanism by which the SSVEP attention effect appears in simpler designs.

While these results do not provide any clarification of the relationship between the block-wise SSVEP attention effect and slow fluctuations of SSVEP power throughout task performance, the difficulty in reproducing even the basic attention effect using this slightly more complicated design emphasizes the understated limitations of the SSVEP paradigm as a whole and confirms that the mechanisms and properties of the SSVEP signal have not yet been fully explored.

SSVEP Frequency Sweep: Demonstration of a Stimulus Device

Introduction

LCD monitors and other computer displays are a convenient approach to eliciting SSVEPs, but these devices can accurately generate stimuli for a limited number of frequencies and with substantial constraints on the shape of the waveform (Volosyak et al, 2009). Special techniques can expand the stimulus capabilities of computer displays (Nakanishi et al, 2013), but these methods are inherently imprecise and may negatively impact experimental outcomes (Szalowski and Picovici, 2015). The restrictions caused by frame rate are a significant shortcoming of commercial video products in SSVEP applications. The use of LCD monitors can be particularly problematic in the study of SSVEPs using concurrent fMRI and EEG, where large electronic devices pose safety concerns and introduce significant noise.

Frequency-dependent characteristics have been demonstrated in the mechanisms and effects of SSVEPs (Ding et al, 2006; Pastor et al, 2006). Exploring the influence of stimulus frequency on the strength, variability, and other properties of SSVEPs requires a method for precisely generating stimuli over a range of frequencies. To meet these requirements, a device was designed and constructed with the ability to modulate an LED with high precision at virtually any frequency between one flash per hour and tens of thousands of flashes per second. The capabilities of the device allow the flicker frequency to be varied continuously and arbitrarily throughout stimulation; this implementation permits many experimental designs that would not be possible using a monitor.

The following experiment illustrates the efficacy of a custom stimulus device when presenting a driving waveform that sweeps across a frequency range. The precision and stability of the device was validated using an oscilloscope prior to data collection. In addition to

demonstrating the new device, this study assesses the ability of a generated SSVEP to change frequency continuously while remaining distinguishable in the EEG. The quality of the resulting SSVEP signals will verify the feasibility of future research plans.

Methods

A single adult subject passively viewed a flickering stimulus while an Electrical Geodesics 256-channel EEG system recorded the subject's neural activity. The subject provided informed written consent prior to the experiment. The recording was taken using a 250 Hz sample rate in a room equipped with electromagnetic shielding to reduce EEG artifact. A custom electronic device, built using an Arduino UNO microcontroller, generated the stimulus by driving a white LED that projected a round light spot onto a screen made of white paper. The light spot was positioned 76 centimeters from the subjects with a diameter of 12 centimeters, corresponding to visual angle of approximately 9º.

Throughout the stimulus presentation, the LED underwent square wave oscillation with a 50% duty cycle. The frequency of the stimulus changed continually over two seven-minute blocks. The first block began with a frequency of 7 Hz and steadily increased to 17 Hz over seven minutes. The second block began at 17 Hz and decreased to 7 Hz. Two blocks were used to balance the order of the frequencies but not to compare results between increasing and decreasing sweeps. The two blocks were separated by a rest period, during which no stimuli were presented and no EEG data were collected. To maintain a 50% duty cycle at all times, changes to the stimulus frequency took place only between completed square wave periods. At the end of a full on/off cycle, the duration of the next square wave was calculated by the device firmware according to the progression through the block, with an average rate of change of 1.429 Hz per minute. For example, at the beginning of the first block, a single square wave was shown

for 142.86 milliseconds, corresponding to the 7 Hz start point. After the first complete cycle, the duration was updated to 138.81 milliseconds, corresponding to 7.2 Hz. The square wave duration was updated at the end of each complete period in this manner for the remainder of the block. Figure 4.4 illustrates this method at the beginning, middle, and end of the increasing frequency sweep.

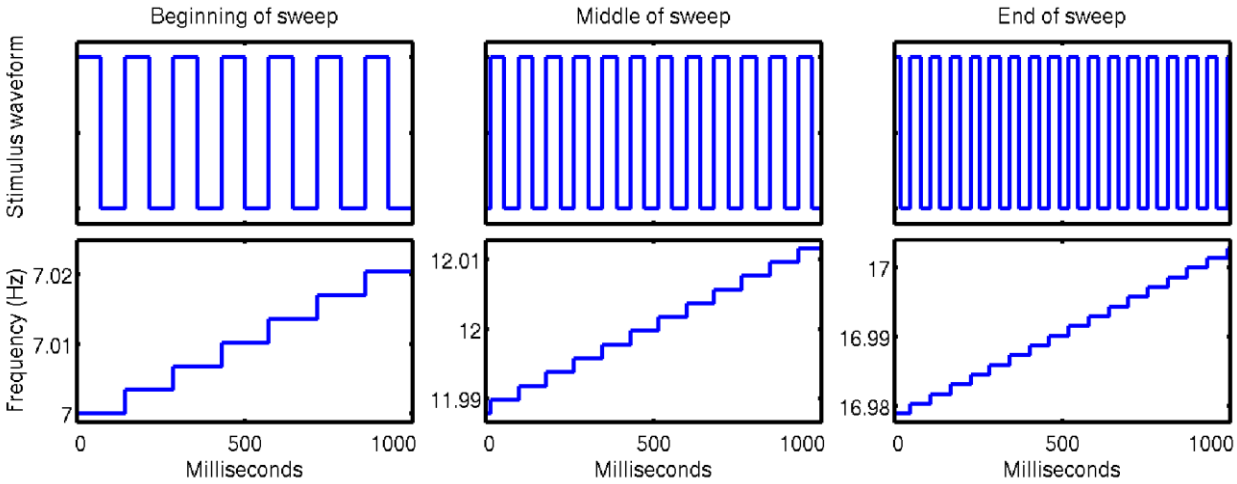

Figure 4.4. Increasing stimulus frequency over 1-second windows at three points in the sweep. Changes occurred more often and with finer resolution at faster stimulus frequencies, because updates were made at the end of each period.

Analyses

Spectral analyses on the EEG data were performed in MATLAB using the O_Z channel. First, the FFT of both stimulus blocks were calculated to determine the frequency at which the subject had the strongest alpha signal. Later analyses of changes in alpha power throughout the blocks were limited to a 1 Hz band around this peak frequency, because the stimulus was in the general alpha vicinity throughout most of the experiment. Next, each seven-minute stimulus block was divided into 28 non-overlapping 15-second segments using Hanning windows, and the FFT of each window was taken individually. Within each window, the mean power was calculated for the band corresponding to the range of stimulus frequencies presented during that

time. The presence of SSVEPs was determined for each window by comparing power in the stimulus band to power in the same frequency range in windows under different stimulus conditions (background power) using one-sample t-tests. To assess the presence of second harmonic SSVEP signals, the mean power at twice the stimulus frequency range was also calculated for each window (2f power) and compared to average power in that range during other windows, again using one-sample t-tests. Mean power in a 1 Hz band containing the subject's peak alpha frequency was calculated as well, to explore any possible relationship between stimulus frequency and enhancement or inhibition of alpha generation. Correlation was calculated between blocks in SSVEP power, 2f power, and alpha power to evaluate the consistency of the results (in relation to stimulus frequency, not time). Additional power spectra were generated after dividing each block into ten 42-second windows, for visualization of the SSVEPs across each sweep.

Results

Over the entirety of the two stimulus blocks, the subject exhibited the largest alpha signal between 9.5 Hz and 10.5 Hz, shown in Figure 4.5, so this band was chosen to assess the strength of alpha activity for individual stimulus windows. The spectra of the sliding windows revealed the presence of SSVEPs within the stimulus frequency bands, and significant increases in power were shown in all but a handful of windows in each block. Table 4.3 lists the mean SSVEP power during each 15-second window as well as the ratio of SSVEP power to background power. Figure 4.6 presents the spectra from the 42-second windows. SSVEP power, alpha power, and 2f power varied considerable across the range of stimulus frequencies. SSVEP power was significantly correlated between the two blocks ($R = 0.55$, $p = 0.0026$), as was 2f power ($R = 0.926$, $p = 1.6 \times 10^{-12}$), but alpha power was not significantly correlated ($R = 0.32$, $p = 0.10$).

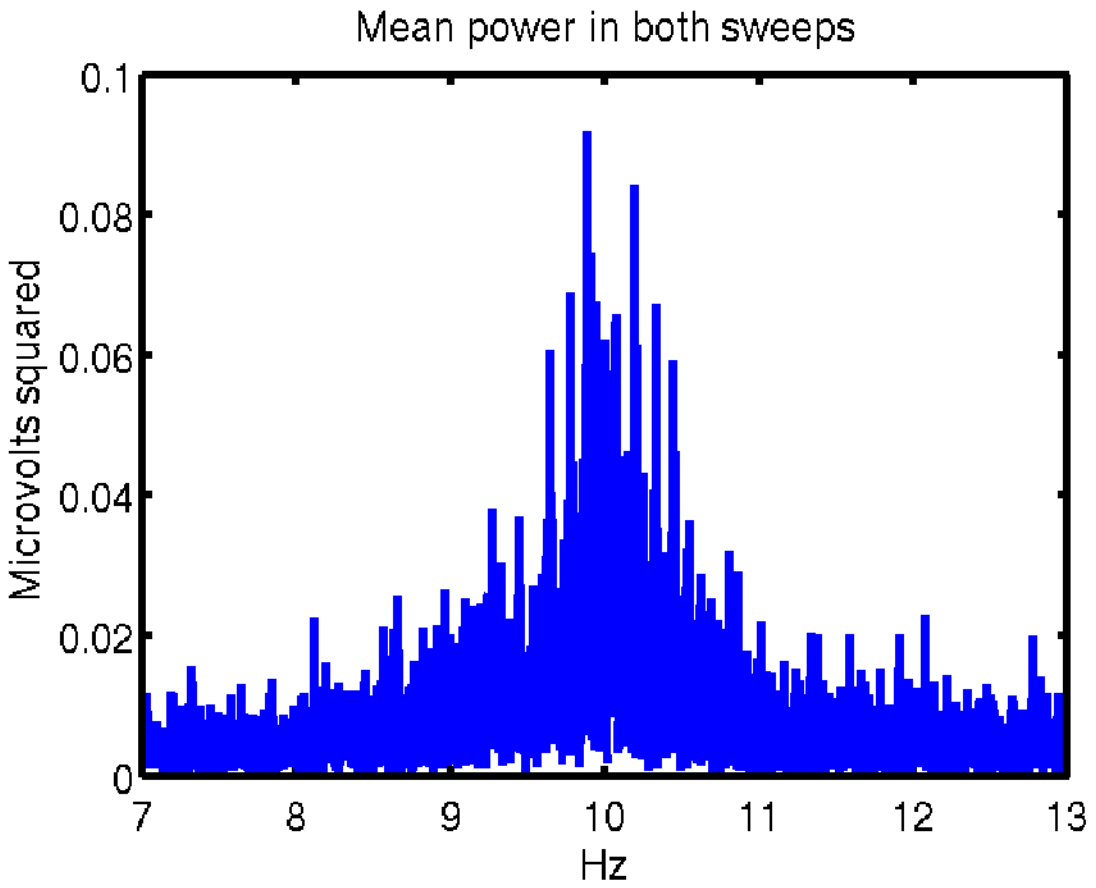

Figure 4.5. Average power in the alpha band across both stimulus sweeps.

Table 4.3
SSVEP Power and SSVEP/Background Power Ratio

Center Frequency	Power (Microvolts Squared)			SSVEP/Background Ratio		
	Sweep Up	Sweep Down	Mean	Sweep Up	Sweep Down	Mean
7.18 Hz	0.04	0.13	0.09	1.9	4.5	3.2
7.54 Hz	0.02	0.04	0.03	0.74	1.6	1.2
7.89 Hz	0.05	0.03	0.04	1.7	0.95	1.3
8.25 Hz	0.32	0.02	0.17	8.4	0.49	4.5
8.61 Hz	0.54	0.13	0.33	15	2.9	8.7
8.96 Hz	0.21	0.07	0.14	4	0.94	2.5
9.32 Hz	0.58	0.38	0.48	11	3.2	7.1
9.68 Hz	0.79	1.1	0.94	10	7.2	8.6
10.0 Hz	0.13	0.64	0.38	1.1	2.2	1.7
10.4 Hz	0.23	0.27	0.25	2.6	1.7	2.1
10.8 Hz	0.26	0.1	0.18	3.3	1.2	2.3
11.1 Hz	0.28	0.22	0.25	8.6	3.7	6.1
11.5 Hz	0.12	0.32	0.22	2.2	5.3	3.8
11.8 Hz	0.05	0.13	0.09	1	2.5	1.8
12.2 Hz	0.14	0.21	0.18	3.6	5	4.3
12.5 Hz	0.11	0.29	0.2	3	7.3	5.1
12.9 Hz	0.14	0.38	0.26	3.6	9.5	6.6
13.2 Hz	0.27	0.23	0.25	10	7.1	8.6
13.6 Hz	0.16	0.29	0.22	6.3	8.6	7.5
14.0 Hz	0.36	0.3	0.33	15	12	13
14.3 Hz	0.18	0.31	0.25	7.4	7.4	7.4
14.7 Hz	0.07	0.29	0.18	3.8	11	7.3
15.0 Hz	0.25	0.2	0.23	6.8	4.2	5.5
15.4 Hz	0.24	0.13	0.19	10	4.9	7.6
15.8 Hz	0.17	0.15	0.16	4.7	4.1	4.4
16.1 Hz	0.23	0.07	0.15	12	4	8.1
16.5 Hz	0.07	0.1	0.09	2.2	2.6	2.4
16.8 Hz	0.13	0.03	0.08	8.9	1.4	5.1

Note. Highlighted values indicate no significance ($p > 0.05$) using a one-sample t-test.

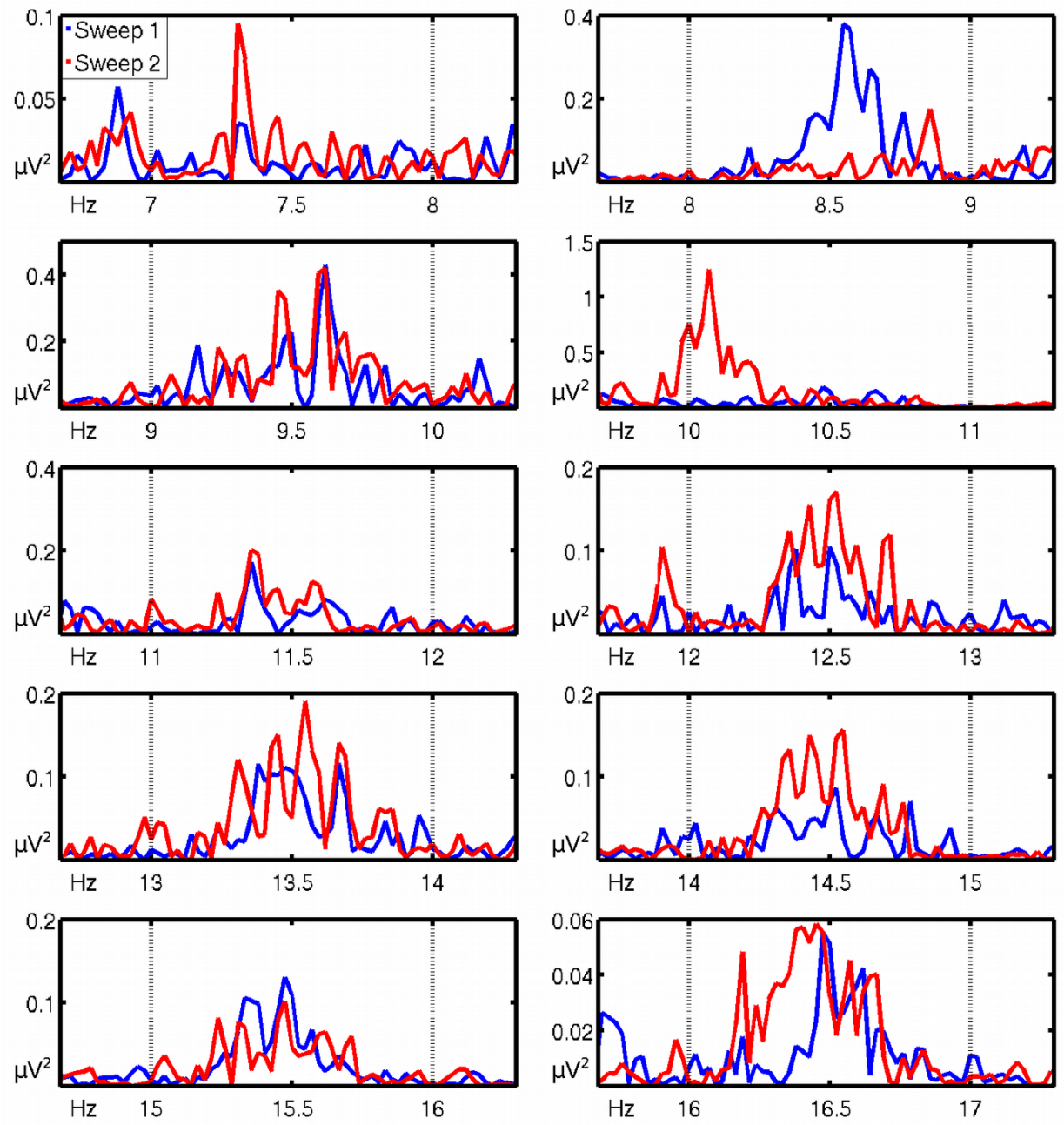

Figure 4.6. Power spectra calculated across 42-second windows. Stimulus frequency increased over the duration of sweep 1 (blue) and decreased over the duration of sweep 2 (red). Vertical broken lines mark the range of stimulus frequencies in each window.

Figure 4.7 demonstrates the relationships between stimulus frequency and SSVEP, alpha, and 2f power. Mean power in the stimulus band was greater during windows where the stimulus frequency was in the 8-12 Hz alpha range ($p = 0.0035$, two-sample t-test), but this was a result of

intrinsic alpha power, as there was no significant difference in the SSVEP to background ratio ($p = 0.90$, two-sample t-test). Mean alpha power between 9.5 Hz and 10.5 Hz increased for windows with stimulus frequencies between 10.5 Hz and 13.5 Hz relative to windows with stimulus frequencies outside of the 9.5-13.5 Hz range ($p = 2.6 \times 10^{-5}$, two-sample t-test). The asymmetry in this test was necessary to avoid confusing SSVEP and alpha power. Power at twice the stimulus frequency band was greatest for stimulus frequencies below 9 Hz, with and without incorporating the background ratio ($p = 1.3 \times 10^{-11}$ and 1.5×10^{-18}, two-sample t-test).

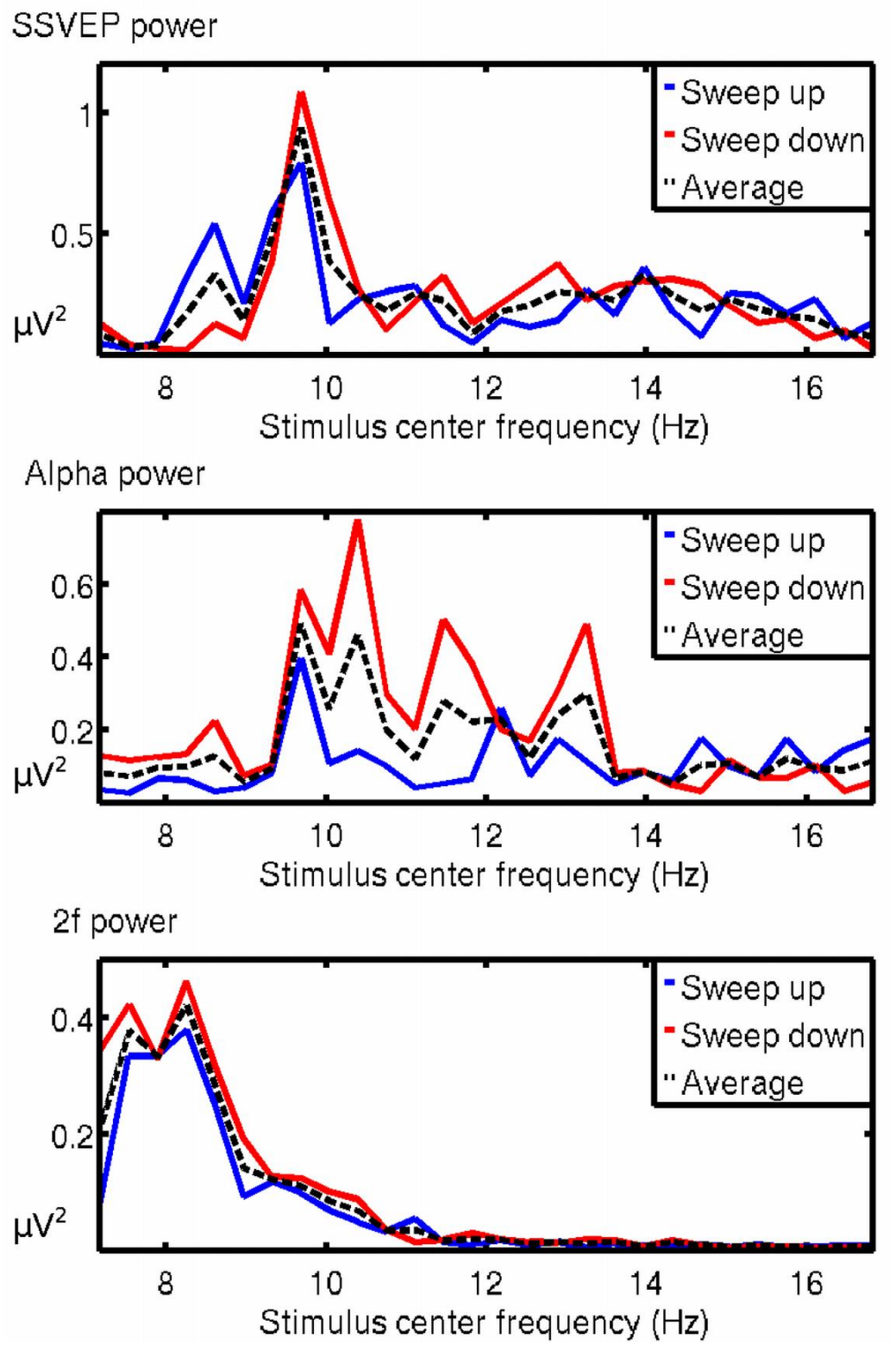

Figure 4.7. SSVEP power, alpha power, and 2f power with respect to stimulus frequency. Increased alpha power was exhibited when SSVEP frequencies were within the alpha range. SSVEP power peaked near the alpha maximum, but 2f power was greatest for stimulus frequencies below the alpha range.

Discussion

The presence of increased power within the appropriate spectral bands across the sliding windows demonstrates the ability to elicit responses that follow the driving frequency even without a truly periodic stimulus, although these nominal SSVEPs technically are not really in a "steady state", as the flicker frequency was not really stable. This result might suggest that neural entrainment can be adjusted continuously, such that intrinsic oscillations will align with the phase and frequency of a changing driving stimulus. However, this result could also indicate that the SSVEP signal arises from individual responses to each of a series of flashing stimuli, without the entrainment of intrinsic oscillations. Regardless of the underlying neural mechanisms, this experiment has illustrated the feasibility of generating continuously variable stimuli to drive responses measurable in EEG over a range of frequencies.

Prior to this study, the custom stimulus device had been validated in terms of waveform fidelity and accuracy, but this experiment was the first attempt at a practical demonstration. The dynamic range of the stimulus showcases the versatility of the system, and the consistency of results between the forward and reverse sweeps illustrates the precision of the implementation. This study could not have been conducted using an LCD monitor, and the performance of the device is merely a proof of concept that can be adapted to a number of potential experimental designs.

Effects of Duty Cycle and Luminance on SSVEP Characteristics

Introduction

One of the most useful SSVEP properties is that the frequency of the driving stimulus determines the fundamental frequency of the induced EEG signal (Regan, 1989). Many paradigms take advantage of this property to compare responses to stimuli over a range of frequencies or to distinguish between responses to multiple simultaneous stimuli based on frequency tagging. Eliciting SSVEPs at more than one frequency, either sequentially or concurrently, can introduce confounding variables when stimulus waveforms differ in ways other than frequency. For example, an experimental design that increases the presentation rate of light flashes without a proportional decrease in flash duration will cause an inverse relationship between duty cycle and frequency. Studies that vary the duty cycle of a stimulus as a result of altering its frequency do not typically address this confound (Pastor et al, 2003; Ding et al, 2006; Pastor et al, 2006). The relevance of changing the duty cycle or other parameters of the stimulus may not be readily apparent, particularly to application-oriented research, because the fundamental frequency of an elicited SSVEP matches the driving frequency regardless of these manipulations (Regan, 1989). However, experiments have shown that the duty cycle of a stimulus can affect SSVEPs in other ways. Stimuli with longer duty cycles have been found to increase the SNR of SSVEPs (Cecotti, 2010), and improvements to BCI accuracy have been demonstrated when using a 50% duty cycle square wave in comparison to rectangular waves with shorter duty cycles (Teng et al, 2011). While the fundamental frequency of an SSVEP will match the stimulus regardless of duty cycle, the number and strength of additional harmonic components are sensitive to duty cycle changes (Lee et al, 2011). These studies have illustrated that design choices such as stimulus duty cycle can have subtle consequences, but they primarily

pertained to BCI and were not without their own limitations.

Investigations into the effects of stimulus duty cycle (Cecotti, 2010; Lee et al, 2011; Teng et al, 2011) usually fail to mention another confounding factor: stimuli that differ in duty cycle will also differ in average luminance. For individual flashes, the perception of brightness depends on both the luminance and the duration of a flash (Stevens, 1966). If two periodic stimuli have the same luminance but unequal duty cycle conditions, then the stimulus with the longer duty cycle will emit more total light throughout a single period. This effect is particularly evident when subjects view the two stimuli simultaneously, because the stimulus with the longer duty cycle will be perceived as being brighter than the other. Even when stimuli are presented sequentially, differences in average luminance may influence subject perception or alter the elicited SSVEPs.

Better knowledge of the ramifications of certain design choices can improve future research methods and outcomes while also adding clarity to the interpretation of the existing SSVEP data. The primary objectives of this experiment were to determine whether interactions between stimulus duty cycle and average luminance are consequential to the strength and quality of SSVEPs and to assess whether this potential confound may have influenced the results of previous literature. This study explored the impact stimulus duty cycle and luminance on spectral and temporal characteristics of SSVEP signals. The implementation employed a single stimulus frequency and lacked an attention task as efforts to isolate the desired effects. The analyses provided a quantification of SSVEP variability introduced by adjustments to the driving waveforms, which was used to inform the development of the later multimodal imaging study. Drawing contrasts between the EEG responses to various distinct stimuli illustrated the subtle design considerations necessary to the development of truly controlled SSVEP experiments.

Methods

Ten adult subjects passively viewed a flickering stimulus while an Electrical Geodesics 256-channel EEG system recorded the subjects' neural activity. The recordings were taken using a 500 Hz sample rate in a room equipped with electromagnetic shielding to reduce EEG artifact. A custom electronic device, built using an Arduino UNO microcontroller, generated the stimulus by driving a white LED that projected a round light spot onto a screen made of white paper. The light spot was positioned 76 centimeters from the subjects with a diameter of 12 centimeters, corresponding to visual angle of approximately 9º. All subjects provided informed written consent prior to their participation.

Throughout the stimulus presentation, the LED underwent 10 Hz rectangular wave oscillation with a variety of values in two parameters: duty cycle and luminance. Duty cycle parameter values included 10%, 25%, 50%, and 75%, referring to the portion of each rectangular wave during which the LED was on. Luminance parameter values included 13.33%, 20%, 40%, and 100%, relative to the maximum brightness of the LED. All combinations of duty cycle and luminance values were displayed, resulting in sixteen distinct stimulus waveform conditions (Table 4.4). Parameter values were chosen to balance the average luminance, and therefore the stimulus brightness as perceived by the subject, across four of the conditions (increasing duty cycle matched with decreasing luminance). Luminance was controlled using pulse width modulation (PWM) of the active phase of the 10 Hz stimulus with a switching frequency of 326.8 Hz and pulse width increments of 12 microseconds. To achieve the desired precision, PWM was implemented through custom interrupt service routines triggered by hardware timers on the stimulus device rather than through the built-in PWM functionality.

Table 4.4
Matrix of Sixteen Conditions, One Block per Condition

		Luminance			
		13.33%	**20%**	**40%**	**100%**
Duty Cycle	**10%**	1	2	3	4
	25%	5	6	7	8
	50%	9	10	11	12
	75%	13	14	15	16

Note. Block numbers here are for organizational convenience. Presentation order was balanced across subjects.

Stimulus presentation occurred over sixteen 40-second blocks, with each block utilizing one of the sixteen waveform conditions. Stimulus blocks were separated by periods of rest lasting 25 seconds, and the presentation order of the sixteen conditions was balanced across subjects. The timings of the beginning and end of each stimulus block were inserted as event markers in the EEG recording, as were individual events for the onset and offset of each light flash making up the 10 Hz stimulus. The stimulus device communicated the event markers directly to the EEG recording system using transistor-transistor logic (TTL), providing a high degree of precision.

Analyses

Temporal and spectral analyses on the EEG data were performed in MATLAB, beginning with processing of the individual subject data. First, the EEG time series was band-pass filtered between 0.5 Hz and 55 Hz using a finite impulse response filter included in the EEGLAB toolbox (Delorme and Makeig, 2004). Next, the EEG time series was segmented into the sixteen 40-second blocks in preparation for further analyses. The FFT was applied to the unfiltered EEG time series from each of the sixteen blocks to obtain the power spectra for all electrodes not excluded in earlier steps. The O_Z spectral component at the 10 Hz stimulus frequency (the SSVEP power) was selected in each block for comparison of SSVEP strength

across conditions. The SSVEP signal-to-noise ratio (SNR) was calculated for each block by comparing SSVEP power to the mean power between 8 Hz and 12 Hz, excluding the band between 9.75 Hz and 10.25 Hz. Additionally, aggregate power over the first five harmonic frequencies (10 Hz to 50 Hz) was calculated for each block.

The effects of stimulus duty cycle and luminance on SSVEP power, SNR, and harmonic power were investigated in each subject via least-squares linear regression, using the stimulus parameter values as predictor variables of the SSVEP measures for each block. Duty cycle and luminance were tested individually as predictors of SSVEP power, SSVEP SNR, and aggregate harmonic power. Following the completion of individual analyses for all subjects, least-squares linear regression was repeated at the group level.

Further segmentation was then performed according to the flash onset event markers, splitting the filtered EEG data into periods of 100 ms containing the response potentials to each flash (SSVEP waveforms). The individual SSVEP waveform segments were gathered by block to allow comparisons according to stimulus parameters. For each subject, correlation coefficients were calculated between pairs of individual SSVEP waveforms that shared one parameter while differing in the other. For example, each individual waveform generated by the 10% duty cycle and 100% luminance stimulus was paired with each waveform generated during blocks with the same duty cycle but a different luminance. The correlation coefficients were then organized into two sets. One set contained all the correlation coefficients between any two individual SSVEP waveforms with the same stimulus duty cycle but different luminance values, and the other set contained all the correlation coefficients between any two individual SSVEP waveforms with the same stimulus luminance but different duty cycle values. The two sets were compared using a two-sample t-test of the hypothesis that stimuli with the same duty cycle would elicit SSVEP

waveforms with greater correlation than SSVEP waveforms elicited by stimuli with the same luminance.

Next, the individual SSVEP waveforms were averaged by block to create a mean SSVEP waveform for each block. Correlation coefficients were calculated between the mean SSVEP waveforms from each of the sixteen blocks within each subject. The values were sorted into three sets according to the shared stimulus parameters of the two blocks used in each calculation. One set contained all the correlation coefficients between blocks with the same stimulus duty cycle, and a second set contained all the correlation coefficients between blocks with the same stimulus luminance. Correlation coefficients from blocks that differed in both duty cycle and luminance (such as one block with 10% duty cycle and 100% luminance and another block with 25% duty cycle and 40% luminance) were placed into a third control set. The correlation coefficients from the duty cycle, luminance, and control sets were compared using two-sample t-tests, with the hypotheses that the shared duty cycle and shared luminance sets would both have greater correlation than the control set and that the shared duty cycle set would have greater correlation than the shared luminance set. Following the completion of individual analyses for all subjects, the sets were combined across subjects, and the statistical tests were repeated at the group level. Note that the three sets of correlation coefficients were combined across subjects, but the calculations of the correlation coefficients were only performed between two mean SSVEP waveforms from the same subject.

The Fourier spectra of two rectangular waveforms with the same frequency but different duty cycle values will exhibit disparity in the magnitude and phase of their frequency components. Phase changes in a Fourier spectrum are equivalent to shifts in the temporal domain (Ziemer et al, 1998), so the mean SSVEP waveforms were analyzed to determine the extent to

which correlation would increase as a result of circular shifts of one of the two waveforms. Each of the mean SSVEP waveforms from blocks with 25%, 50%, and 75% duty cycles were shifted to determine the time delay resulting in maximum correlation with the corresponding mean SSVEP waveform having a 10% duty cycle and the same luminance. The shifts providing maximum correlation were collected from all subjects and grouped according to the duty cycle of the shifted waveforms. Mean and standard error values were calculated for each duty cycle, and the distributions were compared against a null hypothesis of uniform distribution using chi-square goodness of fit tests. The increased correlation coefficients were compared against the correlations between waveforms with shared duty cycle using a two-sample t-test. As changes in luminance should not alter the Fourier spectra of the SSVEPs, these analyses were not performed with respect to the luminance parameter.

Results

Spectral plots of the FFT data revealed consistent SSVEP signals precisely at the 10 Hz stimulus frequency with the exception of a few blocks, particularly for a single subject. Figure 4.8 illustrates the range of the quality of the spectra. Topographic maps of the SSVEP power confirmed that occipital and parietal electrodes exhibited the greatest SSVEP strength, as shown by the group average in Figure 4.9.

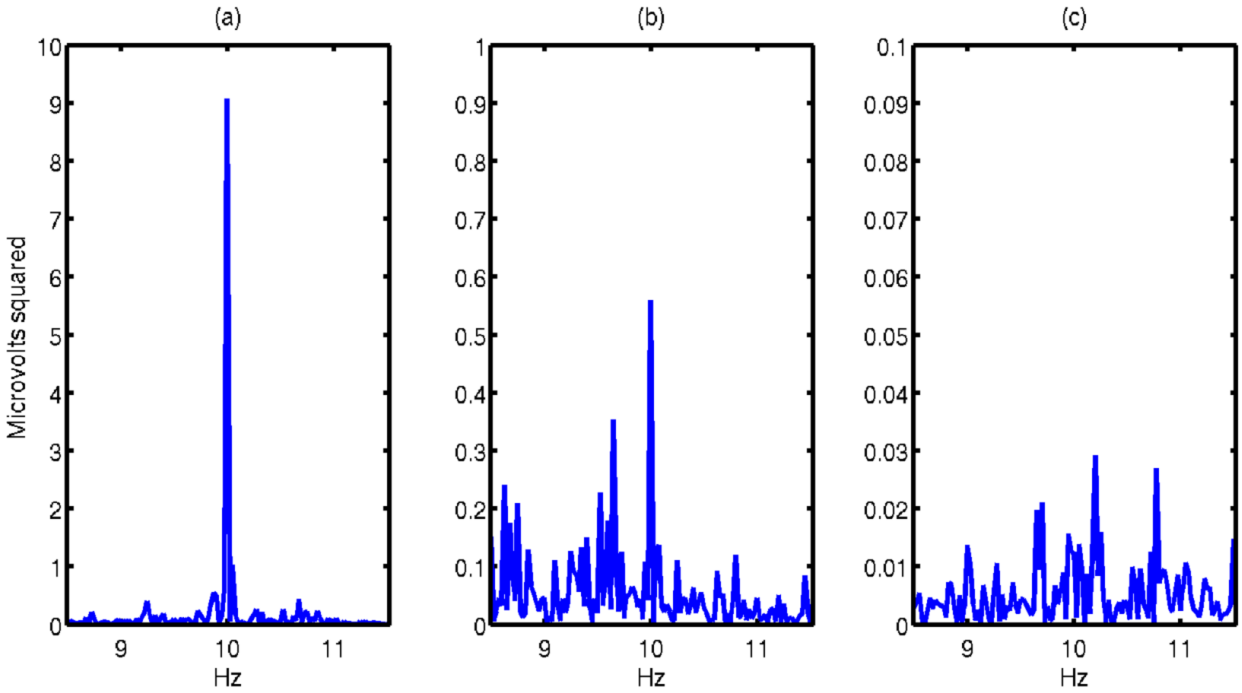

Figure 4.8. Spectra near the SSVEP frequency. Analyses of most blocks revealed SSVEPs with high SNR (a). Some blocks had evident but weaker SSVEPs (b), and a few blocks lacked detectable peaks (c).

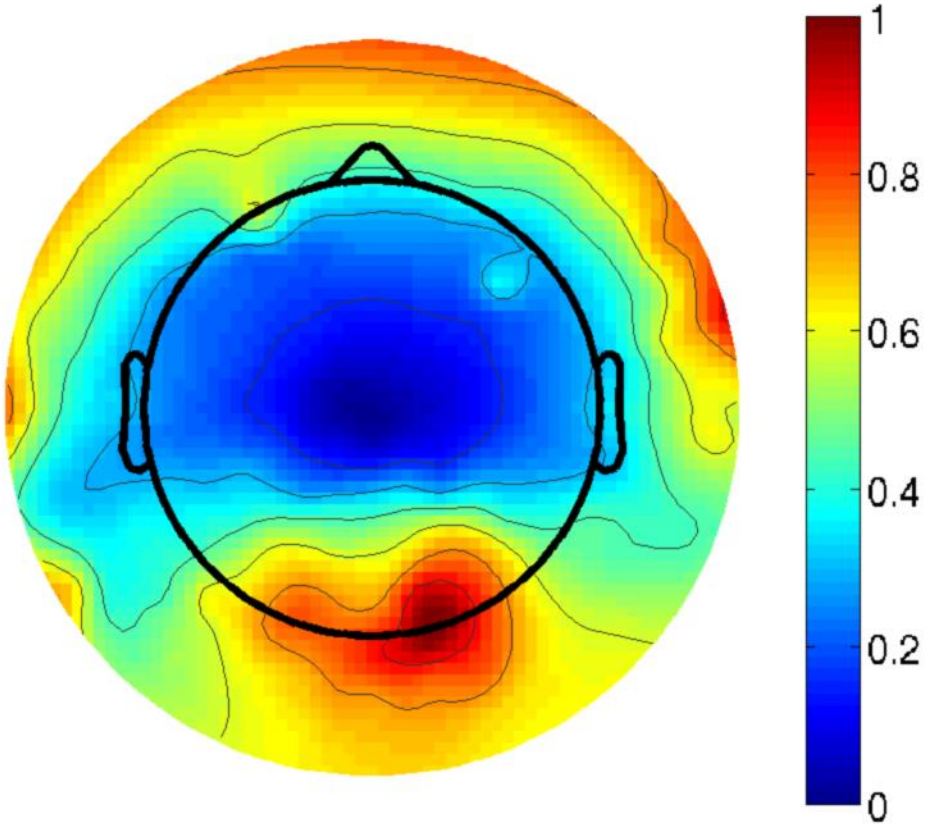

Figure 4.9. Topography of spectral power at the driving frequency, averaged across subjects and blocks after normalizing within subjects.

Table 4.5 presents the mean power and SNR of the SSVEP signals, as well as the mean aggregate harmonic power, for each subject at the O_Z electrode. Standard error values were calculated using bootstrapped sampling over 1000 iterations.

Table 4.5
SSVEP Measurements for Each Subject, Mean and Standard Error across Blocks

Subject	SSVEP Power	SSVEP SNR	Aggregate Harmonic Power
1	2.2 ± 0.59	37 ± 9.9	2.9 ± 0.72
2	0.30 ± 0.041	6.1 ± 1.1	0.45 ± 0.070
3	0.31 ± 0.10	27 ± 4.9	0.34 ± 0.11
4	2.3 ± 0.28	62 ± 7.8	4.5 ± 0.47
5	0.66 ± 0.15	57 ± 15	0.84 ± 0.16
6	0.26 ± 0.064	36 ± 6.0	0.33 ± 0.062
7	1.3 ± 0.21	150 ± 20	1.4 ± 0.21
8	5.6 ± 0.61	370 ± 45	6.2 ± 0.65
9	0.54 ± 0.068	14 ± 2.0	4.2 ± 0.48
10	0.87 ± 0.14	77 ± 14	1.4 ± 0.13

Power, SNR, and aggregate harmonic power for each block are listed in Tables 4.6, 4.7, and 4.8. Of the ten subjects, three subjects exhibited high-SNR SSVEPs (SNR above 10) across all 16 blocks, and another five subjects exhibited high-SNR SSVEPs in all but a one or two blocks. One subject exhibited high-SNR SSVEPs in ten blocks, and another subject exhibited SSVEPs of high SNR in only three blocks. SSVEP power was still calculated for blocks without clear peaks at the stimulus frequency, due to the consistency in frequency of the evident peaks.

Table 4.6
SSVEP Power per Block for Each Subject in Microvolts Squared

	Sbj. 1	**2**	**3**	**4**	**5**	**6**	**7**	**8**	**9**	**10**
Block 1	1.5	0.17	0.24	1.6	1.4	0.24	2.5	7.5	0.56	0.043
2	1.8	0.19	0.88	3.8	0.23	0.23	2.0	7.2	0.94	0.94
3	1.3	0.35	0.10	0.91	0.56	0.28	1.7	9.0	0.15	0.59
4	9.1	0.47	1.7	2.4	1.2	0.37	1.3	8.0	0.16	0.32
5	2.5	0.42	0.075	0.88	2.0	0.016	3.3	5.7	0.84	0.28
6	2.4	0.69	0.042	3.0	0.35	0.14	1.2	9.0	0.54	0.36
7	1.2	0.52	0.18	2.2	0.23	0.04	1.1	3.5	0.50	0.90
8	0.29	0.16	0.14	1.5	0.23	0.16	1.3	8.5	0.47	1.4
9	8.0	0.16	0.42	3.8	1.9	0.10	0.46	3.6	0.40	0.20
10	2.1	0.063	0.30	2.7	0.30	0.29	0.67	7.0	0.70	1.1
11	0.72	0.10	0.065	1.9	0.22	0.50	1.5	5.7	1.2	1.4
12	1.4	0.37	0.090	0.84	0.16	0.077	0.83	4.8	0.67	1.9
13	0.86	0.11	0.21	5.1	0.36	0.19	0.86	2.1	0.35	1.8
14	0.87	0.29	0.13	2.3	0.034	0.039	0.68	3.7	0.64	0.95
15	0.32	0.39	0.10	2.0	0.25	0.43	0.29	2.3	0.35	1.2
16	0.80	0.32	0.31	2.0	1.2	1.1	0.55	2.6	0.21	0.60

Note. Block numbers correspond to Table 4.4. Actual block presentation order was balanced across subjects.

Table 4.7
SSVEP SNR per Block for Each Subject

	Sbj. 1	**2**	**3**	**4**	**5**	**6**	**7**	**8**	**9**	**10**
Block 1	23	3.9	13	38	140	35	310	330	12	3.9
2	16	2.8	39	100	21	25	220	290	21	120
3	21	6.3	24	30	43	46	180	540	3.3	44
4	150	7.5	88	54	87	38	170	390	8.4	30
5	55	14	12	21	130	3.2	320	380	35	19
6	47	13	17	97	37	33	180	760	17	41
7	12	16	47	58	26	13	130	340	9.0	62
8	5.3	2.4	12	52	12	28	140	620	15	90
9	110	3.9	32	85	200	13	43	210	7.6	16
10	55	1.3	48	64	22	47	88	620	18	91
11	14	4.5	5.3	58	11	83	200	320	23	140
12	25	6.0	12	23	15	16	84	410	19	190
13	18	1.7	18	140	39	28	90	77	11	140
14	14	7.2	28	67	3.7	9.5	92	360	16	86
15	6.8	3.6	15	57	18	69	38	140	6.2	90
16	18	4.0	18	45	94	90	79	210	5.6	62

Note. Block numbers correspond to Table 4.4. Actual block presentation order was balanced across subjects.

Table 4.8
Aggregate Harmonic Power per Block for Each Subject in Microvolts Squared

	Sbj. 1	**2**	**3**	**4**	**5**	**6**	**7**	**8**	**9**	**10**
Block 1	2.0	0.27	0.26	2.9	1.5	0.32	2.8	8.6	2.9	0.84
2	2.6	0.22	0.93	5.0	0.30	0.24	2.3	7.9	8.4	1.6
3	2.8	0.37	0.12	2.8	0.60	0.35	1.8	9.9	2.9	0.85
4	10	0.61	1.8	3.7	1.2	0.38	1.6	8.7	3.2	0.56
5	2.7	0.52	0.11	2.5	2.2	0.12	3.6	6.5	5.4	0.92
6	2.7	1.2	0.049	5.7	0.40	0.30	1.2	9.6	4.6	1.8
7	2.0	1.1	0.22	5.2	0.33	0.21	1.2	3.9	4.5	1.4
8	1.3	0.19	0.17	2.9	0.34	0.20	1.4	9.2	6.4	1.7
9	9.7	0.43	0.44	7.1	2.1	0.21	0.64	4.0	3.1	1.2
10	2.3	0.37	0.32	4.8	0.62	0.41	0.82	7.7	6.7	2.1
11	1.3	0.16	0.099	4.5	0.72	0.55	1.6	6.4	5.2	1.6
12	2.0	0.44	0.11	5.3	0.19	0.14	0.92	5.3	4.6	2.2
13	1.3	0.16	0.23	8.8	0.97	0.21	1.0	2.3	2.3	2.2
14	1.3	0.38	0.15	5.7	0.23	0.043	0.94	4.2	3.7	1.2
15	0.73	0.42	0.12	2.8	0.46	0.46	0.37	2.4	1.9	1.3
16	1.8	0.16	0.42	3.8	1.9	0.10	0.46	3.6	0.94	0.36

Note. Block numbers correspond to Table 4.4. Actual block presentation order was balanced across subjects.

Linear regression analyses on the individual subject data did not reveal many significant relationships between the stimulus parameters and the SSVEP measurements. Results of regression of stimulus duty cycle on SSVEP power, SSVEP SNR, and aggregate harmonic power are shown in Table 4.9. In two subjects, duty cycle was found to be a significant predictor of SSVEP power, SNR, and aggregate harmonic power. The magnitude of the regression coefficients and the R-squared statistics were quite low, even among subjects with significant p-values. Linear regression of stimulus luminance on SSVEP measures revealed significant relationships in only a single subject, as can be seen in Table 4.10. This subject was not one of the two subjects with significant results in the analyses of duty cycle. The results of linear

regression performed using data from all subjects are included in Tables 4.9 and 4.10 as well. Duty cycle was a significant predictor only of aggregate harmonic power across subjects, but the regression coefficient and the R-squared value were close to zero. Luminance was not a significant predictor of any SSVEP measures at the group level.

Table 4.9
Linear Regression per Subject: Duty Cycle as a Predictor of Three SSVEP Measures

	Regressand: Power			**Regressand: SNR**			**Regressand: Aggregate Harmonic Power**		
Sbj.	**β**	**R^2**	**p**	**β**	**R^2**	**p**	**β**	**R^2**	**p**
1	-0.029	0.082	0.28	-0.40	0.066	0.34	-0.036	0.10	0.22
2	-0.0016	0.058	0.37	-0.057	0.11	0.22	-0.0028	0.060	0.36
3	-0.0062	0.13	0.17	-0.26	0.099	0.24	-0.0065	0.14	0.15
4	0.012	0.068	0.33	0.31	0.059	0.36	0.022	0.096	0.24
5	-0.0053	0.044	0.43	-0.41	0.032	0.51	-0.0018	0.0051	0.79
6	0.0032	0.10	0.23	0.30	0.088	0.26	0.0025	0.070	0.32
7	-0.021	0.47	0.0035	-2.4	0.51	0.0019	-0.023	0.46	0.0041
8	-0.078	0.67	0.00012	-3.5	0.24	0.054	-0.087	0.68	0.000086
9	-0.00064	0.0033	0.83	-0.044	0.019	0.61	-0.034	0.20	0.082
10	0.011	0.23	0.060	0.90	0.19	0.096	0.0056	0.072	0.31
All	-0.012	0.021	0.066	-0.56	0.012	0.16	-0.016	0.026	0.043

Note. Highlighted values indicate significance.

Table 4.10
Linear Regression per Subject: Luminance as a Predictor of Three SSVEP Measures

	Regressand: Power			**Regressand: SNR**			**Regressand: Aggregate Harmonic Power**		
Sbj.	**β**	**R^2**	**p**	**β**	**R^2**	**p**	**β**	**R^2**	**p**
1	0.015	0.041	0.45	0.23	0.042	0.44	0.014	0.029	0.53
2	-0.0015	0.086	0.27	-0.0048	0.0014	0.89	-0.0013	0.026	0.55
3	-0.0016	0.018	0.62	-0.12	0.041	0.45	-0.0016	0.017	0.63
4	0.013	0.15	0.14	0.28	0.096	0.24	0.019	0.14	0.16
5	0.011	0.36	0.013	1.1	0.44	0.0053	0.013	0.48	0.0028
6	-0.0027	0.14	0.16	-0.32	0.19	0.087	-0.0025	0.13	0.18
7	0.0087	0.15	0.14	0.77	0.10	0.23	0.010	0.17	0.11
8	-0.011	0.027	0.54	-1.7	0.10	0.23	-0.010	0.018	0.62
9	0.00087	0.012	0.69	0.057	0.061	0.35	-0.0047	0.0072	0.75
10	-0.0054	0.11	0.20	-0.53	0.13	0.18	0.00011	0.000056	0.98
All	0.0010	0.0019	0.58	-0.0077	0.000029	0.95	0.0014	0.0024	0.54

Note. Highlighted values indicate significance.

Correlation coefficients between individual 100-ms SSVEP waveforms differed when sorting by duty cycle and by luminance. Table 4.11 lists the mean and standard error (via 1000 bootstrapped samples per subject) of the correlation coefficients in the two parameter sets as well as the difference between the sets. Correlations between individual waveforms with the same duty cycle were significantly stronger than correlations between individual waveforms with the same luminance ($p < 10^{-10}$ for every subject using two-sample t-tests), confirming the hypothesis.

Table 4.11
Correlation between Individual Event Responses Grouped by Parameters

Subject	Shared Duty Cycle	Shared Luminance	Duty Cycle - Luminance
1	0.069 ± 0.00025	-0.017 ± 0.00025	0.090
2	0.0038 ± 0.00022	-0.0019 ± 0.00022	0.0057
3	0.033 ± 0.00026	-0.016 ± 0.00026	0.049
4	0.12 ± 0.00023	-0.039 ± 0.00024	0.16
5	0.020 ± 0.00022	-0.017 ± 0.00022	0.037
6	0.055 ± 0.00022	-0.017 ± 0.00022	0.072
7	0.082 ± 0.00018	0.0025 ± 0.00018	0.079
8	0.25 ± 0.00018	-0.033 ± 0.00020	0.28
9	0.12 ± 0.00021	-0.040 ± 0.00021	0.16
10	0.15 ± 0.00024	-0.038 ± 0.00024	0.19

Note. Differences were significant in all subjects.

Temporal averaging of the individual event responses for each block generated SSVEP waveforms with shapes and features that varied between subjects and that varied within subjects between conditions. The averaged waveforms from each block within a single example subject are plotted in Figure 4.10.

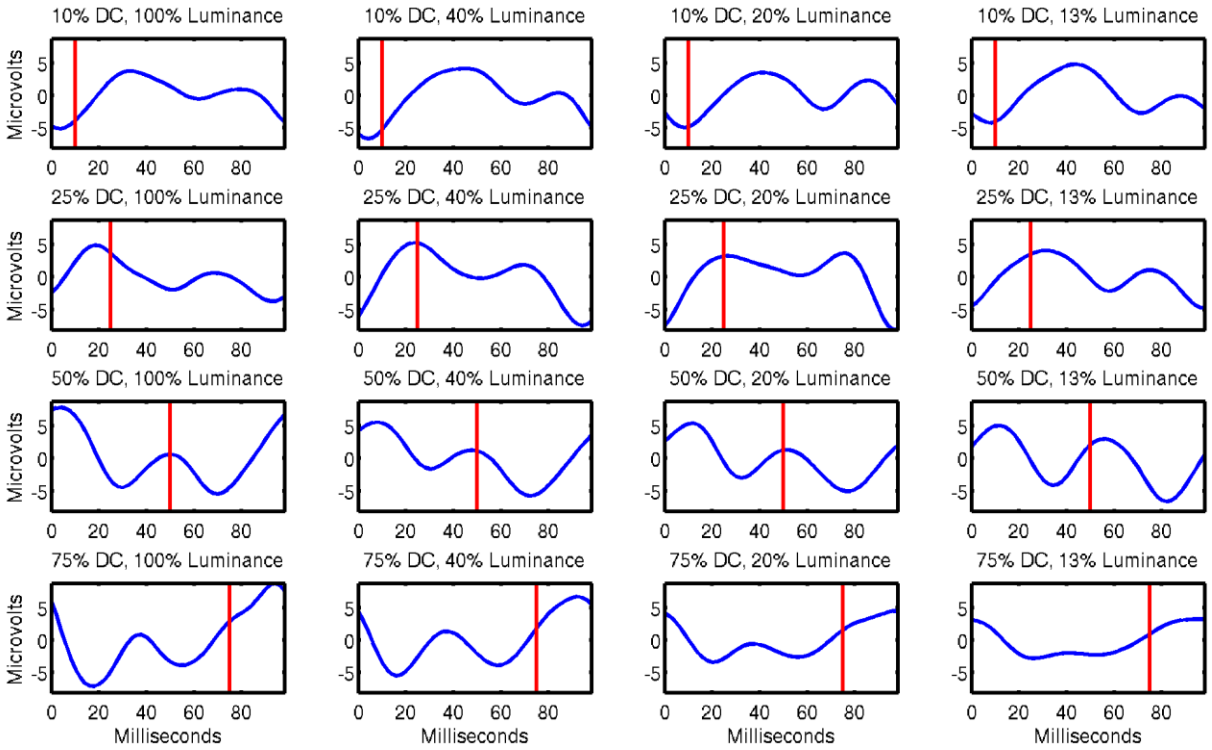

Figure 4.10. Averaged SSVEP waveforms of each block from subject 4. Stimulus onset begins at 0 ms; stimulus offset is denoted by the vertical red line. Each row contains a single duty cycle value, and each column contains a single luminance value.

Correlation coefficients were higher between averaged SSVEP waveforms than between individual waveforms, as an expected consequence of noise reduction. Tables 4.11 and 4.12 present these correlation results for each subject organized by the parameters shared between blocks, and Table 4.13 presents the correlation results for the control set. Table 4.13 also includes the p-values of the two-sample t-tests for each subject. In all ten of the subjects, correlation coefficients between averaged waveforms with the same duty cycle were shown to be significantly greater than those in the control group using two-sample t-tests. Correlation coefficients in the duty cycle set were significantly greater than those in the luminance set for nine of the subjects. The luminance set was not found to be significantly different from the control set in any of the subjects. Averages across subjects of the correlation coefficients and the

relevant p-values are included also in Tables 4.12 through 4.14. Two-sample t-tests using data from all subjects confirmed that correlation coefficients in the duty cycle set were significantly greater than those both in the control set and in the luminance set. The luminance set was not significantly greater than the control set.

Table 4.12
Correlation between Averaged Waveforms with Shared Duty Cycle

	Shared Duty Cycle Correlation			
Sbj.	**10%**	**25%**	**50%**	**75%**
1	0.36 ± 0.16	0.69 ± 0.061	0.79 ± 0.047	0.64 ± 0.10
2	0.025 ± 0.27	0.13 ± 0.29	0.11 ± 0.18	0.32 ± 0.22
3	0.41 ± 0.22	0.23 ± 0.23	0.75 ± 0.057	0.32 ± 0.21
4	0.87 ± 0.024	0.78 ± 0.05	0.77 ± 0.070	0.87 ± 0.041
5	0.31 ± 0.22	0.32 ± 0.17	0.23 ± 0.25	0.18 ± 0.22
6	0.83 ± 0.040	0.57 ± 0.11	0.88 ± 0.029	0.75 ± 0.086
7	0.82 ± 0.047	0.79 ± 0.042	0.84 ± 0.034	0.51 ± 0.16
8	0.99 ± 0.0026	0.98 ± 0.0049	0.84 ± 0.059	0.75 ± 0.086
9	0.81 ± 0.064	0.71 ± 0.084	0.70 ± 0.090	0.59 ± 0.12
10	0.68 ± 0.081	0.60 ± 0.13	0.72 ± 0.083	0.84 ± 0.048
All	0.61 ± 0.055	0.58 ± 0.055	0.66 ± 0.046	0.58 ± 0.051

Table 4.13
Correlation between Averaged Waveforms with Shared Luminance

	Shared Luminance Correlation			
Sbj.	**13.33%**	**20%**	**40%**	**100%**
1	-0.082 ± 0.18	-0.26 ± 0.19	-0.07 ± 0.18	-0.23 ± 0.16
2	0.34 ± 0.16	-0.13 ± 0.16	-0.24 ± 0.25	0.10 ± 0.20
3	-0.21 ± 0.22	-0.09 ± 0.28	-0.31 ± 0.31	-0.32 ± 0.26
4	-0.28 ± 0.18	-0.22 ± 0.16	-0.28 ± 0.15	-0.27 ± 0.17
5	-0.15 ± 0.20	-0.22 ± 0.19	-0.22 ± 0.26	-0.033 ± 0.22
6	-0.28 ± 0.15	-0.25 ± 0.13	-0.18 ± 0.19	-0.22 ± 0.26
7	-0.13 ± 0.22	-0.17 ± 0.20	0.28 ± 0.21	0.071 ± 0.22
8	-0.28 ± 0.20	-0.21 ± 0.25	-0.20 ± 0.25	-0.058 ± 0.28
9	-0.22 ± 0.20	-0.23 ± 0.18	-0.25 ± 0.17	-0.17 ± 0.19
10	-0.082 ± 0.12	-0.25 ± 0.18	-0.29 ± 0.18	-0.18 ± 0.22
All	-0.14 ± 0.060	-0.20 ± 0.058	-0.17 ± 0.068	-0.13 ± 0.065

Table 4.14
Correlation between Averaged Waveforms without Shared Parameters and Tests of Hypotheses

Sbj.	**Control Set Correlation**	**p-Values**		
		D.C. > Control	**Lum. > Control**	**D.C. > Lum.**
1	-0.094 ± 0.056	$< 10^{-5}$	0.73	$< 10^{-5}$
2	-0.10 ± 0.061	0.03	0.17	0.21
3	-0.13 ± 0.074	$< 10^{-5}$	0.74	$< 10^{-5}$
4	-0.23 ± 0.052	$< 10^{-5}$	0.61	$< 10^{-5}$
5	-0.056 ± 0.064	0.01	0.78	$< 10^{-5}$
6	-0.19 ± 0.053	$< 10^{-5}$	0.65	$< 10^{-5}$
7	0.028 ± 0.064	$< 10^{-5}$	0.55	$< 10^{-5}$
8	-0.18 ± 0.071	$< 10^{-5}$	0.52	$< 10^{-5}$
9	-0.15 ± 0.063	$< 10^{-5}$	0.71	$< 10^{-5}$
10	-0.18 ± 0.047	$< 10^{-5}$	0.58	$< 10^{-5}$
All	-0.13 ± 0.019	$< 10^{-50}$	0.80	$< 10^{-50}$

Note. Highlighted values indicate significance.

Circular shifts of the averaged waveforms appreciably increased the correlation between blocks of differing stimulus duty cycle. The shift amounts providing maximum correlation exhibited specificity to the duty cycle of the shifted waveform and consistency across subjects. Table 4.15 lists the mean and standard error of the circular shifts and of the resulting increases in correlation for each stimulus duty cycle. Histograms of the circular shifts from all subjects sorted according to stimulus duty cycle are presented in Figure 4.11. Chi-square goodness of fit tests confirmed that the shifts were not uniformly distributed (p-values below 10^{-4} for all three tests). The increased correlation coefficients were closer to those between averaged SSVEP waveforms with the same duty cycle, but the shared duty cycle correlations were still significantly greater (p-value of 0.037).

Table 4.15
Circular Shifts for Maximum Correlation and Resulting Correlation Increase

Duty Cycle	**Shift Amount (milliseconds)**	**Correlation Increase**
25%	15 ± 1.3	0.27 ± 0.096
50%	37 ± 2.2	0.58 ± 0.15
75%	54 ± 2.0	0.63 ± 0.13

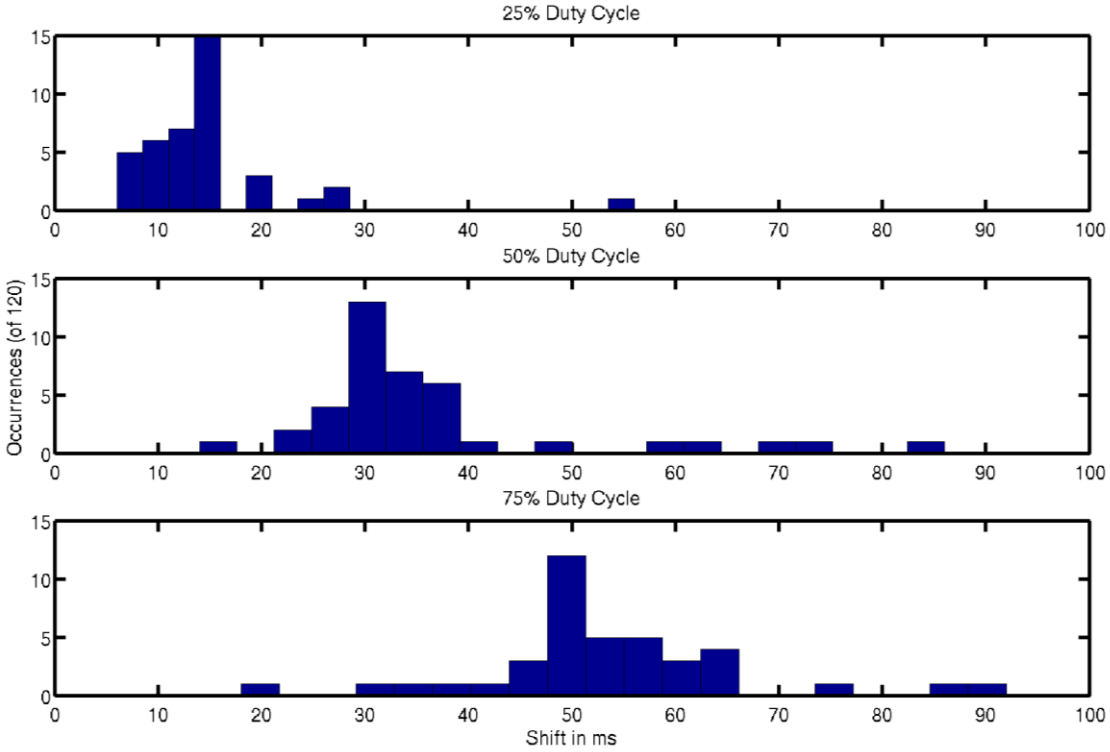

Figure 4.11. Circular shifts in milliseconds providing maximal correlation between averaged SSVEP waveforms of the indicated duty cycle and the 10% duty cycle reference waveform.

Discussion

The main goal of this experiment was to investigate the consequences of stimulus duty cycle and luminance changes on SSVEPs. The results did not establish a relationship between the stimulus parameters and SSVEP spectral measures. However, correlational analyses of individual and averaged flash responses demonstrated that stimuli with different duty cycle values evoke EEG waveforms with dissimilar temporal characteristics. Improvement of the correlation between two of such responses was attained by circularly shifting one of the waveforms to compensate for difference in duty cycle. These outcomes indicated that stimulus duty cycle influences SSVEP signals, but the findings did not identify average stimulus luminance as an important confound.

Linear regression of the individual subject data and across all subjects did not reveal

consistent effects between either of the stimulus parameters and any of the spectral SSVEP measures. These outcomes failed to replicate the previously reported relationship between duty cycle and SNR (Cecotti, 2010) and provide no indication that differences in luminance contributed to the prior results. The lack of a demonstrated relationship between stimulus luminance and SSVEP power was somewhat unexpected and may have been related to the way in which the stimulus was presented to subjects. The flashing LED was the only source of light in the recording room, with the exception of a few indicator LEDs on other hardware that were far dimmer than the stimulus, and so the amount of light perceived by the subjects was dominated by changes in the luminance parameter values. The effect of varying the luminance of the stimulus may have been lessened as a result of the adaptive dynamic range of the human visual system. An experimental design in which the presence of ambient light mitigates the impact of the driving stimulus on the overall light level could obtain a better characterization of the relationship between stimulus luminance and SSVEP signals.

Temporal analyses of individual stimulus responses and of block-wise averaged response waveforms provided more informative results. The outcomes of the correlational analyses demonstrated that changes in stimulus duty cycle alter the shape of the responses. For all subjects, individual SSVEP waveforms from blocks with the same stimulus duty cycle had significantly greater correlation than did SSVEP waveforms from blocks with the same luminance condition, and analyses of the correlation coefficients between averaged SSVEP waveforms agreed with the results from the individual SSVEP waveforms. Additionally, averaged SSVEP waveforms with shared duty cycle showed higher correlation than a control set of waveforms with no shared stimulus parameters, whereas correlation coefficients between averaged waveforms with the same luminance were not significantly greater than the control set. It is reasonable that changes

to stimulus luminance would not alter the shape of the induced SSVEP waveform, even if the strength of the SSVEPs had varied as a function of luminance. These outcomes confirm that stimulus duty cycle must be considered carefully during the design of an SSVEP experiment, and stimulus duty cycle should be kept constant between various conditions whenever possible.

Correlation between averaged SSVEP waveforms was lower for blocks with different stimulus duty cycles, but correlation was substantially increased after applying a circular shift to one of the waveforms. The duty cycle specificity and the consistency across subjects of the optimal shift durations show that the consequences of stimulus design in SSVEP experiments can be quantified and generalized. Such temporal shifts reflect differences in the spectra of the SSVEPs, in agreement with the previous investigation of changes to SSVEP harmonic components as an outcome of variations in stimulus duty cycle (Lee et al, 2011). The number of conditions in this case prohibited a conclusive test of a linear relationship between duty cycle and shift duration, but the results here are encouraging for future investigations of the linearity of SSVEP characteristics.

With respect to experimental design choices, the ability to change stimulus parameters with high precision offered a significant advantage over SSVEP generation using a computer display. The high precision of the stimulus as well as of the timing used for marking events was illustrated by the successful temporal averaging of SSVEP waveforms, which exhibited characteristics dependent on stimulus duty cycle. Methods of SSVEP generation relying on video display devices cannot offer the flexibility and precision of an LED driven by a microcontroller.

Responses to Periodic and Aperiodic Stimuli At Multiple Frequencies using EEG/fMRI

Introduction

Despite the inclusion of SSVEPs in a range of experimental paradigms, several fundamental questions remain unanswered regarding the generation of SSVEPs and their sources of variability (Vialatte et al, 2010). Clarifying the origins of the signal itself could facilitate the interpretation of SSVEP effects. Given the large number of applications that utilize SSVEPs solely for the purpose of achieving other goals, such as attention monitoring or BCI, a comprehensive understanding of the basic principles behind the SSVEP phenomenon has not been a recent priority. However, gaps in knowledge can lead to study designs that introduce confounds or diminish stimulus efficacy, as demonstrated in the preceding sections of this manuscript. Confirming the mechanisms by which SSVEPs appear and the factors that influence their stability are important objectives, even to research with other primary motives.

One uncertainty is whether an SSVEP arises as a simple summation of reactions to individual events or as a specific response triggered only by periodic stimulation. If the SSVEP is composed of the linear combinations of separate evoked potentials, then features of transient VEPs should explain SSVEP characteristics such as frequency selectivity. Conversely, if the visual system is sensitive to periodicity itself, then there should be nonlinear relationships between SSVEPs and responses to irregular flashes. The prior literature has not yet produced a definitive answer. Some data have indicated that SSVEPs result from the phase alignment of intrinsic oscillations such as alpha waves (Moratti et al, 2007; Klimesch et al, 2007), akin to the phase reset model of event-related potentials (Sauseng et al, 2007). Another group has reported the ability to predict SSVEP observations based on transient potentials (Gaume et al, 2014a; Gaume et al, 2014b), but these transient potentials were provoked also by periodic stimuli, albeit

at a frequency below traditional SSVEPs. Further exploration of the degree of similarity between SSVEPs and responses to arrhythmic stimuli is needed to resolve these questions.

The final experiment comprising this manuscript employs simultaneous EEG/fMRI (functional magnetic resonance imaging) to investigate SSVEPs in comparison to evoked potentials elicited by aperiodic flashes. As SSVEP outcomes have been shown to vary with stimulus rate (Ding et al, 2006; Pastor et al, 2006; Bayram et al, 2011; Huang et al, 2012), this design includes both periodic and aperiodic stimuli over a range of frequencies. The slowest conditions allow sufficient time between events to categorize the resulting activity as transient VEPs (Regan, 1989). This study contrasts periodic and aperiodic induced activity, evaluates frequency dependence in responses to both types of stimuli, and assesses the capacity of transient VEPs to explain EEG signals driven at higher frequencies. Elucidating the roles of periodicity and presentation rate in the generation of evoked potentials will contribute to better-informed conclusions in SSVEP research and may reveal ways to improve stimulus implementations.

Methods

Six adult subjects viewed a flickering stimulus passively during the concurrent acquisition of EEG and fMRI, following procedures established by colleagues at the same facility (Lenartowicz et al, 2016). MRI data were collected using a 3 T Siemens Trio MRI scanner. T2*-weighted echoplanar images (EPI) were acquired during visual stimulation (3 mm slice thickness, 36 slices, 64 x 64 matrix, 2.16 second repetition time, 30 ms echo time, 90º flip angle, 192 mm field of view). A T2-SPACE structural image (1 mm slices thickness, 224 slices, 256 x 256 matrix, 3.2 second repetition time, 213 ms echo time, 256 mm field of view, sagittal plane) and a T2-weighted matched bandwidth structural scan having bandwidth parameters corresponding to the EPI were used to register functional images to Montreal Neurological

Institute (MNI) standard space. EEG recordings were made with an Electrical Geodesics (Eugene, OR) 256-channel EEG system whose sampling at 1000 Hz was synchronized to the EPI sequence. Electrocardiogram (ECG) data were recorded via the EEG system as well. All subjects provided informed written consent prior to their participation.

Stimuli were presented via a custom electronic device, built using an Arduino UNO microcontroller, driving a white LED shining onto a rear projection screen situated behind the MRI scanner, superior to the supine subjects. Subjects viewed the stimuli through a mirror mounted on the MRI head coil. The projected light spot had a diameter of 12 centimeters at a distance of approximately 110 centimeters, corresponding to a visual angle of approximately 6.25º. The stimulus electronics remained outside of the scanner room during the experiment, connecting to the LED via an RF filtered BNC cable, as illustrated in Figure 4.12. Other sources of light were eliminated from the scanner room during data collection.

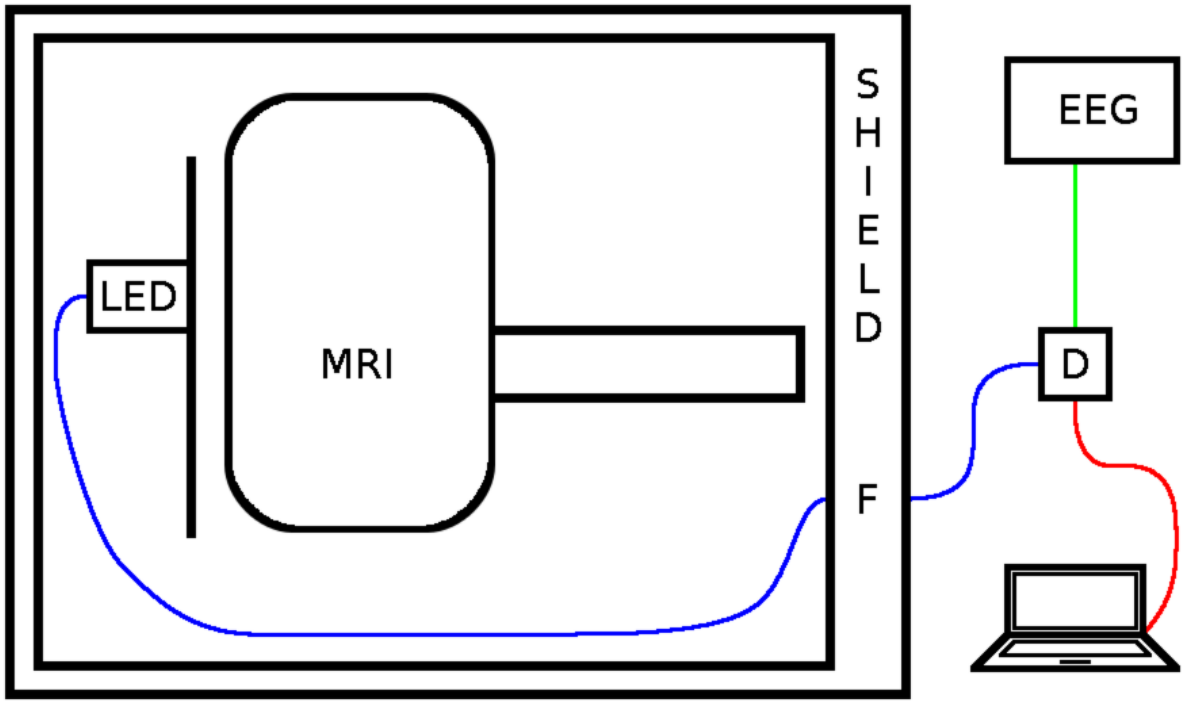

Figure 4.12. Arrangement during data collection. A personal computer communicates with the stimulus device (D) over USB (red). The device controls the LED from outside the shielded MRI room via BNC cable (blue) with an in-line RF filter (F). The device sends timed event markers to the EEG recording computer with a direct TTL connection (green).

Over the course of the experiment, subjects viewed periodic and aperiodic light flashes at multiple rates amounting to eight unique conditions in a block design. Periodic stimulus frequencies included 1.55 Hz (slowest), 4.65 Hz (low), 9.30 Hz (mid), and 15.5 Hz (high), which were chosen to sample a common band in SSVEP literature and to avoid confounding covariance with either 60 Hz noise or the MRI sequence. The aperiodic conditions consisted of intermittent flashes of varying inter-stimulus interval (ISI). Each aperiodic condition contained five ISI values, with the median and the mean ISI in each condition corresponding to one of the four periodic stimulus frequencies; Table 4.16 specifies the presentation rates for all conditions. The aperiodic ISI values were selected to provide a linear distribution of durations rather than a linear distribution of frequencies. This choice allowed each of the five ISI values to appear the same number of times per block while keeping the mean and median ISI as well as the block length

equal to those of the corresponding periodic condition. The ISI order of the slowest aperiodic condition followed an m-sequence to ensure balance and low autocorrelation (Buračas and Boynton, 2002), whereas the low, mid, and high aperiodic conditions were varied according to a pseudorandom number generator (PRNG) implemented through the stimulus device. The PRNG was seeded with a different and specific value at the start of each aperiodic block, such that no sequences were repeated in whole or part for a given subject. Stimuli were rectangular waveforms with flash durations of 10 milliseconds in all conditions.

Table 4.16
Periodic and Aperiodic Stimulus Parameters

Condition	Periodic Frequency (Hz)	Aperiodic ISIs (ms)
Slowest	1.55	515, 580, 645, 710, 775
Low	4.65	171, 193, 215, 237, 259
Mid	9.30	86, 97, 108, 119, 130
High	15.5	51, 58, 65, 72, 79

The experiment was divided into sixteen blocks, with each condition appearing in two blocks. The slowest aperiodic and periodic conditions had durations of 120 seconds, with all other blocks lasting 90 seconds each. Blocks were separated by rest periods of 30 seconds, and the experiment was halted after every four blocks to check on the status of the subject. As such, four separate EPI scans were collected, each lasting slightly over eight minutes. Each EPI scan consisted of a different permutation of four stimulus conditions. These conditions were in turn balanced across scans within subjects, and the balancing order was varied from subject to subject. Within each subject, the first and fourth scans contained the same conditions in reversed order, as did the second and third scans. Table 4.17 shows an example of the condition balancing. The timings of the beginning and end of each stimulus block were inserted as event markers in the

EEG recording, as were individual events for the onset and offset of each light flash. The stimulus device communicated the event markers directly to the EEG recording system using transistor-transistor logic (TTL), providing a high degree of precision.

Table 4.17
Condition Balancing across Four EPI Scans

EPI 1:	Low P.	Rest	High A.	Rest	Mid P.	Rest	Slowest A.
EPI 2:	Low A.	Rest	Slowest P.	Rest	Mid A.	Rest	High P.
EPI 3:	High P.	Rest	Mid A.	Rest	Slowest P.	Rest	Low A.
EPI 4:	Slowest A.	Rest	Mid P.	Rest	High A.	Rest	Low P.

Note. P = Periodic (blue) and A = Aperiodic (red). Frequencies and ISIs match those from Table 4.16. The slowest blocks lasted 120 seconds; all other stimulus blocks lasted 90 seconds. Each rest block lasted 30 seconds. Scan order and block order within scans was varied across subjects, but the two condition subsets were consistent in all subjects.

Analyses

Preprocessing of the EEG data was performed in MATLAB using several third-party tools. First, EEG channels with impedances above 50 kilohms, as measured at the time of the recording, were excluded from the remainder of the analyses. Excessively high impedances were identified in as few as one channel and in no more than 59 channels per subject, with a median of 22. Table 4.18 includes the number of channels rejected for each subject. Next, the gradient artifact generated during EPI acquisition was removed from the EEG and ECG time series without template subtraction using an EEG/fMRI cleaning method developed in the lab (Rodriguez, 2016).

Decimation of the EEG and ECG from 1000 Hz to 250 Hz followed elimination of the gradient artifact, to expedite later processing and to reduce file size. As part of the gradient removal and decimation, the data were band-pass filtered between 0.9 Hz and 100 Hz. Subsequently, EEG channels with poor signal quality were identified and excluded from further analyses with automated channel rejection implemented in EEGLAB (Delorme and Makeig,

2004), based on abnormally low correlation between neural signals and artifact (Delorme et al, 2011). Spherical interpolation was then applied to the noisy and high-impedance channels via EEGLAB (see Table 4.18).

Table 4.18
Number of Channels Rejected per Subject

Subject	High Impedance	Improbable Signal	Total Interpolated
1	59	43	102
2	29	28	57
3	8	29	37
4	1	37	38
5	15	21	36
6	35	27	62

Detection and cleaning of ballistocardiogram (BCG) contamination in the EEG (Debener et al, 2008; Mullinger et al, 2013) took place in two steps. The timing of BCG events was determined using an automated algorithm (Rodriguez et al, 2014) and verified with the ECG recording. The BCG artifact was removed from the EEG data using the FMRIB plug-in for EEGLAB, provided by the University of Oxford Centre for Functional MRI of the Brain (FMRIB), based on principal component analysis (Niazy et al, 2005; Iannetti et al, 2005).

Independent component analysis (ICA) was performed outside of MATLAB with binary Infomax ICA by Sigurd Enghoff, based on the MATLAB version of Scott Makeig and collaborators (Makeig et al, 1996). ICA results were imported into MATLAB and assessed by the Multiple Artifact Rejection Algorithm (MARA) to label artifactual components (Winkler et al, 2011; Winkler et al, 2014). EEGLAB was used to reconstruct the EEG data without rejected components as labeled by MARA, completing the EEG preprocessing.

The preprocessed EEG data were segmented according to the sixteen stimulus blocks for

further analyses (90-second blocks for all but the slowest conditions, which were 120-second blocks). The FFT was applied to the EEG time series from each of the sixteen blocks to obtain the power spectra for the O_Z electrode. For each periodic block, the spectral component at the stimulus frequency was selected to identify SSVEP power. For aperiodic blocks, power was calculated at the five frequencies corresponding to the five ISI values for comparison but without the expectation of detectable SSVEPs.

Further segmentation was performed on the slowest periodic and aperiodic blocks according to the stimulus event markers. Separate 700-ms windows were extracted beginning at each flash onset, totaling 372 responses for each of the two conditions. Time averaging was performed across the individual events from each condition, producing the mean periodic and aperiodic VEPs for the O_Z electrode (pVEP and aVEP, respectively). The spectral content of each VEP was assessed using the FFT to identify components at the three higher stimulus frequencies (4.65 Hz, 9.30 Hz, and 15.5 Hz). Least squares linear regression was used to examine the relationship between the spectral components of the slow VEPs and the power of the SSVEPs elicited by faster stimuli. The spectral components were assessed as the predictor variable for the SSVEP power in the corresponding periodic blocks, to test the hypothesis that the SSVEP frequency response matches the spectral characteristics of transient VEPs.

The extent to which SSVEPs derive from individual transient VEPs was tested by constructing simulated EEG data based on the averaged responses to the slow stimuli. A stimulus waveform time series was created for each block using the flash onset and offset event markers. Each stimulus time series matched the sample rate and the duration of the EEG segment from the corresponding block. Predictive models were made by convolving the stimulus time series with each averaged VEP as the assumed transfer function of the flash response. Three separate

predictions were made for each block by using the pVEP, the aVEP, and a standard flash VEP (sVEP) reported in the literature (Odom et al, 2004). The pVEP and aVEP waveforms were truncated to 300 ms prior to convolution to match the duration of the canonical flash VEP. Correlation coefficients were calculated between the recorded EEG and each prediction; strong correlation would indicate that slow transient responses can explain SSVEPs and responses to faster aperiodic stimuli. Paired t-tests were used to compare the magnitudes of the correlation coefficients between the three models at the group level, determining which VEP provided the best approximation of the transfer function.

Analyses of the structural and functional MRI recordings were performed in FMRIB Software Library (FSL) v5.0 (Smith et al, 2004; Jenkinson et al, 2012; Woolrich et al, 2014) after conversion of the original DICOM files to NifTI format using dcm2nii (www.mricro.com). Preprocessing in FSL included motion correction applied to the EPI scans via MCFLIRT (Jenkinson et al, 2002) and the removal of non-brain tissue from all images through BET (Smith, 2002). Multilevel analyses of the functional data were completed using FEAT (Jezzard et al, 2001; Smith et al, 2001) following confirmation that all preprocessing steps had finished successfully.

The generalized linear model for the first-level functional analyses contained four stimulus condition regressors generated from the EEG event markers and six nuisance regressors for the translation and rotation parameters calculated with MCFLIRT. Regressors were convolved with a gamma hemodynamic response function (HRF), and temporal derivatives were added to the model. Corrections for temporal autocorrelation were applied to the data using FILM pre-whitening (Woolrich et al, 2001). Data were spatially smoothed (5 mm full- width-half-maximum Gaussian kernel) and high-pass filtered at a frequency selected by FSL based on

the explanatory variables. Each EPI session was registered with three degrees of freedom (DOF) to the T2 matched-bandwidth scan, which was registered with seven DOF to the T2-SPACE image, in turn registered to standard space using twelve DOF.

Two parallel second-level analyses were conducted within each subject to integrate the two pairs of sessions with matching conditions. A fixed effects model was applied to determine the mean activation per condition within each subject. Registration transforms were reused from the first-level analyses. Third-level analyses assessed fMRI activation across subjects according to ten contrasts, including averages of the eight individual stimulus conditions, a contrast between periodic and aperiodic blocks, and a test of linearity with respect to frequency. Fixed effects models were also used in the third-level analyses, along with the first-level registration transforms. Activated structures were identified according to the Harvard-Oxford cortical and subcortical structural atlases (Frazier et al, 2005; Makris et al, 2006; Desikan et al, 2006; Goldstein et al, 2007).

Results

Spectral plots of the FFT data revealed clear SSVEP signals during most periodic stimulation blocks, but strength and SNR varied considerably within and across subjects. Figure 4.13 provides example spectra from two subjects. The 15.5 Hz condition produced the weakest signals, followed by the 4.65 Hz condition. SSVEP power was still calculated for blocks without clear peaks at the stimulus frequency, due to the previously demonstrated precision of the stimulus device and the consistency in frequency of the evident peaks. Table 4.19 lists the SSVEP power at each frequency for all subjects. As expected, aperiodic blocks did not exhibit increased power corresponding to the ISIs, demonstrated by the spectrum in Figure 4.14. Temporal analyses produced averaged VEPs that resembled standard flash responses, but the

apparent noise in these waveforms was substantial in some subjects. Averaged VEPs from two subjects are plotted in Figure 4.15.

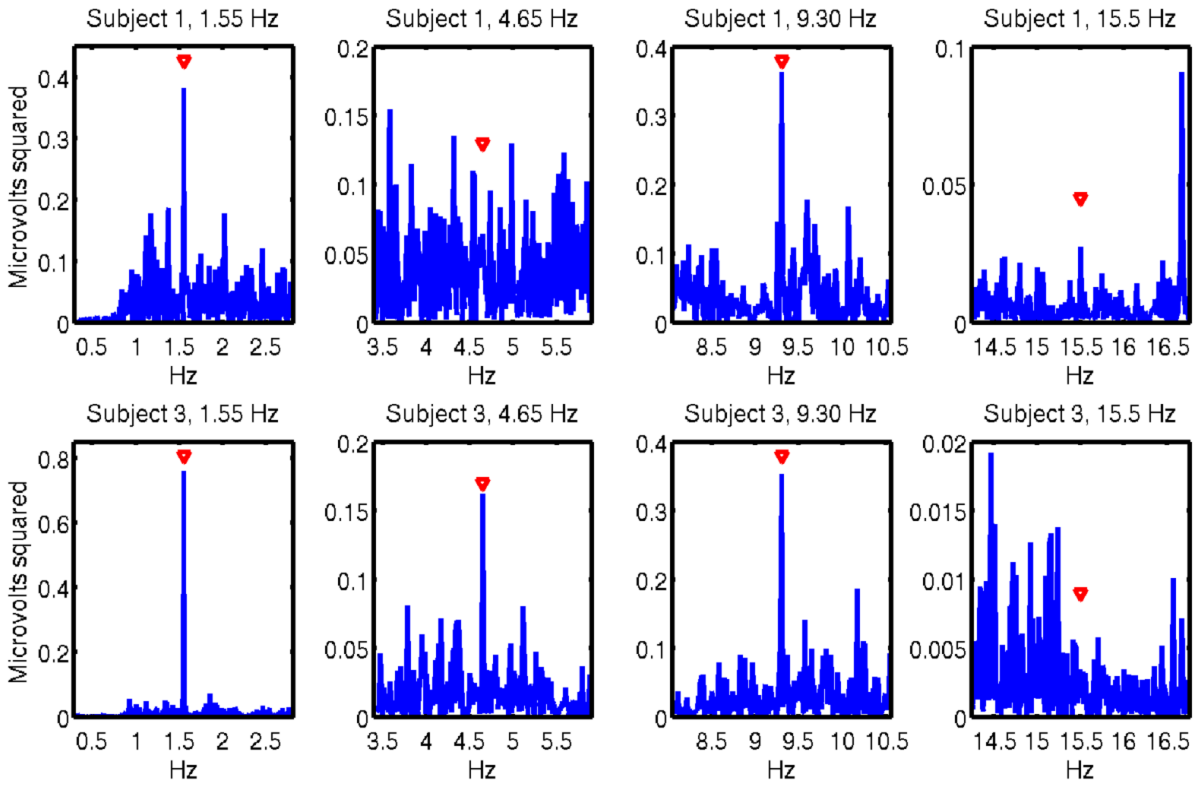

Figure 4.13. Spectra near the stimulus frequency (red triangles) reveal SSVEPs.

Table 4.19
Mean SSVEP Power at Four Stimulus Frequencies (Microvolts Squared)

Sbj.	1.55 Hz	4.65 Hz	9.30 Hz	15.5 Hz
1	0.29	0.070	0.26	0.046
2	0.12	0.25	0.72	0.042
3	0.68	0.15	0.58	0.0037
4	0.25	0.12	0.33	0.015
5	0.58	0.91	0.40	0.029
6	0.42	0.020	0.52	0.0075

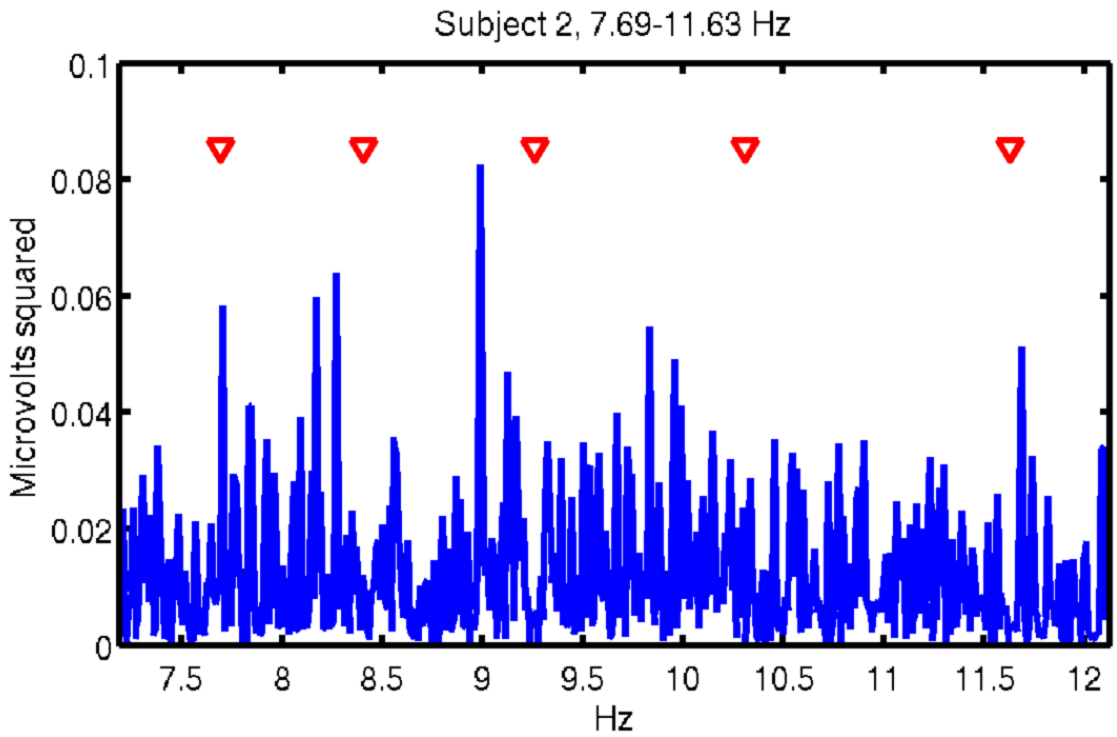

Figure 4.14. Spectral power not increased at frequencies corresponding to aperiodic ISIs.

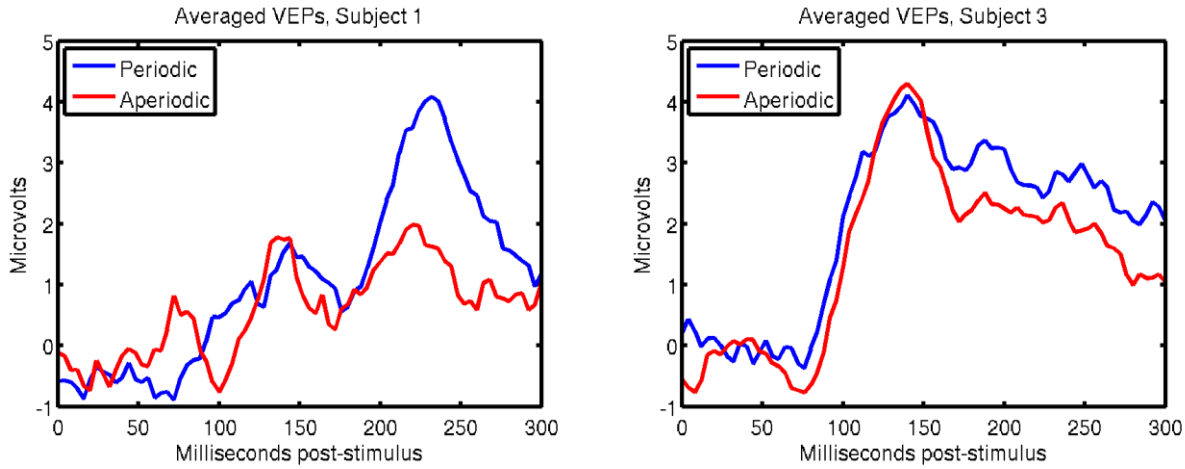

Figure 4.15. Averaged VEPs generated from the two slowest stimulus conditions.

Analyses produced positive linear regression coefficients between the spectral components of the VEPs (regressor) and the SSVEP power during the corresponding blocks (regressand). Table 4.20 displays the spectral components of the VEPs for all subjects, and Table 4.21 presents the regression results. Linear regression was calculated using VEP spectral

components and SSVEP power paired within subjects, then pooled across subjects. A significant regression coefficient with a modest R-squared value was found using the spectral components of the aVEPs but not using the components of the pVEPs. The strongly significant result indicates that an averaged VEP generated with aperiodic stimulation may closely approximate the general SSVEP frequency response.

Table 4.20
Spectral Power of VEPs at Frequencies Corresponding to Other Stimuli (Microvolts Squared)

	Power at 4.65 Hz		**Power at 9.30 Hz**		**Power at 15.5 Hz**	
Sbj.	**aVEP**	**pVEP**	**aVEP**	**pVEP**	**aVEP**	**pVEP**
1	0.0019	0.034	0.0017	0.018	0.020	0.00023
2	0.049	0.041	0.043	0.025	0.0040	0.0027
3	0.084	0.051	0.048	0.0058	0.0011	0.0019
4	0.13	0.047	0.12	0.011	0.0082	0.0045
5	0.25	0.030	0.15	0.054	0.0026	0.0032
6	0.060	0.034	0.031	0.021	0.0087	0.00037

Table 4.21
Linear Regression between VEP Spectral Components and Corresponding SSVEP Power

VEP	***β* (95% C.I.)**	**R^2**	**p**
Aperiodic	2.5 (1.2, 3.8)	0.31	5.1×10^{-5}
Periodic	3.5 (-2.1, 9.0)	0.046	0.21

Note. C.I. = Confidence Interval.

Low correlation was found between the recorded EEG and the simulated models, but the majority of these correlations were significant. Additionally, the correlations with the real EEG were significantly different between the three models. The aVEP predictions and pVEP predictions both had stronger correlation than the sVEP predictions ($p = 9.9 \times 10^{-6}$ for aVEP > sVEP, $p = 0.015$ for pVEP > sVEP), and correlations with the aVEP predictions were significantly stronger than correlations with the pVEP predictions ($p = 3.1 \times 10^{-5}$). Table 4.22

summarizes the correlation results of all three predictive models; standard error values were calculated using bootstrapped sampling over 1000 iterations. The increased correlation and greater number of significant correlations seen in the aVEP models suggest that transient VEPs generated by intermittent flashes are more reflective of a general impulse response.

Table 4.22
Correlation between Simulated and Real EEG

VEP	Correlation Magnitude	Percent Significant
Aperiodic	0.073 ± 0.0072	84%
Periodic	0.059 ± 0.0068	76%
Standard	0.042 ± 0.0048	77%

Note. Both subject-specific models (aVEP and pVEP) had significantly higher correlations than the models based on a standard flash response. The aVEP models also showed significantly higher correlations than the pVEP models.

The multi-level fMRI analyses produced activation maps identifying various cortical regions sensitive to different stimulus conditions. Figure 4.16 presents the thresholded results ($z > 2.3$) from the two main contrasts: aperiodic vs periodic stimulation and linearity with respect to frequency. Aperiodic conditions showed greater activation than periodic conditions, specifically in the right superior, middle, and inferior temporal gyri as well as in the calcarine sulcus and lingual gyrus. Activity in some frontal regions demonstrated a positive linear relationship with stimulus frequency, including the frontal pole and anterior cingulate cortex; this relationship was also found in the lateral occipital cortex, lingual gyrus, and fusiform gyrus. The middle temporal gyrus appeared to have a negative relationship with stimulus frequency, although the strength of this effect was not as pronounced.

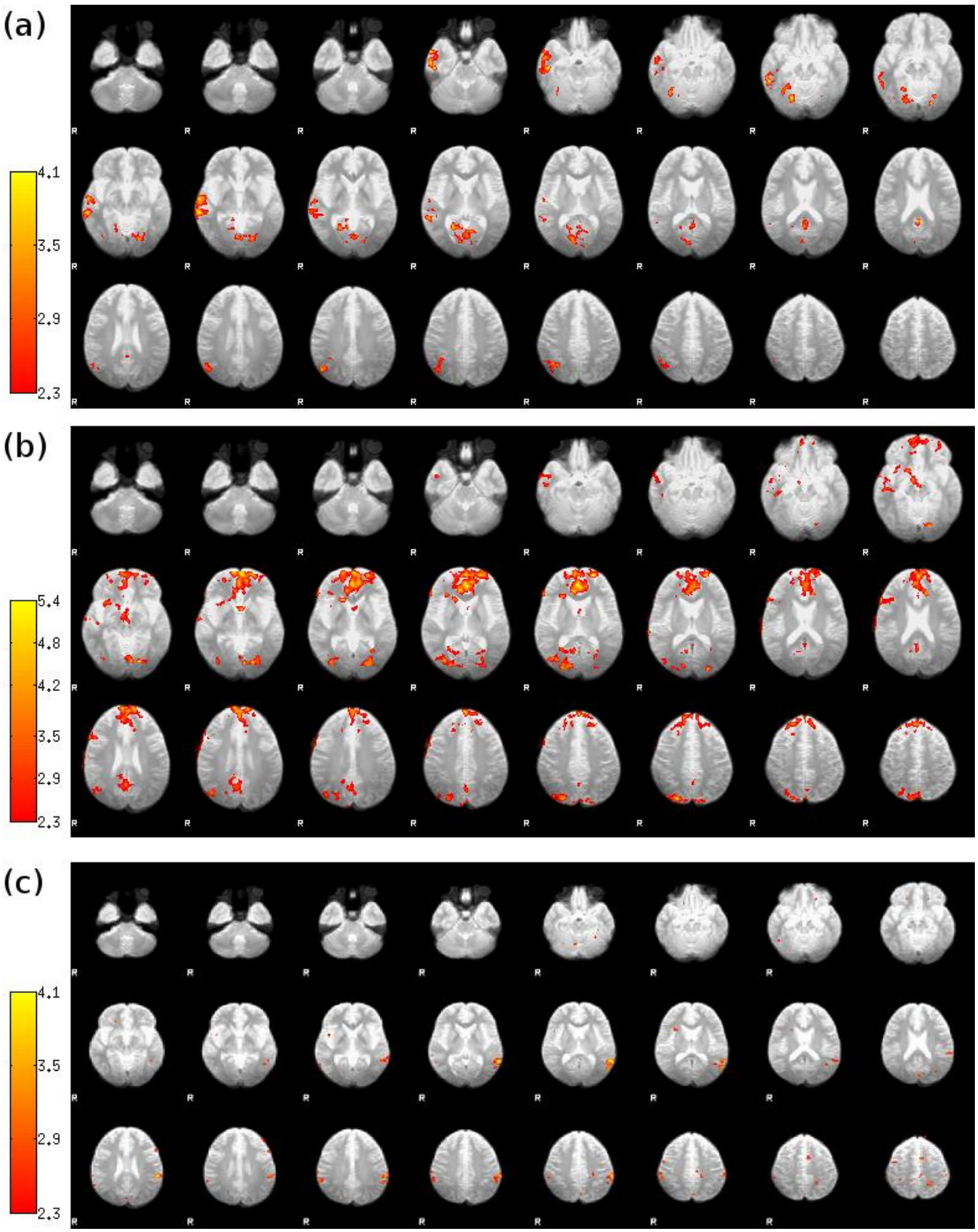

Figure 4.16. Group-level fMRI activation maps for three contrasts. (a): Regions with greater activation in aperiodic blocks than in periodic blocks. (b): Regions with activation that varied directly with stimulus frequency. (c): Regions with activation that varied inversely with stimulus frequency.

The average activation maps for the eight individual conditions revealed some commonalities across stimulus types. At least one occipital region was activated in every condition, and a number of stimuli also resulted in decreased activity in occipital regions. Five of the contrasts illustrated increased activation in the precentral and postcentral gyri, and seven conditions exhibited decreased activation in the cuneus or precuneus. Table 4.23 contains the list of regions with significant changes in each condition

Table 4.23
Brain Regions Activated per Stimulus Condition

Condition	Increased Activation	Decreased Activation
Slowest aperiodic	Occipital cortex	Precuneus, cuneus, occipital pole
Slowest periodic	Precentral gyrus, postcentral gyrus, supramarginal gyrus, middle temporal gyrus, lateral occipital cortex	Precuneus, cuneus, occipital pole, lateral occipital cortex
Low aperiodic	Precentral gyrus, postcentral gyrus, supramarginal gyrus, occipital pole, lateral occipital cortex	Superior frontal gyrus, cingulate cortex, precuneus
Low periodic	Lateral occipital cortex, angular gyrus	Superior frontal gyrus, precuneus, cuneus
Mid aperiodic	Precentral gyrus, postcentral gyrus, middle temporal gyrus, lateral occipital cortex, superior frontal gyrus, intracalcarine cortex, paracingulate gyrus	Frontal pole
Mid periodic	Precentral gyrus, postcentral gyrus, lateral occipital cortex, occipital pole	Precuneus, cuneus, occipital fusiform gyrus, lingual gyrus
High aperiodic	Occipital pole, lateral occipital cortex, occipital fusiform gyrus	Cuneus, lateral occipital cortex, frontal pole
High periodic	Precentral gyrus, postcentral gyrus, supramarginal gyrus, lateral occipital cortex	Cuneus

Discussion

The outcomes of this investigation revealed interesting characteristics distinguishing responses to periodic and to aperiodic stimuli and connecting transient evoked potentials and SSVEPs over a range of frequencies. Analyses of the EEG data demonstrated a relationship

between the spectra of transient VEPs and the overall SSVEP frequency response, but the EEG recordings also indicated a degree of disparity between periodic and aperiodic driven activity. Effects of periodicity were also shown by the fMRI analyses, along with evidence of frequency sensitivity in certain brain regions.

Results of the regression analyses illustrate a connection between spectral characteristics of transient VEPs elicited in the slowest aperiodic condition and SSVEPs induced by the low-, mid-, and high-frequency stimuli, providing evidence that transient and steady-state VEPs occur via shared or similar mechanisms. Interestingly, a significant relationship was not found using the spectral components of the periodically driven VEP, and while the presentation rates during the slowest conditions were infrequent enough for the responses to be considered transient VEPs (Regan, 1989), the shape of waveforms differed with periodicity.

The comparisons of real EEG data and simulations constructed using transient VEPs further established the relationships between transient and steady-state VEPs and across a range of stimulus rates. These results agree with the outcomes of similar previous research (Gaume et al, 2014a; Gaume et al, 2014b). The inclusion in this study of aperiodic VEPs, which the prior experiments lacked, proved to be an advantage, as the analyses revealed greater effects for the aperiodic condition.

The low correlation between the simulated data and the recorded EEG should not be interpreted to suggest that transient VEPs cannot explain responses at higher frequencies, because most of the correlations were highly significant. The combination of low correlation and high significance can be explained by the large number of samples contributing to each comparison (over 22,500 samples per block). It is also important to remember that many signals are contained in the EEG, from both neural and external sources, and the flash-induced responses

are only a portion of the recorded time series.

The higher correlation seen with the predictions that used the subject-specific VEPs, as opposed to the standard flash response, provides evidence of success in these models and supports explanations of SSVEPs based on transient responses. The finding that simulated data generated from aVEPs showed higher correlation than those from pVEPs indicates that aperiodic stimulation produces a more generalizable response, possibly as a consequence of frequency-specific structures or networks being activated by periodic stimuli. Clearly some of the attributes of SSVEPs are derived from transient VEP mechanisms irrespective of frequency, but it also seems unlikely that no SSVEP processes would be selectively sensitive to periodicity.

The results of the fMRI analyses also provide evidence of different mechanisms governing the responses to periodic and aperiodic stimuli, most notably in the increased activation seen in aperiodic conditions in contrast to periodic conditions. SSVEP generation via alignment of intrinsic oscillations should have lower metabolic requirements than the summation of individual responses, because in the latter case the neurons must fire when they would not otherwise, in addition to synchronizing to the phase of the stimulus. The reduced activation seen in periodic blocks suggests that this mechanism is at play during the generation of SSVEPs, in accordance with arguments in prior literature (Moratti et al, 2007). However, the difference between the attentional demands of the periodic and aperiodic stimuli could also explain the activation effects. Multiple cortical areas exhibited a linear relationship to stimulus frequency, but activation maps between the conditions overlapped to a large extent. The consistency of the activated regions across the range of stimulation rates indicates that VEPs and SSVEPs emerge through common processes, which supports the EEG findings here as well as outcomes in prior literature.

The contrasts of the individual conditions revealed areas with decreased activation during stimulation. Previous studies have illustrated negative correlations between EEG alpha rhythms and fMRI activation in many of the same brain regions (Goldman et al, 2002; Laufs et al, 2003; Gonçalves et al, 2006). Accordingly, inhibition of alpha rhythms may have driven the reductions in activity seen in this experiment. The salience of these flashes is quite high, so it is possible that a number of these fMRI outcomes reflect not only the processes of VEP and SSVEP generation but also induced changes in other structures or networks as a consequence of stimulation. Correlational analyses cannot escape the inability to determine causality.

In total, this experiment demonstrates that characteristics of transient VEPs can predict and explain SSVEP effects with some degree of success, and SSVEPs may be generated in part by the superimposition of repeated responses to each flash. However, additional factors must be involved, as data in both imaging modalities have revealed distinctions between aperiodic and periodic conditions as well as frequency-dependent activation of certain brain regions. The duality of these outcomes illustrates the complexity of the SSVEP phenomenon.

CHAPTER 5: CONCLUSIONS AND REFLECTIONS

As this manuscript has demonstrated, SSVEPs can be quite useful in many types of neuroscience, psychology, and engineering research, but experimental designs must be constructed with consideration of the more subtle characteristics of this phenomenon, particularly its sources of variability related to implementation choices. This project has shown that reports of robust effects in SSVEP publications may belie their ease of replication. However, iterative improvements to methodology and careful scrutiny of the assumptions about SSVEPs have succeeded in developing studies with a higher degree of precision and in producing more-informative results.

The experiments in Chapter 2 applied SSVEPs to the investigation of visual attention and ADHD; those outcomes illustrate the encouraging nature of the easily discernible SSVEP signals but also exemplify the difficulty of reproducing higher-order effects such as attentional modulation. Some of the design choices at this stage were influenced by presumptions about the stability of certain SSVEP characteristics, and a need for particularity in this respect was not indicated by the diversity of SSVEP implementations across previous research (Vialatte et al, 2010; Zhu et al, 2010). The initial pilot data seemed to hint that interesting conclusions regarding SSVEP fluctuations and attention regulation were close at hand, limited only by the small sample size of this first exploration. Unfortunately, the subsequent expanded attention study did not succeed in associating SSVEP measures with behavioral performance and failed even in confirming the established phenomenon of SSVEP attentional modulation (Morgan et al, 1996; Müller et al, 1998; Russo et al, 2002; Kelly et al, 2005). Inadvertent deficiencies in the experimental design were assumed to be the origin of these shortcomings, as the literature was not suggestive of inconsistencies in this effect.

The iterative experimental design process described in Chapter 3 identified a number of stimulus parameters and presentation schemes having consequences in data outcomes that were not initially obvious. Abandonment of the frequency approximation method (Nakanishi et al, 2013) improved the precision of the driving waveforms thereby removing a source of potentially significant instability in the elicited SSVEPs, the effects of which have been demonstrated more recently (Szalowski and Picovici, 2015). Optimizations of the flicker contrast and of the background luminance were implemented based on a combination of quantitative analysis and subjective participant feedback. The use of a third periodic stimulus as a fixation target provided the new setup with an indicator of gaze and an instrument for assessing SSVEP variance unrelated to the task, which also extends the possible future analyses of the data. Modifications to the block design balanced the ability to detect block-wise effects against the windows in which slow fluctuations of attention could emerge. Resting EEG blocks were included to offer a more-accurate baseline recording and further expand the utility of the data set for later research. The creation of a processing algorithm for rapidly assessing the quality of SSVEPs using different stimulus conditions granted reduced likelihood of collecting fruitless recordings, as the task specifications can be tailored to each subject. Some alternative stimulus concepts, such as the quadrant configuration, were not incorporated into the final implementation, but the evaluation of these rejected methods provided valuable affirmation of the strengths of the original version.

Studies employing the revised experimental design are currently ongoing. Early results indicate that the effort was as success: anticipated outcomes from the new implementation include multiple publications as well commercialization of an ADHD assessment system. (For information about these ongoing projects, see the acknowledgments preceding this manuscript.)

The original motivation behind this endeavor was the development of techniques for examining attention, but the process additionally revealed unaddressed sources of SSVEP variability, inspiring successive experiments seeking a better understanding of the SSVEP phenomenon.

Chapter 4 recounts a series of investigations into the intrinsic principles of SSVEPs. The first of these experiments concerned attentional modulation in simultaneously attended SSVEPs, but its purpose was to clarify the properties of the SSVEP itself rather than to use SSVEPs as a lens through which to inspect other systems. Similarly to the work in Chapter 2, this study failed to replicate prior attention effects and did not answer any other questions pertaining to SSVEP fluctuations. The lack of findings were interpreted as evidence of the limits of SSVEPs, particularly in such a complex stimulus presentation. Subsequent designs emphasized simplicity and explored SSVEPs at a basic level to characterize their sources of variability.

While LCD monitors are an attractive choice for implementing SSVEP paradigms, they impose serious constraints on the displayed stimuli (Volosyak et al, 2009). The design and construction of a custom electronic stimulus device was essential to the success of the research depicted in the final sections of Chapter 4. Production of the device required knowledge of circuit analysis and the C programming language as well as soldering and prototyping skills. An evaluative testing and debugging procedure demonstrated the utility of the device and its ability to generate stimulus waveforms with high precision over a wide range of characteristics, including stimuli with continuously varying parameters. Completion of the device also enabled plans for a simultaneous EEG/fMRI study.

The penultimate experiment in Chapter 4 illustrated that changes to the duty cycle of a driving stimulus can alter the elicited SSVEP. Temporal shifts were able to increase correlation between SSVEPs elicited by stimuli differing in duty cycle; this results from qualities of the

frequency spectra that change with duty cycle, such as harmonic components, which prior research had established (Lee et al, 2011). This outcome also validated the substantial attention to detail invested in the redesign process chronicled throughout Chapter 3. However, a previously reported effect of duty cycle on SNR was not replicated (Cecotti, 2010). The conclusions of this experiment, including the failure to replicate the prior finding, supported suspicions that the variety of methodologies employed throughout the SSVEP literature may have unintended consequences. Stimulus luminance was expected to be identified as a problematic confound as well, but it was not shown to impact SSVEPs. This null result reinforces the prior literature that employed stimuli without matching average luminance (Pastor et al, 2003; Ding et al, 2006; Pastor et al, 2006). Final development of the simultaneous EEG/fMRI study was then completed with consideration of the duty cycle effect and without concern for luminance.

The comparison of responses to periodic and aperiodic stimuli at multiple frequencies using simultaneous EEG/fMRI was the culmination of an intricate project that faced many obstacles over several years. This last step was a huge undertaking, as multimodal imaging introduced additional noise and complexity to a design that already struggled with unknown sources of variability. Fortunately, the efforts to identify optimal stimulus methods and to eliminate confounding variance wherever possible seem to have been worth the investment: the final experiment established a relationship between VEPs driven at slow presentation rates and the characteristics of responses to stimuli at higher frequencies. Simulated data based on these slow VEPs were somewhat successful in predicting the recorded responses to faster stimuli, in line with similar preceding research (Gaume et al, 2014a; Gaume et al, 2014b). The results from both modalities also drew a contrast between periodic and aperiodic responses, favoring of the

proposed phase alignment mechanism of SSVEP generation (Moratti et al, 2007). The small sample size was one limiting factor of this study, but the encouraging outcomes demonstrated the feasibility of elucidating sources of SSVEP variability through meticulous methodology.

In conclusion, the attractive qualities of SSVEPs must be weighed against their many subtle sources of variation whenever they are incorporated into an experimental design. Many of the experiments presented in this manuscript failed to replicate SSVEP effects that were believed to be rather robust. The successful outcomes described in the later chapters illustrated that precise methodology allows investigation of SSVEP phenomena while avoiding confounding characteristics.

APPENDIX

Firmware Version 1 (Sweep)

```
const int ledPin1 = 31;
const int ledPin2 = 27;
const int ledPin3 = 25;
const int ledPin4 = 23;
const int ledPin5 = 29;
int ledState1 = LOW;
unsigned long t0 = 0; // Sweep start.
unsigned long ts = 0; // Last phase switch.
unsigned long t = 0; // Current time.
unsigned long dur = 5*60*1000000; // Sweep duration.
float fstart = 5; // Start frequency.
float fend = 25; // End frequency.
float frange = 20; // Sweep range.
float fpm = frange/((float)dur); // Change in frequency per us.
float f = 5; // Current frequency.
double phalf = 0; // Half period of current square.
double pnext = 500000/f; // Half period of next square.
boolean sweeping = false; // Sweeping/idle flag.
int inputStep = 0; // Serial parameter tracker.
float tmpfl;
String tmpst;

void setup() {
  pinMode(ledPin1, OUTPUT);
  pinMode(ledPin2, OUTPUT);
  pinMode(ledPin3, OUTPUT);
  pinMode(ledPin4, OUTPUT);
  pinMode(ledPin5, OUTPUT);
  digitalWrite(ledPin1, LOW);
  digitalWrite(ledPin2, LOW);
  digitalWrite(ledPin3, LOW);
  digitalWrite(ledPin4, LOW);
  digitalWrite(ledPin5, LOW);
  Serial.begin(9600);
}

void loop() {
  if (sweeping) {
    t = micros();
    if (t - t0 <= dur) {
      if (t - ts > phalf) {
        if (ledState1 == LOW) {
          digitalWrite(ledPin1, HIGH);
          ts = micros();
          phalf = pnext;
```

```
        f = ((float)(ts - t0 + phalf*2))*fpm + fstart;
      }
      else {
        digitalWrite(ledPin1, LOW);
        ts = micros();
        pnext = round(500000/f);
      }
      ledState1 = !ledState1;
    }
  }
  else {
    digitalWrite(ledPin1, LOW);
    Serial.println("Sweep finished.");
    Serial.println(" ");
    sweeping = false;
    inputStep = 0;
  }
}
else {
  if (inputStep == 0) {
    Serial.print("Duration in seconds:");
    inputStep++;
  }
  else if (Serial.available() > 0){
    if (inputStep < 4) {
      tmpfl = Serial.parseFloat();
    }
    else {
      tmpst = Serial.readString();
    }
    switch (inputStep) {
      case 1:
        dur = tmpfl*1000000; // Convert to us.
        Serial.print("Start frequency:");
        break;
      case 2:
        fstart = tmpfl;
        Serial.println("End frequency:");
        break;
      case 3:
        fend = tmpfl;
        frange = fend - fstart;
        fpm = frange/((float)dur);
        pnext = 500000/fstart;
        Serial.print("Start? y/n:");
        break;
      case 4:
        if (tmpst == "y") {
          sweeping = true;
          phalf = 0;
          ledState1 = LOW;
```

```
            Serial.println("Sweeping.");
            t0 = micros();
            ts = micros();
          }
          else if (tmpst == "n") {
            inputStep = -1;
            Serial.println("Paramters cleared.");
            Serial.println("");
          }
          else {
            inputStep--;
          }
          break;
        }
        inputStep++;
      }
    }
  }
```

Firmware Version 2 (Duty Cycle and Luminance)

```
volatile uint8_t pwmn = 255;
int nhi = 1;
volatile uint16_t sfn = 65535;
unsigned int sfnhi = 75;
unsigned int sfnlo = 100;
int inputStep = 0;
String tmpstr;
unsigned long dur;
unsigned long tbeg;
const int ttlBeg = 2;
const int ttlFin = 3;

void setup() {
  pinMode(11, OUTPUT); // LED
  pinMode(4, OUTPUT); // LED On;
  pinMode(5, OUTPUT); // LED Off;
  pinMode(ttlBeg, OUTPUT);
  pinMode(ttlFin, OUTPUT);;

  cli(); // Disable all interrupts.
  // Set up Timer 1 for stim frequency:
  TCCR1A = 0;
  TCCR1B = 0;
  // Counter to 0:
  TCNT1 = 0;
  // Compare match register:
  OCR1A = 1999;
  // Turn on CTC:
  TCCR1B |= (1 << WGM12);
  // 8 prescale:
  TCCR1B |= (1 << CS11);
  // Set up Timer 2 for PWM:
  TCCR2A = 0;
  TCCR2B = 0;
  // Counter to 0:
  TCNT2 = 0;
  // Compare match register:
  OCR2A = 23;
  // Turn on CTC:
  TCCR2A |= (1 << WGM21);
  // 8 prescale:
  TCCR2B |= (1 << CS21);
  sei(); // Enable all interrupts.

  Serial.begin(115200);
  Serial.setTimeout(2);
}
```

```
void loop() {
  if (inputStep == 0) {
    Serial.println("On duration? (ms)");
    inputStep++;
  }
  else if (Serial.available() > 0) {
    switch (inputStep) {
      case 1:
        sfnhi = Serial.parseInt();
        inputStep++;
        Serial.println("Off duration? (ms)");
        break;
      case 2:
        sfnlo = sfnhi + Serial.parseInt();
        inputStep++;
        Serial.println("Luminance? (1-256)");
        break;
      case 3:
        nhi = Serial.parseInt();
        inputStep++;
        Serial.println("Block duration? (s)");
        break;
      case 4:
        dur = Serial.parseInt() * 1000000;
        inputStep++;
        Serial.println("Ready to begin?");
        break;
      case 5:
        tmpstr = Serial.readString();
        if (tmpstr == "y") {
          // Start marker:
          digitalWrite(ttlBeg, HIGH);
          delay(8);
          digitalWrite(ttlBeg, LOW);
          // Stimulus:
          startStim();
          tbeg = micros();
          while ( micros() - tbeg < dur) {};
          stopStim();
          // Stop marker:
          digitalWrite(ttlFin, HIGH);
          delay(8);
          digitalWrite(ttlFin, LOW);
          inputStep = 0;
          Serial.println("Done.");
        }
        else if (tmpstr == "n") {
          Serial.println("Resetting.");
          inputStep = 0;
        }
        else {
```

```
          Serial.println("Enter 'y' to begin or 'n' to reset.");
        }
        break;
    }
    delay(20);
  }
}

void startStim() {
  TIMSK1 |= (1 << OCIE1A); // Turn on Timer 1 interrupts.
}
void stopStim() {
  TIMSK1 &= (0 << OCIE1A); // Turn off Timer 1 interrupts.
  TIMSK2 &= (0 << OCIE2A); // Turn off Timer 2 interrupts.
  PORTB &= ~_BV(PB3); // Turn off LED.
}
void startPWM() {
  pwmn = 255;
  TIMSK2 |= (1 << OCIE2A); // Enable CTC interrupt.
  PORTD |= _BV(PD4); // "Stim on" marker goes high.
  PORTD &= ~_BV(PD5); // "Stim off" marker goes low.
}
void stopPWM() {
  TIMSK2 &= (0 << OCIE2A); // Disable CTC interrupt.
  PORTB &= ~_BV(PB3); // Turn off LED.
  PORTD |= _BV(PD5); // "Stim off" marker goes high.
  PORTD &= ~_BV(PD4); // "Stim on" marker goes low.
}

// Timer for stim frequency:
ISR(TIMER1_COMPA_vect){
  sfn++;
  if (sfn == sfnlo) {
    startPWM();
    sfn = 0;
  }
  else if (sfn == sfnhi) {
    stopPWM();
  }
}
// Timer for PWM:
ISR(TIMER2_COMPA_vect){
  pwmn++;
  if (pwmn == 0) {
    PORTB |= _BV(PB3); // Turn on LED.
  }
  else if (pwmn == nhi) {
    PORTB &= ~_BV(PB3); // Turn off LED.
  }
}
```

Firmware Version 3 (Periodic vs Aperiodic)

```
const int ledPin1 = 11;
const int ttlStimOn = 6;
const int ttlStimNo = 5;
const int ttlBegPeri = 4;
const int ttlFinPeri = 3;
const int ttlBegAper = 2;
const int ttlFinAper = 9;
const int ttlStimOn2 = 8;
const int ttlStimNo2 = 7;
int ledState1 = LOW;
boolean idle = true;
int inputStep = 0;
String tmpstr;
long tmpint;
float tmpflt;
int mode;
boolean ending = false;
unsigned long phalf;
unsigned long nextph;
unsigned long t;
unsigned long tswitch;
unsigned long tbeg;
unsigned long dur;

void setup() {
  pinMode(ledPin1, OUTPUT);
  pinMode(ttlStimOn, OUTPUT);
  pinMode(ttlStimNo, OUTPUT);
  pinMode(ttlBegPeri, OUTPUT);
  pinMode(ttlFinPeri, OUTPUT);
  pinMode(ttlBegAper, OUTPUT);
  pinMode(ttlFinAper, OUTPUT);
  pinMode(ttlStimOn2, OUTPUT);
  pinMode(ttlStimNo2, OUTPUT);
  digitalWrite(ledPin1, LOW);
  digitalWrite(ttlStimOn, LOW);
  digitalWrite(ttlStimNo, LOW);
  digitalWrite(ttlBegPeri, LOW);
  digitalWrite(ttlFinPeri, LOW);
  digitalWrite(ttlBegAper, LOW);
  digitalWrite(ttlFinAper, LOW);
  digitalWrite(ttlStimOn2, LOW);
  digitalWrite(ttlStimNo2, LOW);
  Serial.begin(115200);
  Serial.setTimeout(2);
```

```
}

void loop() {
  if (idle) {
    if (inputStep == 0) {
      Serial.println("Stimulus mode?");
      inputStep++;
    }
    else if (Serial.available() > 0) {
      switch (inputStep) {
        case 1:
          tmpstr = Serial.readString();
          if (tmpstr == "p") {
            mode = 0; // Periodic
            inputStep++;
            Serial.println("Stimulus half-period in microseconds?");
          }
          else if (tmpstr == "a") {
            mode = 1; // Aperiodic
            inputStep++;
            Serial.println("Initial half-period in microseconds?");
          }
          else if (tmpstr == "q") {
            mode = 2; // Cue
            phalf = 0;
            nextph = 50000;
            dur = 500000;
            idle = false;
            ending = false;
            inputStep = 0;
            tbeg = micros();
            tswitch = tbeg;
          }
          else {
            Serial.println("Invalid mode.");
            inputStep = 0;
          }
          delay(100);
        break;
        case 2:
          tmpint = Serial.parseInt();
          nextph = tmpint;
          phalf = 0;
          inputStep++;
          if (mode == 1) {
            inputStep++;
            dur = 600000000;
            Serial.println("Aperiodic mode.");
            Serial.println("Ready to begin?");
          }
          else {
```

```
          Serial.println("Block duration in seconds?");
        }
        delay(100);
      break;
      case 3:
        tmpint = Serial.parseInt();
        dur = tmpint * 1000000;
        inputStep++;
        Serial.print(nextph);
        Serial.print(" us for ");
        tmpflt = round((float)dur / 1000000.);
        Serial.print(tmpflt);
        Serial.println(" seconds.");
        Serial.println("Ready to begin?");
        delay(100);
      break;
      case 4:
        tmpstr = Serial.readString();
        if (tmpstr == "y") {
          idle = false;
          ending = false;
          inputStep = 0;
          if (mode == 0) {
            digitalWrite(ttlBegPeri, HIGH);
            delay(50);
            digitalWrite(ttlBegPeri, LOW);
          }
          else {
            digitalWrite(ttlBegAper, HIGH);
            delay(50);
            digitalWrite(ttlBegAper, LOW);
          }
            tbeg = micros();
          tswitch = tbeg;
        }
        else if (tmpstr == "n") {
          Serial.println("Resetting.");
          inputStep = 0;
        }
        else {
          Serial.println("Enter 'y' to begin or 'n' to reset.");
        }
      break;
    }
  }
}
// If not idle:
else {
  t = micros();
  if (!ending && t - tbeg > dur) {
    ending = true;
```

```
  if (ledState1 == LOW) {
    while (micros() - tswitch < phalf) {}
    idle = true;
    // Prevent extra cycles in very rare cases:
    phalf = 10000000;
    if (mode == 0) {
          digitalWrite(ttlFinPeri, HIGH);
          delay(50);
          digitalWrite(ttlFinPeri, LOW);
        }
        else if (mode == 1) {
          digitalWrite(ttlFinAper, HIGH);
          delay(50);
          digitalWrite(ttlFinAper, LOW);
        }
    Serial.println("Done.");
  }
}
if (t - tswitch > phalf) {
  digitalWrite(ledPin1, !ledState1);
  tswitch = t;
  // ledState1 is the previous state at this point
  if (ledState1 == LOW) {
    // Stimulus is *on*
    digitalWrite(ttlStimOn, HIGH);
    digitalWrite(ttlStimOn2, HIGH);
    digitalWrite(ttlStimNo, LOW);
    digitalWrite(ttlStimNo2, LOW);
    phalf = nextph;
    if (mode == 1) {
      Serial.println("?");
    }
  }
  else {
    // Stimulus is *off*
    digitalWrite(ttlStimOn, LOW);
    digitalWrite(ttlStimOn2, LOW);
    digitalWrite(ttlStimNo, HIGH);
    digitalWrite(ttlStimNo2, HIGH);
    if (Serial.available() > 0 && mode == 1) {
      nextph = Serial.parseInt();
      if (nextph == 0) {
        ending = true;
      }
    }
    if (ending == true) {
      while (micros() - tswitch < phalf) {}
      digitalWrite(ttlStimNo, LOW);
      digitalWrite(ttlStimNo2, LOW);
      if (mode == 0) {
          digitalWrite(ttlFinPeri, HIGH);
```

```
            delay(50);
            digitalWrite(ttlFinPeri, LOW);
          }
          else if (mode == 1) {
            digitalWrite(ttlFinAper, HIGH);
            delay(50);
            digitalWrite(ttlFinAper, LOW);
          }
        idle = true;
        Serial.println("Done.");
      }
    }
    ledState1 = !ledState1;
  }
 }
}
```

BIBLIOGRAPHY

Amiri, S., Rabbi, A., Azinfar, L., & Fazel-Rezai, R. (2013). A Review of P300, SSVEP, and Hybrid P300/SSVEP Brain- Computer Interface Systems. *Brain-Computer Interface Systems - Recent Progress and Future Prospects*.

Bayram, A., Bayraktaroglu, Z., Karahan, E., Erdogan, B., Bilgic, B., Ozker, M., . . . Demiralp, T. (2011). Simultaneous EEG/fMRI Analysis of the Resonance Phenomena in Steady-State Visual Evoked Responses. *Clinical EEG and Neuroscience, 42*(2), 98-106.

Brainard, D. H. (1997). The Psychophysics Toolbox. *Spatial Vision, 10*(4), 433-436.

Brown, R. J., & Norcia, A. M. (1997). A method for investigating binocular rivalry in real-time with the steady-state VEP. *Vision Research, 37*(17), 2401-2408.

Buračas, G. T., & Boynton, G. M. (2002). Efficient Design of Event-Related fMRI Experiments Using M-Sequences. *NeuroImage, 16*(3), 801-813.

Button, K. S., Ioannidis, J. P., Mokrysz, C., Nosek, B. A., Flint, J., Robinson, E. S., & Munafò, M. R. (2013). Power failure: Why small sample size undermines the reliability of neuroscience. *Nature Reviews Neuroscience Nat Rev Neurosci, 14*(5), 365-376.

Castellanos, F. X., Sonuga-Barke, E. J., Scheres, A., Martino, A. D., Hyde, C., & Walters, J. R. (2005). Varieties of Attention-Deficit/Hyperactivity Disorder-Related Intra-Individual Variability. *Biological Psychiatry, 57*(11), 1416-1423.

Cecotti, H. (2010). Effect of the Stimulus Duty Cycle on Steady-State Visual Evoked Potential detection. *5th French Conference on Computational Neuroscience,* 205-209.

Chen, X., Wang, Y., Nakanishi, M., Jung, T., & Gao, X. (2014). Hybrid frequency and phase coding for a high-speed SSVEP-based BCI speller. *2014 36th Annual International Conference of the IEEE Engineering in Medicine and Biology Society*.

Debener, S., Mullinger, K. J., Niazy, R. K., & Bowtell, R. W. (2008). Properties of the ballistocardiogram artefact as revealed by EEG recordings at 1.5, 3 and 7 T static magnetic field strength. *International Journal of Psychophysiology, 67*(3), 189-199.

Delorme, A., & Makeig, S. (2004). EEGLAB: An open source toolbox for analysis of single-trial EEG dynamics including independent component analysis. *Journal of Neuroscience Methods, 134*(1), 9-21.

Delorme, A., Mullen, T., Kothe, C., Acar, Z. A., Bigdely-Shamlo, N., Vankov, A., & Makeig, S. (2011). EEGLAB, SIFT, NFT, BCILAB, and ERICA: New Tools for Advanced EEG Processing. *Computational Intelligence and Neuroscience, 2011*, 1-12. doi:10.1155/2011/130714

Desikan, R. S., Ségonne, F., Fischl, B., Quinn, B. T., Dickerson, B. C., Blacker, D., . . . Killiany, R. J. (2006). An automated labeling system for subdividing the human cerebral cortex on MRI scans into gyral based regions of interest. *NeuroImage, 31*(3), 968-980.

Ding, J., Sperling, G., & Srinivasan, R. (2006). Attentional Modulation of SSVEP Power Depends on the Network Tagged by the Flicker Frequency. *Cerebral Cortex, 16*(7), 1016-1029.

Dwan, K., Gamble, C., Williamson, P. R., & Kirkham, J. J. (2013). Systematic Review of the Empirical Evidence of Study Publication Bias and Outcome Reporting Bias — An Updated Review. *PLoS ONE, 8*(7).

Emerson, G. B., Warme, W. J., Wolf, F. M., Heckman, J. D., Brand, R. A., & Leopold, S. S. (2010). Testing for the Presence of Positive-Outcome Bias in Peer Review. *Arch Intern Med Archives of Internal Medicine, 170*(21).

Frazier, J. A., Chiu, S., Breeze, J. L., Makris, N., Lange, N., Kennedy, D. N., . . . Biederman, J. (2005). Structural Brain Magnetic Resonance Imaging of Limbic and Thalamic Volumes in Pediatric Bipolar Disorder. *American Journal of Psychiatry AJP, 162*(7), 1256-1265.

Gaume, A., Vialatte, F., & Dreyfus, G. (2014). Transient brain activity explains the spectral content of steady-state visual evoked potentials. *2014 36th Annual International Conference of the IEEE Engineering in Medicine and Biology Society*.

Gaume, A., Vialatte, F., & Dreyfus, G. (2014). Detection of steady-state visual evoked potentials using simulated trains of transient evoked potentials. *2014 IEEE Faible Tension Faible Consommation*.

Goldman, R. I., Stern, J. M., Engel, J., & Cohen, M. S. (2002). Simultaneous EEG and fMRI of the alpha rhythm. *NeuroReport, 13*(18), 2487-2492.

Goldstein, J. M., Seidman, L. J., Makris, N., Ahern, T., O'Brien, L. M., Caviness, V. S., . . . Tsuang, M. T. (2007). Hypothalamic Abnormalities in Schizophrenia: Sex Effects and Genetic Vulnerability. *Biological Psychiatry, 61*(8), 935-945.

Gonçalves, S., Munck, J. D., Pouwels, P., Schoonhoven, R., Kuijer, J., Maurits, N., . . . Silva, F. L. (2006). Correlating the alpha rhythm to BOLD using simultaneous EEG/fMRI: Inter-subject variability. *NeuroImage, 30*(1), 203-213.

Gray, M., Kemp, A., Silberstein, R., & Nathan, P. (2003). Cortical neurophysiology of anticipatory anxiety: An investigation utilizing steady state probe topography (SSPT). *NeuroImage, 20*(2), 975-986.

Helps, S., James, C., Debener, S., Karl, A., & Sonuga-Barke, E. J. (2008). Very low frequency EEG oscillations and the resting brain in young adults: A preliminary study of localisation, stability and association with symptoms of inattention. *Journal of Neural Transmission J Neural Transm, 115*(2), 279-285.

Huang, G., Yao, L., Zhang, D., & Zhu, X. (2012). Effect of duty cycle in different frequency domains on SSVEP based BCI: A preliminary study. *2012 Annual International Conference of the IEEE Engineering in Medicine and Biology Society*.

Iannetti, G., Niazy, R., Wise, R., Jezzard, P., Brooks, J., Zambreanu, L., . . . Tracey, I. (2005). Simultaneous recording of laser-evoked brain potentials and continuous, high-field functional magnetic resonance imaging in humans. *NeuroImage, 28*(3), 708-719.

Jenkinson, M., Bannister, P., Brady, M., & Smith, S. (2002). Improved Optimization for the Robust and Accurate Linear Registration and Motion Correction of Brain Images. *NeuroImage, 17*(2), 825-841.

Jenkinson, M., Beckmann, C. F., Behrens, T. E., Woolrich, M. W., & Smith, S. M. (2012). Fsl. *NeuroImage, 62*(2), 782-790.

Jezzard, P., Matthews, P. M., & Smith, S. M. (2001). *Functional MRI: An introduction to methods*. Oxford: Oxford University Press.

Johnson, K. A., Kelly, S. P., Bellgrove, M. A., Barry, E., Cox, M., Gill, M., & Robertson, I. H. (2007). Response variability in Attention Deficit Hyperactivity Disorder: Evidence for neuropsychological heterogeneity. *Neuropsychologia, 45*(4), 630-638.

Kandel, E. R., Schwartz, J. H., & Jessell, T. M. (2000). *Principles of neural science*. New York: McGraw-Hill, Health Professions Division.

Kelly, S., Lalor, E., Reilly, R., & Foxe, J. (2005). Visual Spatial Attention Tracking Using High-Density SSVEP Data for Independent Brain–Computer Communication. *IEEE Trans. Neural Syst. Rehabil. Eng. IEEE Transactions on Neural Systems and Rehabilitation Engineering, 13*(2), 172-178.

Klein, C., Wendling, K., Huettner, P., Ruder, H., & Peper, M. (2006). Intra-Subject Variability in Attention-Deficit Hyperactivity Disorder. *Biological Psychiatry, 60*(10), 1088-1097.

Kleiner M, Brainard D, Pelli D, 2007, "What's new in Psychtoolbox-3?" Perception 36 ECVP Abstract Supplement.

Klimesch, W., Sauseng, P., & Hanslmayr, S. (2007). EEG alpha oscillations: The inhibition–timing hypothesis. *Brain Research Reviews, 53*(1), 63-88.

Laufs, H., Kleinschmidt, A., Beyerle, A., Eger, E., Salek-Haddadi, A., Preibisch, C., & Krakow, K. (2003). EEG-correlated fMRI of human alpha activity. *NeuroImage, 19*(4), 1463-1476.

Lee, P., Yeh, C., Cheng, J. Y., Yang, C., & Lan, G. (2011). An SSVEP-Based BCI Using High Duty-Cycle Visual Flicker. *IEEE Transactions on Biomedical Engineering IEEE Trans. Biomed. Eng., 58*(12), 3350-3359.

Lenartowicz, A., Lu, S., Rodriguez, C., Lau, E. P., Walshaw, P. D., Mccracken, J. T., Cohen, M. S., & Loo, S. K. (2016). Alpha desynchronization and fronto-parietal connectivity during spatial working memory encoding deficits in ADHD: A simultaneous EEG-MRI study. *NeuroImage: Clinical, 11*, 210-223.

Makeig S., Bell A. J., Jung, T-P., & Sejnowski, T.J. (1996) Independent component analysis of electroencephalographic data. In: D. Touretzky, M. Mozer, & M. Hasselmo (Eds.), *Advances in Neural Information Processing Systems 8* (145-151). Cambridge, Massachusetts: The MIT Press.

Makris, N., Goldstein, J. M., Kennedy, D., Hodge, S. M., Caviness, V. S., Faraone, S. V., . . . Seidman, L. J. (2006). Decreased volume of left and total anterior insular lobule in schizophrenia. *Schizophrenia Research, 83*(2-3), 155-171.

Morgan, S. T., Hansen, J. C., & Hillyard, S. A. (1996). Selective attention to stimulus location modulates the steady-state visual evoked potential. *Proceedings of the National Academy of Sciences, 93*(10), 4770-4774.

Moratti, S., Clementz, B. A., Gao, Y., Ortiz, T., & Keil, A. (2007). Neural mechanisms of evoked oscillations: Stability and interaction with transient events. *Human Brain Mapping Hum. Brain Mapp., 28*(12), 1318-1333.

Müller, M. M., Picton, T. W., Valdes-Sosa, P., Riera, J., Teder-Sälejärvi, W. A., & Hillyard, S. A. (1998). Effects of spatial selective attention on the steady-state visual evoked potential in the 20–28 Hz range. *Cognitive Brain Research, 6*(4), 249-261.

Müller, M. M., & Hübner, R. (2002). Can the Spotlight of Attention be Shaped Like A Doughnut? *Psychological Science, 13*(2), 119-124.

Mullinger, K. J., Havenhand, J., & Bowtell, R. (2013). Identifying the sources of the pulse artefact in EEG recordings made inside an MR scanner. *NeuroImage, 71*, 75-83.

Nakanishi, M., Wang, Y., Wang, Y., Mitsukura, Y., & Jung, T. (2013). An approximation approach for rendering visual flickers in SSVEP-based BCI using monitor refresh rate. *2013 35th Annual International Conference of the IEEE Engineering in Medicine and Biology Society (EMBC).*

Niazy, R., Beckmann, C., Iannetti, G., Brady, J., & Smith, S. (2005). Removal of FMRI environment artifacts from EEG data using optimal basis sets. *NeuroImage, 28*(3), 720-737.

O'Connell, R. G., Dockree, P. M., Robertson, I. H., Bellgrove, M. A., Foxe, J. J., & Kelly, S. P. (2009). Uncovering the Neural Signature of Lapsing Attention: Electrophysiological Signals Predict Errors up to 20 s before They Occur. *Journal of Neuroscience, 29*(26), 8604-8611.

Odom, J. V., Bach, M., Barber, C., Brigell, M., Marmor, M. F., Tormene, A. P., & Holder, G. E. (2004). Visual evoked potentials standard (2004). *Documenta Ophthalmologica Doc Ophthalmol, 108*(2), 115-123.

Parsons, O. A., & Miller, P. N. (1957). Flicker Fusion Thresholds in Multiple Sclerosis. *Archives of Neurology And Psychiatry Arch NeurPsych, 77*(2), 134.

Pastor, M. A., Artieda, J., Arbizu, J., Valencia, M., & Masdeu, J. (2003). Human Cerebral Activation during Steady-State Visual-Evoked Responses. *Journal of Neuroscience, 23*(37), 11621-11627.

Pastor, M., Valencia, M., Artieda, J., Alegre, M., & Masdeu, J. (2006). Topography of Cortical Activation Differs for Fundamental and Harmonic Frequencies of the Steady-State Visual-Evoked Responses. An EEG and PET H215O Study. *Cerebral Cortex, 17*(8), 1899-1905.

Pelli, D. G. (1997). The VideoToolbox software for visual psychophysics: Transforming numbers into movies. *Spatial Vision, 10*(4), 437-442.

Perlstein, W. M., Cole, M. A., Larson, M., Kelly, K., Seignourel, P., & Keil, A. (2003). Steady-state visual evoked potentials reveal frontally-mediated working memory activity in humans. *Neuroscience Letters, 342*(3), 191-195.

Regan, D. (1989). *Human brain electrophysiology: Evoked potentials and evoked magnetic fields in science and medicine*. New York: Elsevier.

Ritter, P., Moosmann, M., & Villringer, A. (2009). Rolandic alpha and beta EEG rhythms' strengths are inversely related to fMRI-BOLD signal in primary somatosensory and motor cortex. *Human Brain Mapping Hum. Brain Mapp., 30*(4), 1168-1187.

Rodriguez C., Cohen, M. Lenartowicz, A. (2014). U.S. Patent No. WO2015179567 A1. Systems and methods for measuring cardiac timing from a ballistocardiogram. Regents of the University of California.

Rodriguez, Cameron. (2016). Improvements to Simultaneous Electroencephalography – functional Magnetic Resonance Imaging and Electroencephalographic Source Localization. UCLA: Bioengineering 0288.

Russo, F. D., Teder-Sälejärvi, W. A., & Hillyard, S. A. (2002). Steady-State VEP and Attentional Visual Processing. *The Cognitive Electrophysiology of Mind and Brain*, 259-274.

Sauseng, P., Klimesch, W., Gruber, W., Hanslmayr, S., Freunberger, R., & Doppelmayr, M. (2007). Are event-related potential components generated by phase resetting of brain oscillations? A critical discussion. *Neuroscience, 146*(4), 1435-1444.

Sedra, A. S., & Smith, K. C. (2004). *Microelectronic circuits* (5th ed.). Oxford University Press.

Silberstein, R. B., Schier, M. A., Pipingas, A., Ciorciari, J., Wood, S. R., & Simpson, D. G. (1990). Steady-State Visually Evoked Potential topography associated with a visual vigilance task. *Brain Topogr Brain Topography, 3*(2), 337-347.

Smith, S., Bannister, P. R., Beckmann, C., Brady, M., Clare, S., Flitney, D., . . . Zhang, Y. (2001). FSL: New tools for functional and structural brain image analysis. *NeuroImage, 13*(6), 249.

Smith, S. M. (2002). Fast robust automated brain extraction. *Human Brain Mapping Hum. Brain Mapp., 17*(3), 143-155.

Smith, S. M., Jenkinson, M., Woolrich, M. W., Beckmann, C. F., Behrens, T. E., Johansen-Berg, H., . . . Matthews, P. M. (2004). Advances in functional and structural MR image analysis and implementation as FSL. *NeuroImage, 23*.

Stevens, S. S. (1966). Duration, luminance, and the brightness exponent. *Perception & Psychophysics, 1*(2), 96-100.

Szalowski, A., & Picovici, D. (2015). Investigating the robustness of constant and variable period graphics in eliciting steady state visual evoked potential signals using Emotiv EPOC, MATLAB, and Adobe after effects. *2015 26th Irish Signals and Systems Conference (ISSC)*.

Teng, F., Choong, A. M., Gustafson, S., Waddell, D., Lawhead, P., & Chen, Y. (2010). Steady state visual evoked potentials by dual sine waves. *Proceedings of the 48th Annual Southeast Regional Conference on - ACM SE '10*.

Teng, F., Chen, Y., Choong, A. M., Gustafson, S., Reichley, C., Lawhead, P., & Waddell, D. (2011). Square or Sine: Finding a Waveform with High Success Rate of Eliciting SSVEP. *Computational Intelligence and Neuroscience, 2011*, 1-5.

Vaurio, R. G., Simmonds, D. J., & Mostofsky, S. H. (2009). Increased intra-individual reaction time variability in attention-deficit/hyperactivity disorder across response inhibition tasks with different cognitive demands. *Neuropsychologia, 47*(12), 2389-2396.

Vialatte, F., Maurice, M., Dauwels, J., & Cichocki, A. (2010). Steady-state visually evoked potentials: Focus on essential paradigms and future perspectives. *Progress in Neurobiology, 90*(4), 418-438.

Volosyak, I., Cecotti, H., & Gräser, A. (2009). Impact of Frequency Selection on LCD Screens for SSVEP Based Brain-Computer Interfaces. *Lecture Notes in Computer Science Bio-Inspired Systems: Computational and Ambient Intelligence,* 706-713.

Winkler, I., Haufe, S., & Tangermann, M. (2011). Automatic Classification of Artifactual ICA-Components for Artifact Removal in EEG Signals. *Behavioral and Brain Functions Behav Brain Funct, 7*(1), 30.

Winkler, I., Brandl, S., Horn, F., Waldburger, E., Allefeld, C., & Tangermann, M. (2014). Robust artifactual independent component classification for BCI practitioners. *J. Neural Eng. Journal of Neural Engineering, 11*(3), 035013.

Woolrich, M. W., Ripley, B. D., Brady, M., & Smith, S. M. (2001). Temporal Autocorrelation in Univariate Linear Modeling of FMRI Data. *NeuroImage, 14*(6), 1370-1386.

Woolrich, M. W., Jbabdi, S., Patenaude, B., Chappell, M., Makni, S., Behrens, T., . . . Smith, S. M. (2009). Bayesian analysis of neuroimaging data in FSL. *NeuroImage, 45*(1).

Zhu, D., Bieger, J., Molina, G. G., & Aarts, R. M. (2010). A Survey of Stimulation Methods Used in SSVEP-Based BCIs. *Computational Intelligence and Neuroscience, 2010,* 1-12.

Ziemer, R. E., Tranter, W. H., & Fannin, D. R. (1998). *Signals and Systems: Continuous and Discrete*. Upper Saddle River, NJ: Prentice-Hall.